

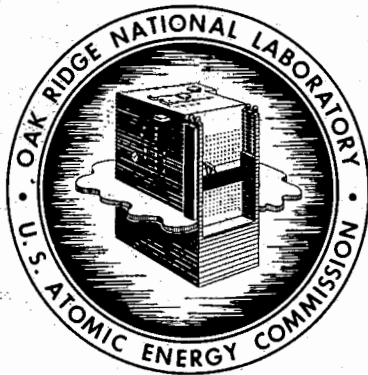
ORNL
MASTER COPY

EXTERNAL DISTRIBUTION AUTHORIZED

ORNL *etc*
Central Files Number
60-12-5
Revised

187

DESIGN STUDY OF A PEBBLE-BED
REACTOR POWER PLANT



NOTICE

This document contains information of a preliminary nature and was prepared primarily for internal use at the Oak Ridge National Laboratory. It is subject to revision or correction and therefore does not represent a final report. The information is not to be abstracted, reprinted or otherwise given public dissemination without the approval of the ORNL patent branch, Legal and Information Control Department.

OAK RIDGE NATIONAL LABORATORY

operated by

UNION CARBIDE CORPORATION

for the

U.S. ATOMIC ENERGY COMMISSION

LEGAL NOTICE

This report was prepared as an account of Government sponsored work. Neither the United States, nor the Commission, nor any person acting on behalf of the Commission:

- A. Makes any warranty or representation, expressed or implied, with respect to the accuracy, completeness, or usefulness of the information contained in this report, or that the use of any information, apparatus, method, or process disclosed in this report may not infringe privately owned rights; or
- B. Assumes any liabilities with respect to the use of, or for damages resulting from the use of any information, apparatus, method, or process disclosed in this report.

As used in the above, "person acting on behalf of the Commission" includes any employee or contractor of the Commission, or employee of such contractor, to the extent that such employee or contractor of the Commission, or employee of such contractor prepares, disseminates, or provides access to, any information pursuant to his employment or contract with the Commission, or his employment with such contractor.

ORNL
Central Files Number
60-12-5
Revised

External Distribution Authorized

Contract No. W-7405-eng-26

DESIGN STUDY OF A PEBBLE-BED REACTOR POWER PLANT

A. P. Fraas

R. S. Carlsmith	S. E. Moore
J. M. Corum	M. L. Myers
J. Foster	M. N. Ozisik
B. L. Greenstreet	A. M. Perry
W. O. Harms	M. W. Rosenthal
T. Hikido	J. C. Suddath
R. B. Korsmeyer	M. M. Yarosh
J. W. Michel	

DATE ISSUED

MAY 11 1961

OAK RIDGE NATIONAL LABORATORY
Oak Ridge, Tennessee
operated by
UNION CARBIDE CORPORATION
for the
U. S. ATOMIC ENERGY COMMISSION

CONTENTS

1. INTRODUCTION AND SUMMARY	1.1
2. PARAMETRIC ANALYSIS FOR SELECTION OF CORE PROPORTIONS	2.1
General Design Requirements	2.1
Reflector	2.1
Core	2.2
Pressure Vessel	2.6
Fluid Flow and Heat Transfer Relations	2.7
Thermal Stresses in Fuel Elements	2.9
Axial Flow Core	2.9
Radial Outflow Cores	2.13
Choice of Reactor Core	2.15
Axial Flow Pattern	2.15
Radial Flow Pattern	2.25
Hot Spot Estimates	2.33
Comparison of Design Problems of Spherical and Prismatic Fuel Element Reactors	2.36
3. REACTOR DESIGN	3.1
Graphite Structure	3.1
Steel Support Structure	3.5
Ball Flow	3.7
Control Rods	3.7
Steam Generators	3.7
4. PLANT LAYOUT	4.1
Site	4.1
Design Data	4.3
General Layout	4.5
Reactor Building	4.8
Helium Storage	4.8
Helium Circulation	4.15
Servicing Equipment	4.15

Viewing Provisions	4.16
Decontamination	4.16
Ventilating System	4.16
5. REACTOR PHYSICS	5.1
6. FUEL ELEMENT FABRICATION	6.1
Fabrication Costs	6.2
7. STRESS ANALYSIS OF FUEL ELEMENTS	7.1
Stress Analysis of Uncoated Fueled Graphite Spheres With Uniform Heat Removal	7.1
Effect of Thermal Stresses Caused by a Nonuniform Heat Transfer Coefficient Over the Surface of a Sphere with Uniform Internal Heat Generation	7.5
Properties of Fueled Graphite	7.10
Discussion of Results	7.16
8. STEAM GENERATORS.....	8.1
General Considerations for Steam Generator Design	8.2
Steam and Gas Conditions in the Steam Generator	8.4
Steam Generator Geometry	8.6
Leak Detection and Maintenance Procedures	8.9
9. BLOWERS AND DRIVES	9.1
10. BALL-HANDLING SYSTEM	10.1
Ball Loading	10.1
Ball Removal	10.2
Development Problems	10.3
11. HELIUM PURIFICATION SYSTEM	11.1
12. STEAM AND ELECTRICAL PLANT	12.1
Turbine Plant	12.1
13. HAZARDS ANALYSES	13.1
Maximum Credible Accident	13.1
Activity Release to the Surroundings Under Normal Conditions	13.5
Activation of Shield Cooling Air	13.6
Activity Escape from Reactor	13.7
Dose at Helium Blowers	13.7
Conclusions	13.9
14. CONSTRUCTION COSTS	14.1

1. INTRODUCTION AND SUMMARY

Sanderson & Porter have carried out a series of studies over the past four years which indicate that the pebble-bed reactor may be an attractive way to obtain low-cost power.^{1,2} At the request of the Atomic Energy Commission, two design studies have been carried out on this concept at the Oak Ridge National Laboratory. The first of these, a preliminary design of a 10-Mw(t) reactor experiment, the PBRE, was initiated September 10, and a report on the study was issued November 1, 1960. The second phase of the work, a conceptual design study of a 330-Mw(e) central station, was initiated November 1, and is the subject of this report.

The over-all design precepts evolved in the course of the work on the PBRE appeared to be applicable and were followed in the development of the design for the 330-Mw(e) plant. In order to avoid duplication, there is no repetition in this report of applicable material presented previously; references are made to pertinent sections of the earlier report.³ Emphasis has been placed on the problems associated with the application of the pebble-bed reactor to a large central station.

A parametric study was carried out to evaluate the characteristics of both axial- and radial-flow pebble-bed reactors. The effects of various limitations associated with the fuel temperature, pressure-vessel fabrication problems, the pumping power-to-heat removal ratio, graphite shrinkage cracking, thermal stresses in the fuel spheres, the core conversion ratio, the core length-to-diameter ratio, and fuel cycle costs were given particular attention. On the basis of this work the choice was narrowed to three reactors, a 14-ft-diam radial-flow core, a 14-ft-diam downflow core, and a 20.5-ft-diam upflow core. The large core with axial upflow was chosen because it gives a higher conversion ratio within the core and hence substantially lower fuel cycle costs and

¹"Design and Feasibility Study of a Pebble Bed Reactor-Steam Power Plant," S&P 1963, May 1, 1958.

²"Pebble Bed Reactor Program Progress Report," NYO-2373, June 1959.

³"Preliminary Design of a 10-Mw(t) Pebble-Bed Reactor Experiment," ORNL CF-60-10-63, November 1, 1960.

better control characteristics. It also gives a less expensive pressure vessel of a size and thickness within the demonstrated techniques of construction, whereas fabrication of the pressure vessels for both the other cores would require extension of known technology. Further, the cost of the pressure vessel for the large core was estimated to be about 60% of the cost of the vessel required for either of the other two reactors. The large-diameter core also has the advantage that the graphite-shrinkage-cracking problem is less severe by a factor of 4, and still higher outputs from this type of reactor seem to be obtainable.

The plant configuration is similar to that for the PBRE and was chosen on the basis of the same design precepts. The reactor auxiliary facilities and equipment are generally similar, but the steam system is designed to generate power rather than to provide a heat dump. Another difference is the use of steam turbines rather than electric motors to drive the blowers. The containment vessel diameter was increased from 80 to 122 ft and its height from 201 to 221 ft. The steam system was modified to provide 1050°F steam at 2400 psi at the turbine, with reheat to 1000°F. The estimated over-all thermal efficiency is 40.5%.

Only seven weeks was available to examine the problems, conceive a design, and prepare this report, as was the case for the preceding study of a 10-Mw(t) pebble-bed reactor experiment. The reactor design presented should be construed as no more than a conceptual design intended to illustrate the problems involved in a large-scale pebble-bed reactor plant and to indicate some of the more promising approaches to their solution. The study indicates that the higher allowable fuel element temperatures permissible with an all-graphite-uranium carbide reactor make possible a net thermal efficiency of about 40%, which is much better than the 32.8% estimated for the GCR-2, and very much better than the efficiencies characteristic of pressurized-water reactor plants. The higher allowable fuel temperature and thermal efficiency also lead to marked reductions in reactor, steam generator, shield, and containment

vessel size for a given reactor power, and hence to lower capital costs - only \$190/kw. The high thermal efficiency also helps reduce the fuel cycle costs, which preliminary estimates indicate are likely to be from about 2.2 to 5.5 mills/kwhr in a first generation plant.

It is by no means evident that the pebble-bed reactor has a cost advantage over other types of all-ceramic reactor. The necessary design compromises lead to lower power densities, lower conversion ratios, and higher pumping power requirements than for cores employing prismatic elements made of the same materials. The higher costs resulting from these factors may more than offset whatever savings may be effected in the fuel-handling system. A definitive evaluation of these factors will require much further work.

The feasibility of a large-scale pebble-bed reactor plant hinges on the same set of research and development problems as were outlined in the PBRE report. Items of particular importance to the design of full-scale plants include the determination of the following:

1. fission-product release rates as functions of fuel composition and fabrication, operating temperature, and burnup;
2. fission-product deposition as a function of surface material, temperature, and gas flow passage length-to-diameter ratio, including any tendencies of surfaces to saturate;
3. effectiveness of fission-product decontamination techniques for surfaces in blowers, fuel-handling equipment, etc.;
4. design limitations imposed by stresses resulting from graphite shrinkage under irradiation and the extent to which shrinkage stresses can be alleviated by slitting, taper drilling, etc.;
5. design limitations imposed by thermal stresses in graphite; and
6. flow behavior of graphite ball beds for a core-to-ball diameter ratio of about 100, both with and without an annular outer layer of balls smaller in diameter than those in the main bed.

2. PARAMETRIC ANALYSIS FOR SELECTION OF CORE PROPORTIONS

The relationships between factors such as ball diameter, core dimensions, and gas-system pressure on the one hand, and the allowable pressure-vessel thickness, pressure drop across the core, and fuel-element temperature and thermal stress on the other are so complex that it is difficult to choose core proportions for a pebble-bed reactor. The problem is further complicated by the necessity for choosing a gas-flow pattern, i.e., axial upflow, axial downflow, or radial outflow. A fairly comprehensive parametric survey of the effects of the principal design parameters was therefore undertaken, and the resulting charts were employed in the selection of a suitable core geometry. In order to give perspective to the results, the characteristics of a typical series of pebble-bed reactors are compared with those of a series of prismatic-fuel-element reactors for the same design conditions.

General Design Requirements

Reflector

There are certain design requirements that must be met irrespective of the type of core flow chosen. The pressure vessel must be properly protected against excessive temperatures, excessive thermal stresses, and fast neutrons. The latter requirement is best satisfied by employing a reflector having a thickness equivalent to approximately 3 ft of graphite. Vessel temperatures and thermal stresses can be kept to reasonable values by thermally isolating the reflector from the vessel with thermal insulation and providing for gas cooling of the interior surface of the vessel. It is also important to inhibit gamma-ray heating of the pressure vessel by absorbing the low-energy neutron leakage from the reflector in a layer of material such as steel or borated graphite. The latter appears to be the more promising

for this application. Structure within the vessel for support of the core and reflector should be similarly protected against excessive temperature. A typical layout designed to satisfy these requirements is shown schematically in Fig. 2.1.

Since irradiation shrinkage cracking will probably limit the life of graphite components exposed to a high fast-neutron flux gradient, graphite so exposed must be designed for replacement. The machined graphite blocks surrounding the vertical sides of the core are therefore protected with a layer of unfueled graphite balls that are fed through the core in much the same way as the fuel. They are smaller than the fuel balls to avoid excessive gas bypass flow through this region. The thickness of the layer of unfueled graphite balls required to protect the fixed graphite is about 1.0 ft. If the fuel charging is carried out in other than batch operations, unfueled graphite balls should not be used to line the reflector at the top and bottom of the reactor. Thus this graphite is designed to be replaceable with special equipment through suitable access tubes. The supports for the top reflector pass through the vessel liner and over the hot-gas plenum for anchorage to the pressure vessel. The guide tubes for the control rods are also exposed to an intense fast-neutron flux and hence are likewise designed for easy replacement, probably on a preventive-maintenance schedule. Cracking of the control rod guide tubes could not be tolerated because control rod operation would be adversely affected.

Core

Reactor core size and shape are influenced by reactor physics considerations in several respects. Probably the most important of these are the effects of core geometry on conversion ratio and consequently on fuel cycle costs. Typical values illustrating these effects are shown in Fig. 2.2, which presents data¹ for a generalized series of

¹A. P. Fraas and M. N. Ozisik, "Relative Capital Charges and Fuel Cycle Costs for All-Ceramic Gas-Cooled Reactors," ORNL CF-60-7-41, July 20, 1960, p. 22.

Unclassified
ORNL-LR-DWG
54494

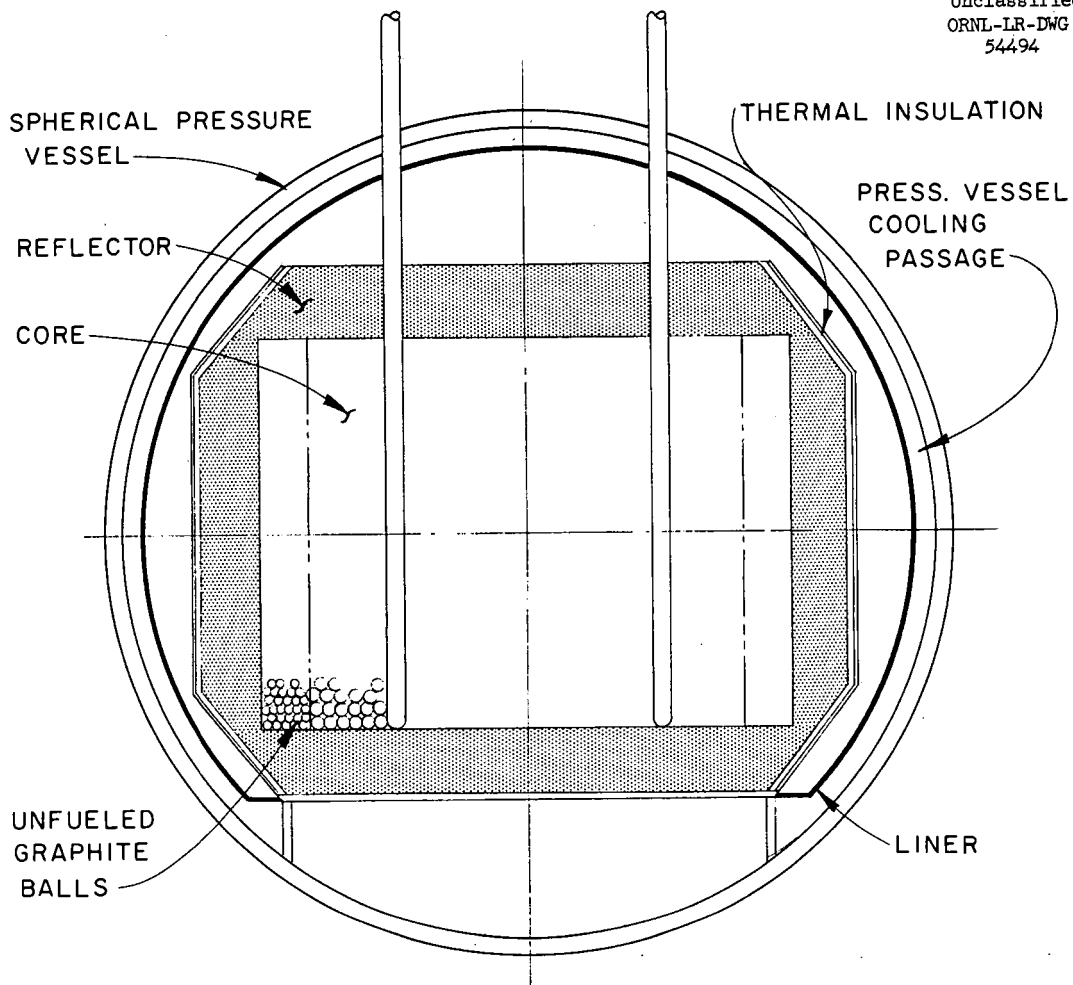


Fig. 2.1. Vertical Section Through an Idealized Axial-Flow Pebble-Bed Reactor Showing the Principal Components.

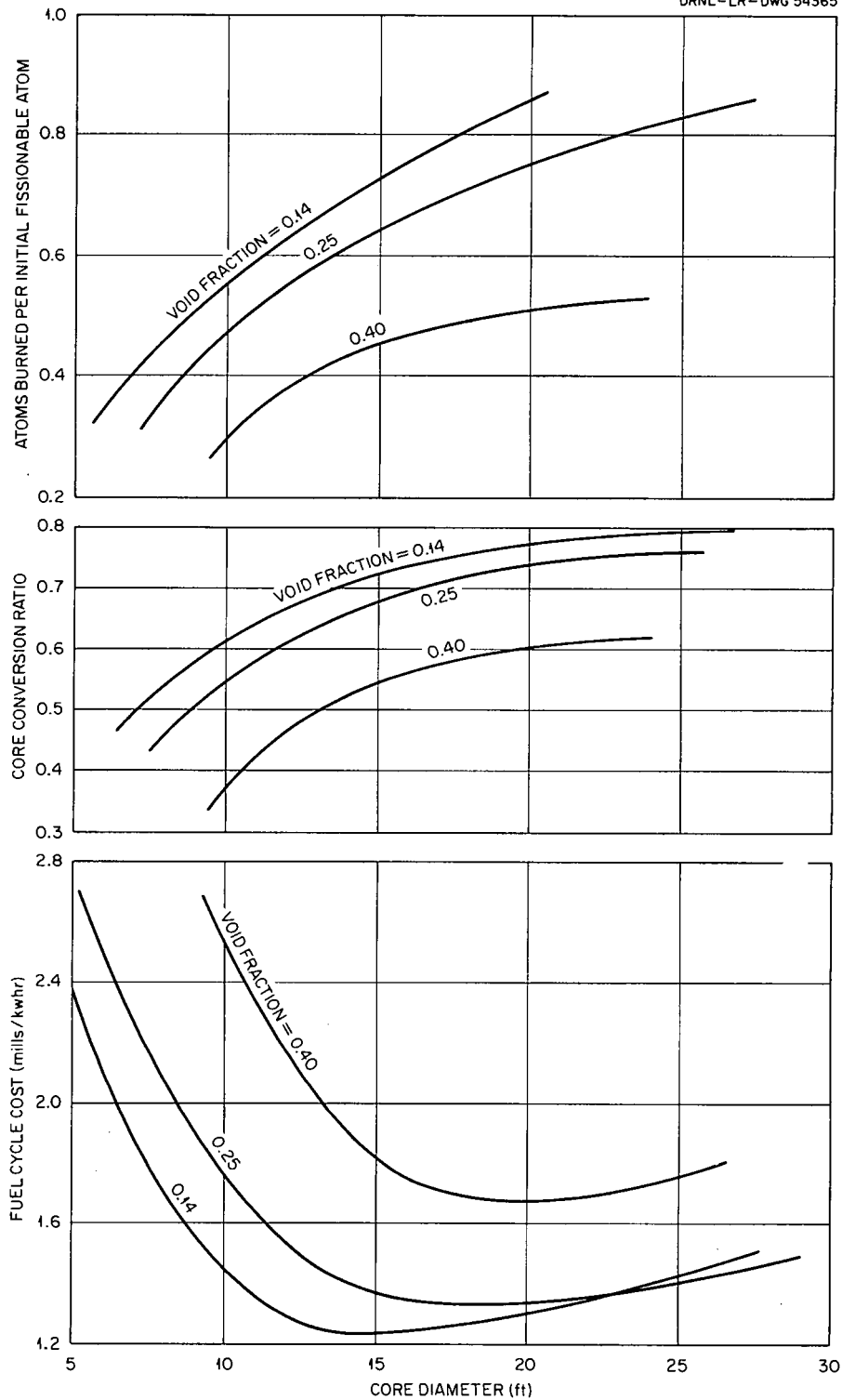


Fig. 2.2. Typical Values for Conversion Ratio, Burnup, and Fuel Cycle Costs as Functions of Core Diameter for 10-ft-Long, Cylindrical, Graphite-Uranium Carbide Pebble-Bed Reactor Cores with Graphite-Thorium Carbide Blankets.

graphite-uranium carbide cores surrounded by graphite-thorium carbide blankets. In preparing Fig. 2.2 it was assumed that the number of fissionable atoms in the fuel should not be allowed to drop to less than 80% of the initial number of fissionable atoms in order to keep the hot-spot problem within reasonable limits. It should be emphasized that the fuel cycle costs estimated in Fig. 2.2 were based on a simplified analysis, and thus there are major uncertainties in fuel fabrication and reprocessing costs. These costs should be considered as indicative rather than absolute. If the fuel fabrication costs were \$100/kg of fuel element instead of the \$10/kg assumed in the calculations, the fuel costs would increase, together with the core diameter for minimum fuel costs. Figure 2.2 implies that, for the 0.39 void fraction characteristic of pebble-bed reactors, the core diameter should be at least 14 ft to give reasonable fuel cycle costs.

The neutron leakage from a core varies with the length-to-diameter ratio for a constant power density. For a bare reactor with a cylindrical core, the minimum neutron leakage loss is obtained with a length-to-diameter ratio of 0.92. The corresponding value for a reflected reactor would be somewhat lower. This is to be compared with a core length-to-diameter ratio of 0.70 for the maximum core volume which can be installed in a given-diameter, spherical, pressure vessel. Thus for both good neutron economy (and low fuel cycle costs) and minimum pressure vessel costs, the core length-to-diameter ratio should be kept between 0.70 and 0.92 if a spherical pressure vessel is to be employed and no other considerations interfere.

A second important factor in the choice of core geometry from the reactor physics standpoint is the power distribution through the core. If a well-proportioned design is to be obtained so that all the fuel is employed to good advantage, the power distribution should be well matched to the cooling-gas flow distribution. Since there appears to be no way of controlling the flow distribution across the face of a pebble-bed reactor, it is important that the power distribution be as nearly uniform as possible. If a thorium blanket is employed in an

axial-flow core, the power density near the core perimeter is so low that a poor gas temperature distribution at the core outlet is unavoidable. Thus it appears to be better to employ a thick reflector rather than a thorium blanket. This has the advantage that, in addition to flattening the power distribution, it increases the conversion ratio in the core. Even though the overall conversion ratio suffers somewhat, the increased cost of fissionable material is offset by reduced fuel fabrication and reprocessing costs.

Pressure Vessel

Practical pressure vessel thicknesses impose limitations on the design of the reactor. At a given pressure level, the thickness requirement for a spherical vessel is half that for a cylindrical vessel of the same diameter. The stress concentrations around penetrations through the reactor vessel for control rods, ducts, or access openings make it necessary to increase the vessel thickness in the vicinity of a penetration by approximately a factor of 3, no matter how small the diameter of the hole. Forging difficulties are serious for vessel sections more than 12 in. thick. If the penetrations are confined to hemispherical heads so that the thickened zones around penetrations will be limited to 12 in., 8-in.-thick cylindrical vessels can be fabricated with nominal head thicknesses of 4 in. X-ray equipment suitable for inspections in the shop is ordinarily limited in capacity to approximately 12-in.-thick sections, while that suitable for field applications is limited to vessel thicknesses of 4 in. These considerations give nominal vessel thicknesses of up to approximately 4 in. for either shop or field fabrication for spherical vessels and 8 in. for cylindrical vessels if shop fabricated.

Shop fabricated vessels up to 14 ft in diameter and 120 ft long have been shipped by rail. Still larger vessels (up to 400 000 lb) have been shipped by water, a mode of transport usually practical for large steam power plants, since the requirement for large amounts of condenser cooling water usually leads to plant locations on navigable water ways. Erection problems at the construction site probably limit

the size of shop-fabricated vessels to around 200 tons. Transportation and erection costs for heavier vessels would be likely to more than offset the extra costs of field fabrication.

The pressure-vessel diameter and thickness can be related to the core diameter and the system pressure level. Layout studies have shown that at least 7 ft must be added to the core diameter to obtain the inside diameter for a cylindrical pressure vessel, while about 11.5 ft must be added to the core diameter to obtain the inside diameter for a spherical vessel. Actually, the diameter of a spherical pressure vessel varies somewhat with a given core diameter depending on the core length-to-diameter ratio. Using the above values and a gas pressure of either 1000 psi or that given by an allowable stress of 16 600 psi, whichever was the smaller, the vessel diameter, thickness, and gas system pressures for both spherical and cylindrical pressure vessels were plotted as a function of core diameter, as shown in Fig. 2.3. As a matter of interest, the weights and estimated costs of these pressure vessels are also plotted in Fig. 2.3 based on the length of the straight cylindrical portion of the vessel being equal to the diameter. The estimated costs do not include costs for penetrations, internal structure, or support structure.

Fluid Flow and Heat Transfer Relations

Materials considerations limit the mean gas temperature at the core outlet to a value in the neighborhood of 1300°F, while good steam-cycle efficiency demands a core inlet gas temperature of at least 500°F (see Sections 8 and 12). Previous studies of other types of gas-cooled reactor² showed that diversion of more than 8 or 10% of the generated power to gas circulation was uneconomical, and that there was often an incentive to make the diversion even less. For thermodynamic efficiencies close to 40%, the ratio of pumping power to total heat generation (W/Q), therefore, cannot exceed 0.03 to 0.04, and, if the

²A. M. Perry, "Economic Effects of Gas-Cooled Reactor Parameters," ORNL CF-59-12-40, December 9, 1959,

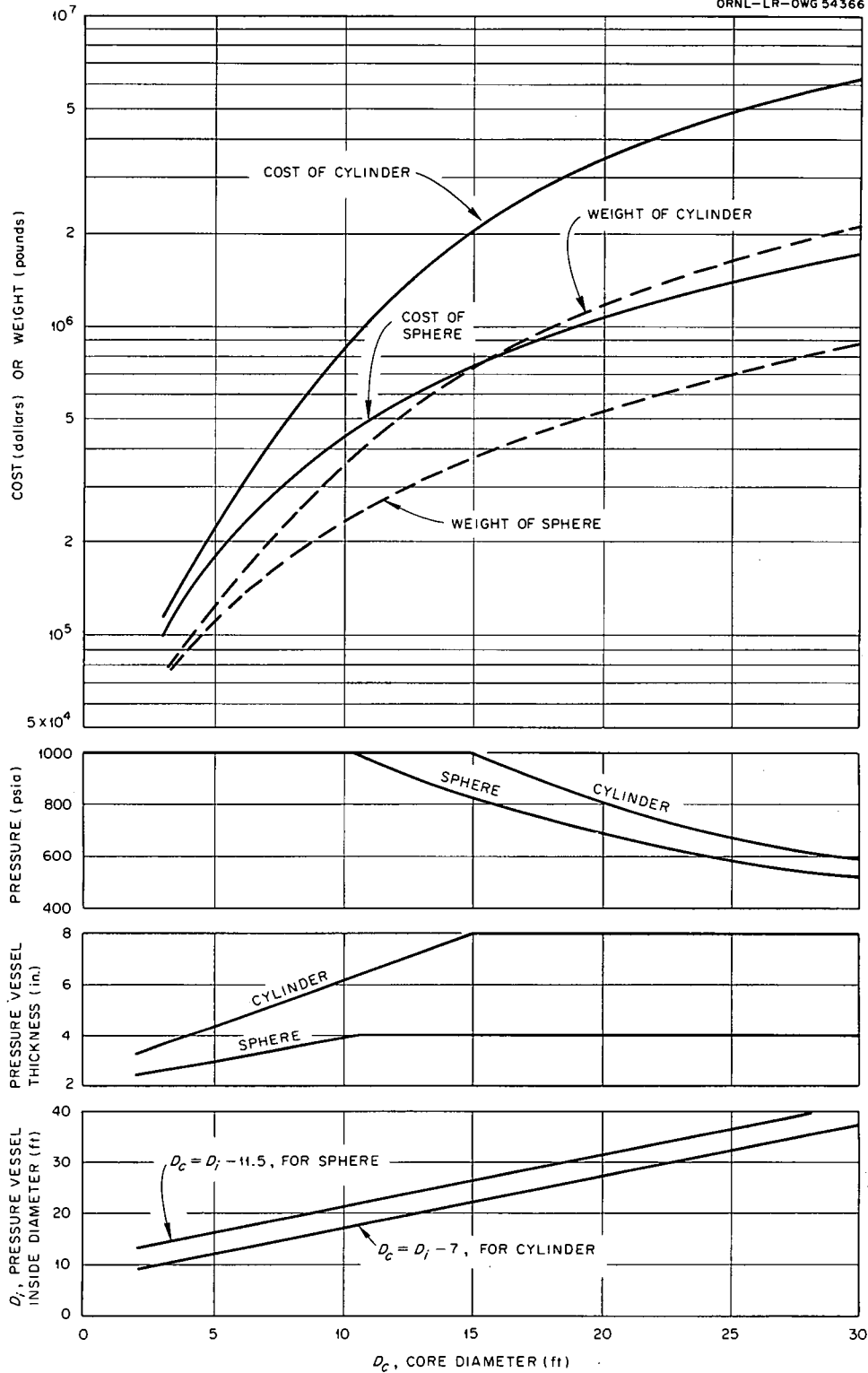


Fig. 2.3. Pressure Vessel Diameter, Allowable System Pressure, and Vessel Cost and Weight Versus Core Diameter for Cylindrical Vessels with a Core Length-to-Diameter Ratio of 0.7 and for Spherical Vessels.

losses in the external system amount to one-half this, the pumping losses in the core alone must not exceed 0.015 to 0.02.

Thermal Stresses in Fuel Elements

The experimental data available on thermal conductivity, modulus of elasticity, and stress to rupture for irradiated fueled graphite are meager. These problems are discussed in some detail in Chapter 7. For the purposes of this section, Fig. 2.4 summarizes the estimated power density and fuel-ball internal temperature drop as a function of ball size for a limiting thermal stress of 2000 psi, a thermal conductivity of 8 Btu/hr·ft²·°F/ft, a modulus of elasticity of 1.5×10^6 psi, a value for Poisson's ratio of 0.3, and a coefficient of thermal expansion of 3×10^{-6} in./in.·°F. Dashed lines for the limiting power density as defined by this thermal stress have been superimposed on the curves of Fig. 2.5.

Axial Flow Cores

The parametric studies covered in this section were based on the relations developed in the PBRE report.³ Equations (23) and (24) on p. 10.16 of that report relate the power density and average film temperature drop to the system pressure, the fuel ball diameter, the temperature rise per unit of core length, and the ratio of pumping power to heat removal. These equations were evaluated for the ranges of variables of interest, and the chart shown in Fig. 2.5 was prepared to facilitate analysis. Note that the temperature rise per unit of core length and the power density define both the core length and the core diameter for any desired reactor power output. The data presented in Fig. 2.5 can be used for other temperatures, void fractions, or gases by multiplying by the appropriate factors given in Fig. 2.6.

³"Preliminary Design of a 10-Mw(t) Pebble-Bed Reactor Experiment," ORNL CF-60-10-63, November 1, 1960, chap. 10.

UNCLASSIFIED
ORNL-LR-DWG 54367

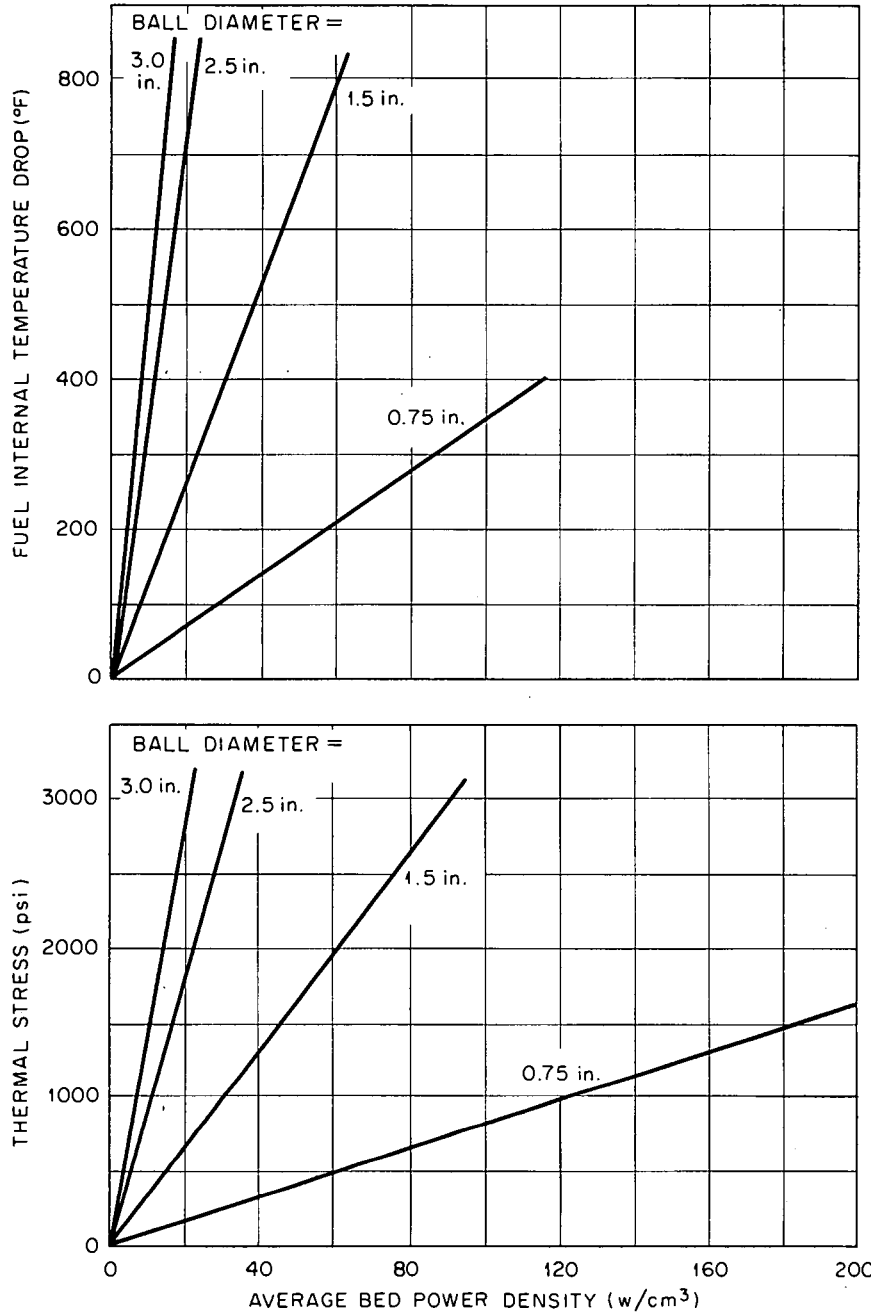


Fig. 2.4. Effects of Power Density and Fuel-Ball Diameter on Thermal Stress and Internal Temperature Drop.

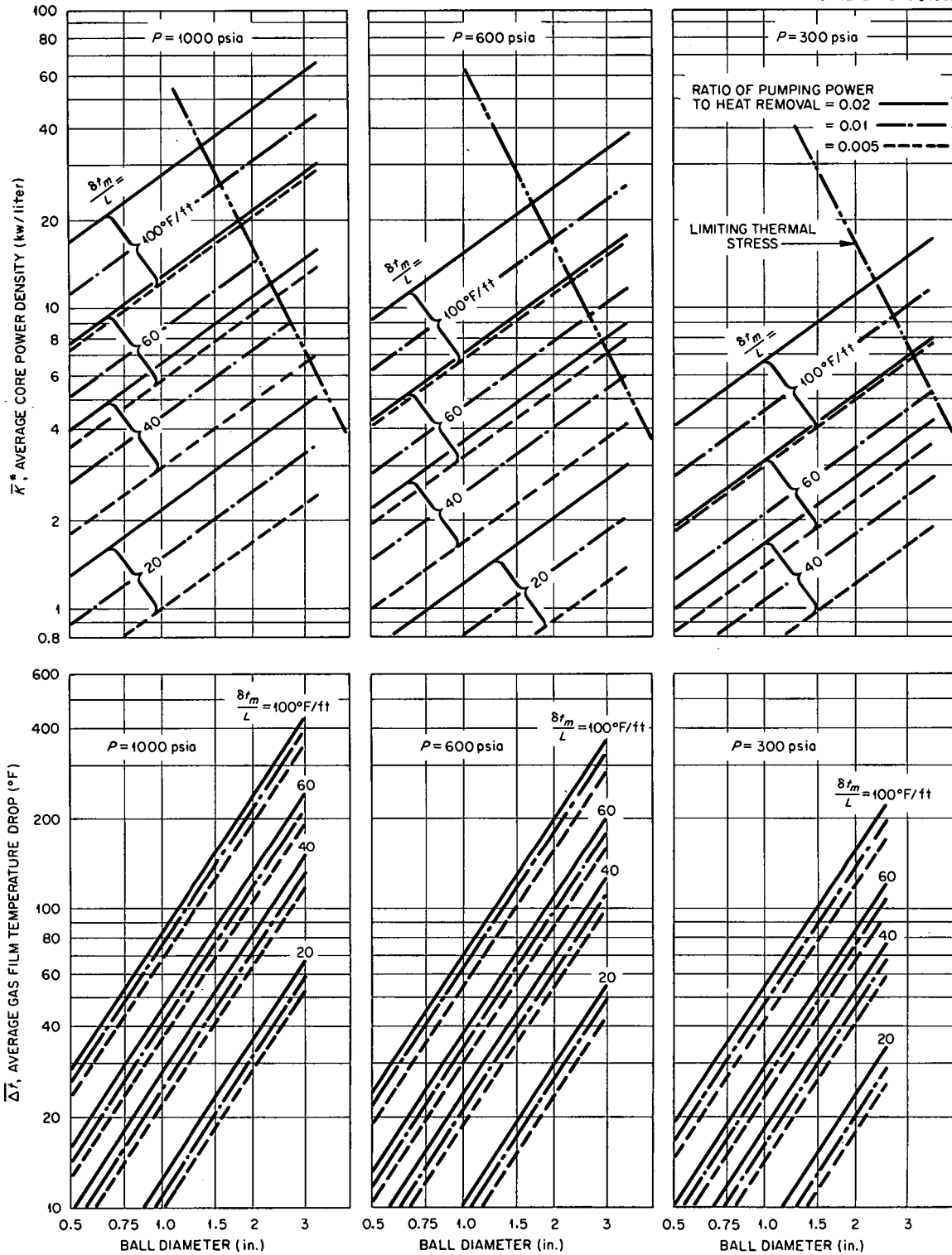


Fig. 2.5. Effects of Fuel-Ball Diameter on Power Density and Film Temperature Drop for Typical Values of System Pressure, Temperature Rise Per Unit Length of Core, and Ratio of Pumping Power to Heat Removal.

FACTORS FOR OTHER GASES:

\bar{K}^* FOR CO₂ = 1.60 (\bar{K}^* FROM FIG. 2.5) $\bar{\Delta}t$ FOR CO₂ = 1.66 ($\bar{\Delta}t$ FROM FIG. 2.5)

\bar{K}^* FOR N₂ = 0.87 (\bar{K}^* FROM FIG. 2.5) $\bar{\Delta}t$ FOR N₂ = 1.51 ($\bar{\Delta}t$ FROM FIG. 2.5)

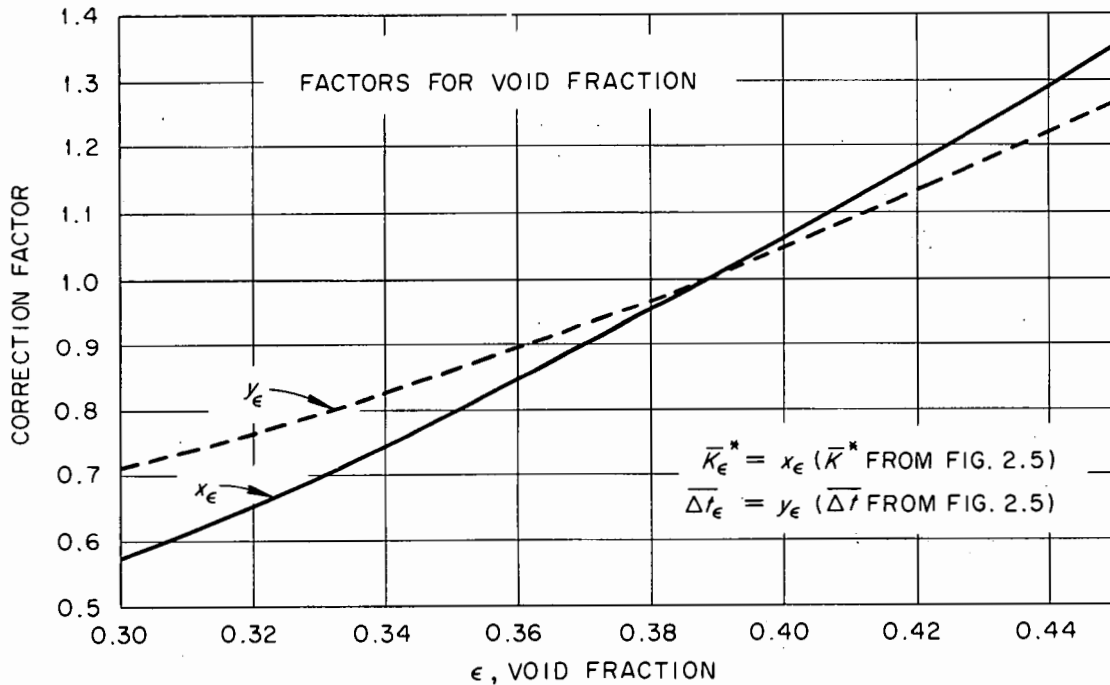
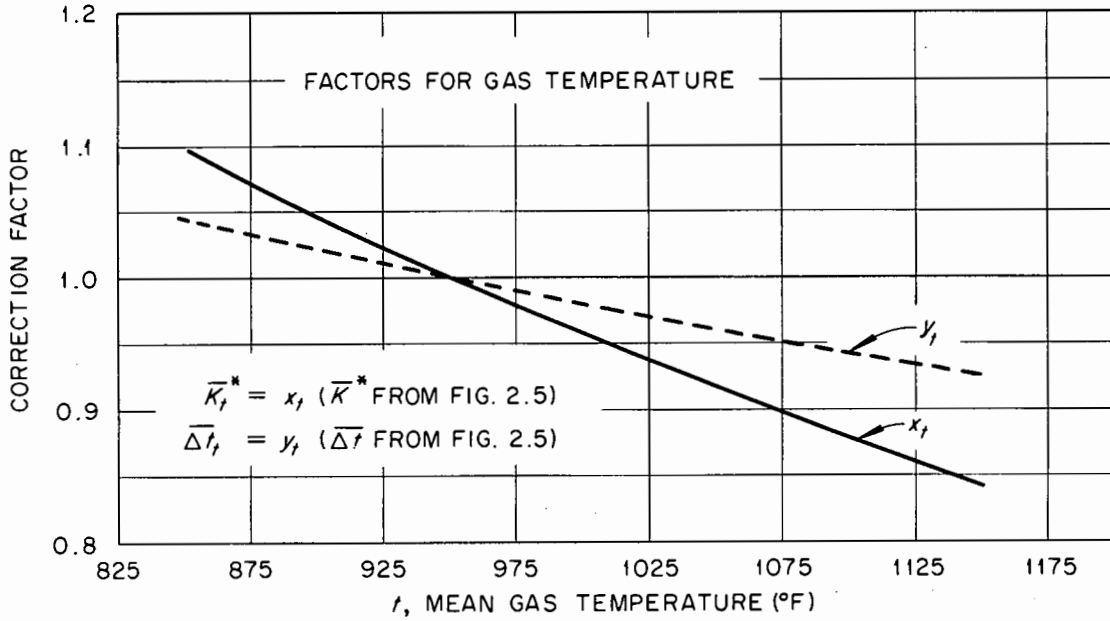


Fig. 2.6. Curves for Correcting Fig. 2.5 for Changes in System Temperature Level, Void Fraction, or Coolant Gas.

Radial Outflow Cores

The general analytical equation relating core power density to the principal variables for radial outflow with a uniform void fraction can be derived readily from the treatment for the axial flow case. Following the derivations of the PBRE report³ and using the same nomenclature, the pressure drop equation in differential form becomes

$$\frac{dP}{dr} = \frac{15}{g} \frac{G^{1.73}}{D_p^{1.27}} \frac{\mu^{0.27}}{\rho} \frac{(1 - \epsilon)^{1.27}}{\epsilon^3}, \quad (1)$$

where r defines the radial position in the core. The local gas flow rate is

$$G = G_0 \frac{r_0}{r},$$

where the subscript zero refers to the core inlet face.

Integrating between r_0 and r_1 , the core inner and outer radii, gives

$$\Delta P = \frac{15}{0.73g} \frac{(G_0 r_0)^{1.73}}{D_p^{1.27}} \frac{\mu^{0.27}}{\rho} \frac{(1 - \epsilon)^{1.27}}{\epsilon^3} \left(r_0^{-0.73} - r_1^{-0.73} \right). \quad (2)$$

The ratio of pumping power to heat removal relation is given by

$$\frac{W}{Q_m} = \frac{1}{778} \frac{\Delta P}{\rho C_p \delta t_m}, \quad (3)$$

where W is the core pumping power and Q_m is the total thermal output (see ref. 3, p. 10.12, Eq. 5). Substituting Eq. (2) in Eq. (3) and solving for G_0 gives

$$G_0 = (7.58 \times 10^5) \left(\frac{W}{Q} \right)^{0.577} D_p^{0.735} \rho^{1.154} \mu^{-0.156} \frac{\epsilon^{1.73}}{(1 - \epsilon)^{0.735}} \times \delta t_m^{0.577} C_p^{0.577} \frac{1}{r_0} \left(r_0^{-0.73} - r_1^{-0.73} \right)^{-0.577}. \quad (4)$$

If $n = r_1/r_0$ and $\rho = PM/1544T$ are substituted in Eq. (4),

$$G_0 = 160 \left(\frac{W}{Q} \right)^{0.577} D_p^{0.735} \left(\frac{PM}{T} \right)^{1.154} \frac{C_p^{0.577}}{\mu^{0.156}} \frac{\epsilon^{1.73}}{(1 - \epsilon)^{0.735}} \times \\ \times \left(\frac{\delta t_m}{r_0} \right)^{0.577} (1 - n^{-0.73})^{-0.577} \quad (5)$$

Further,

$$K_m = \frac{Q_m}{L\pi(r_1^2 - r_0^2)} \quad (6)$$

where L is the core height, and

$$Q_m = G_0 A_0 C_p \delta t_m = G_0 2\pi r_0 L C_p \delta t_m \quad (7)$$

If $n = r_1/r_0$ is substituted in Eq. (6),

$$K_m = \frac{2G_0 C_p}{n^2 - 1} \left(\frac{\delta t_m}{r_0} \right) \quad (8)$$

By substituting Eq. (5) in Eq. (8),

$$K_m = 320 \frac{\epsilon^{1.73}}{(1 - \epsilon)^{0.735}} \frac{C_p^{1.577}}{\mu^{0.156}} \left(\frac{PM}{T} \right)^{1.154} D_p^{0.735} \left(\frac{\delta t_m}{r_0} \right)^{1.577} \times \\ \times \left(\frac{W}{Q} \right)^{0.577} \frac{(1 - n^{-0.73})^{-0.577}}{n^2 - 1} \quad (9)$$

Applying Eqs. (5) and (9) to the case of an 850-Mw(t) reactor circulating helium at 1000 psia through a temperature rise of 700°F and having a core inner radius of 2 ft gives

$$G_0 = (2.37 \times 10^6) \left(\frac{W}{Q} \right)^{0.577} D_p^{0.735} \left(1 - \frac{1}{n^{0.73}} \right)^{-0.577} \quad (10)$$

Conversion to watts per cubic centimeter gives

$$K^* = (2.10 \times 10^4) \left(\frac{W}{Q} \right)^{0.577} D_p^{0.735} \frac{1}{n^2 - 1} \left(1 - \frac{1}{n^{0.73}} \right)^{-0.577} \quad (11)$$

The mass flow can then be expressed in terms of power density as

$$G_0 = 112 (n^2 - 1) K^* \quad , \quad (12)$$

and, for an 850-Mw(t) reactor,

$$L = \frac{4.25 \times 10^3}{(n^2 - 1) K^*} \quad (13)$$

Choice of Reactor Core

Axial Flow Pattern

In choosing a reactor core that would conform to the design limitations outlined above, the first step was to establish the core diameter and length defined by pumping power limitations. For a given system pressure and gas temperature rise through the core, the maximum core depth in the direction of flow was then determined for a given power density, fuel ball size, and ratio of pumping power to heat removal. Once these conditions were established, the core diameter depended only on the total heat generation.

The relationship between core height, diameter, and power density is shown in Fig. 2.7 for various values of the ratio of pumping power to heat removal for a total heat output of 850 Mw, a gas temperature rise of 700°F, a gas pressure of 1000 psia, and a fuel ball diameter of 1.5 in. It is evident that increasing power densities lead to low core length-to-diameter ratios, particularly at low values of the ratio of pumping power to heat removal, and that these are undesirable from the standpoint of neutron economy.

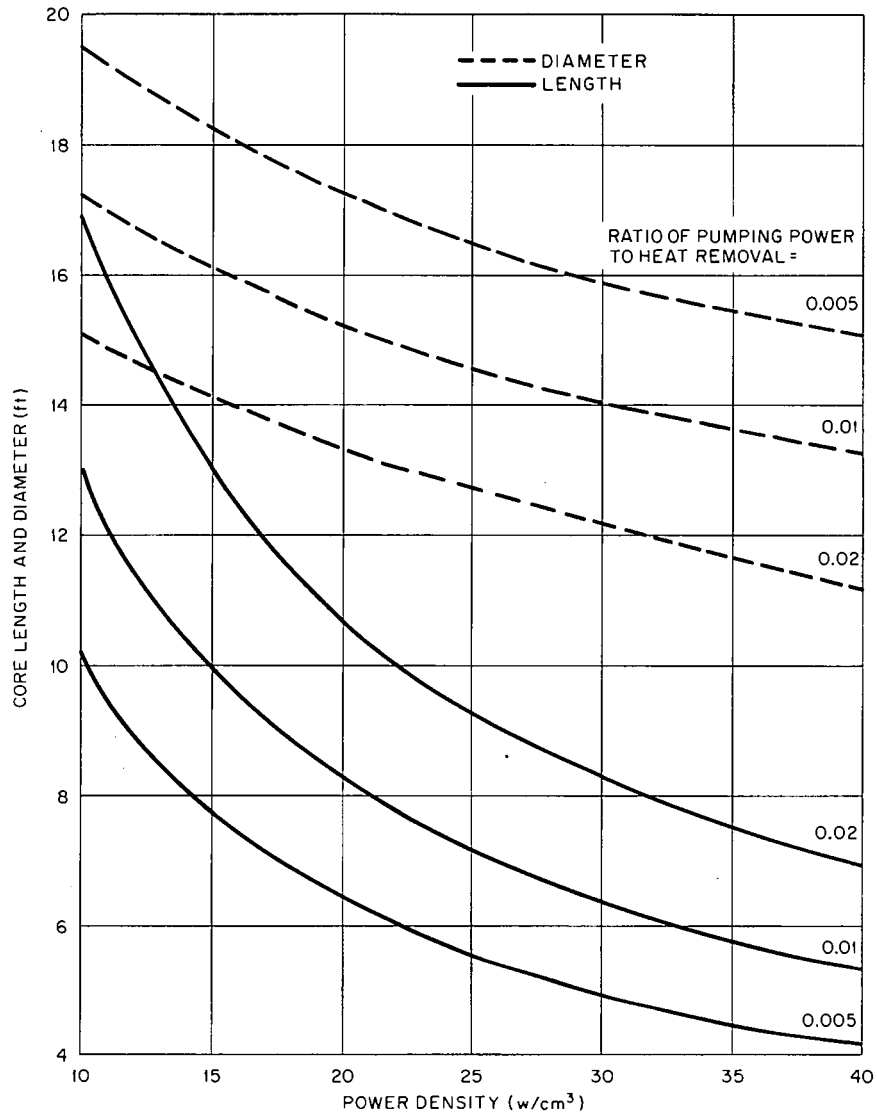
UNCLASSIFIED
ORNL-LR-DWG 54370

Fig. 2.7. Effects of Power Density and Ratio of Pumping Power to Heat Removal on Diameter and Length of an Axial Flow Core with a Total Heat Output of 850 Mw, a Gas Temperature Rise of 700°F, a Fuel Ball Diameter of 1.5 in., and a Gas Pressure of 1000 psia.

Increasing the fuel ball diameter decreases the pumping power, or permits longer cores for the same power density. Thus the core length-to-diameter ratio can be increased simply by increasing the ball diameter, as shown in Fig. 2.8, without adversely affecting the pumping power. The increase in power density obtainable with large fuel balls at a given pumping power-to-heat removal ratio is limited, however, by the allowable thermal stress and internal temperature drop in the balls.

The greater voidage at the core walls permits a considerable fraction of the gas flow to bypass the fueled bed. Additional bypassing occurs through the high voidage regions around the control rod tubes. If a layer of small unfueled graphite balls is used to line the reflector, the interface between the fueled and unfueled layers will be free of a high voidage region and thus should in part offset the bypass flow through such a buffer layer provided ball movement and distribution can be satisfactorily controlled. Preliminary estimates indicate that a 1.0-ft-thick layer of 1.25-in.-diam unfueled graphite balls around a 20-ft-diam bed of 2.5-in. fueled balls would permit approximately 14% of the flow to bypass the core. This requires that the mean gas temperature rise through the fueled region be increased to 800°F, and this value was used in most subsequent studies. While this increases the fuel temperature, it reduces the pumping power requirements and eases the fuel bed levitation problem for upflow cores.

The curves of Fig. 2.2 indicate that, from the fuel cycle cost standpoint, the core diameter should be at least 14 ft, while an examination of fluid flow problems indicates that there is an incentive to increase it to about 20 ft. Figure 2.7 shows that these 14-ft- and 20-ft-diam cores would have lengths of about 12.6 and 10 ft, respectively, and would entail ratios of pumping power to heat removal of about 0.02 and 0.005, respectively. Since these two cores seemed to be representative of those that might be used, they were selected for a more detailed study of their characteristics.

The 14-ft-diam core requires a gas system pressure of 1000 psi if the ratio of pumping power to heat removal is not to exceed the limit

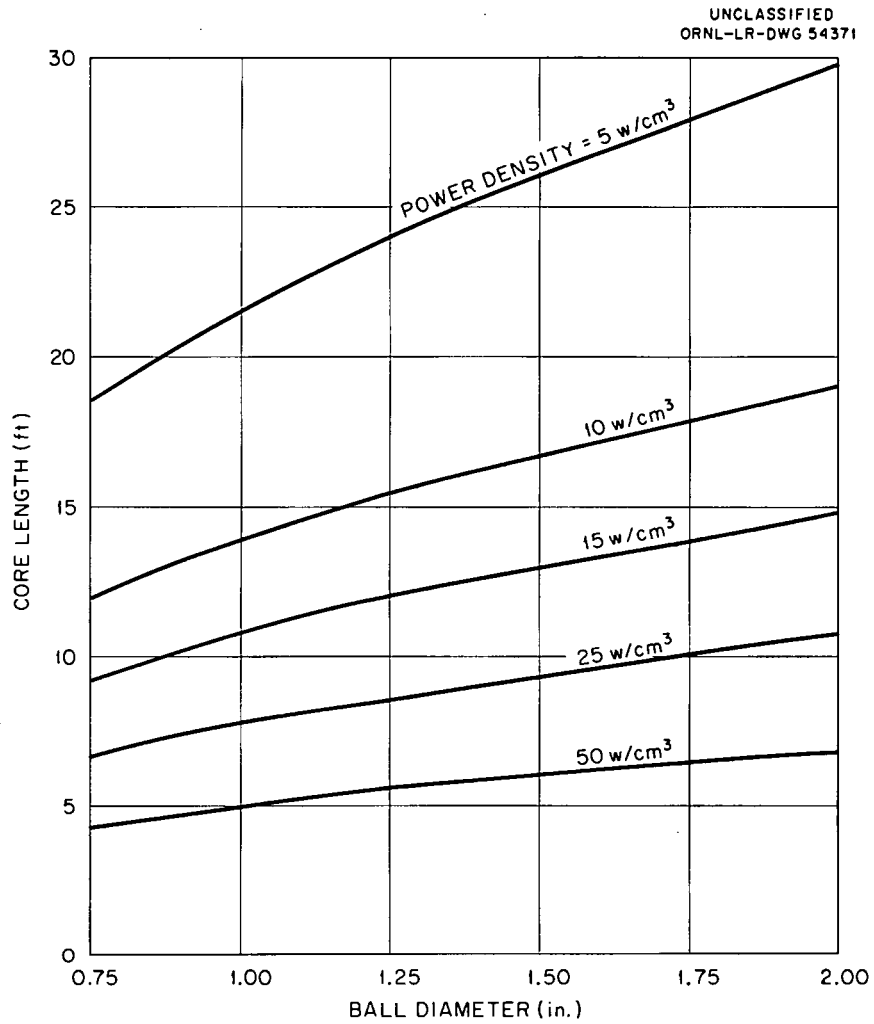


Fig. 2.8. Effects of Fuel-Ball Diameter and Power Density on the Length of an Axial Flow Core for a Pumping Power-to-Heat Removal Ratio of 0.02 and a Gas Pressure of 1000 psia.

of 0.02 established early in the study. Figure 2.3 indicates that this requires an 8-in.-thick, 21-ft-diam cylindrical pressure vessel — a size close to the upper limit of feasibility, and well beyond the limits of existing experience.

The pressure drop across the 14-ft-diam core is much greater than that required to "float" the bed if an upflow core is used. As discussed in Chapter 3 of the PBRE report,³ the design of a reactor to operate under such conditions involves many uncertainties which it would be desirable to avoid. If a downflow core is employed, the very hot gas leaving the core passes through the core and reflector support structure. That structure, therefore, must either be made of a ceramic material or be cooled reliably to a satisfactory working temperature for, say, stainless steel. This temperature is about 500°F below the highest local gas temperatures to be expected at the core exit, and no good way to accomplish the required cooling has been demonstrated. If the support structure is constructed of massive graphite pieces, the misalignment and failure problems associated with irradiation shrinkage and differential thermal expansion are formidable, and frequent replacement might be a necessity. While it has been suggested that graphite slabs might be laid on a layer of loose or sintered graphite spheres, these would support the slabs at only two or three points, and the slabs would tend to teeter unpredictably like flat stones laid on a bed of rounded boulders. Thus the axial downflow concept would be selected only if a thorough examination of other arrangements revealed that downflow would give pronounced advantages in other respects and a thorough analysis showed that the support structure proposed would be satisfactory.

Cores about 20 ft in diameter can be designed to have a pressure drop sufficiently low so that bed flotation will not occur with an upflow core. It has been found that the bed will begin to float at a pressure drop per unit of length 87% of the bed density and that it would be best to design for a limiting core pressure drop per unit of length of not more than 80% of the bed density.⁴ For graphite fuel

⁴"Progress Report, Pebble Bed Reactor Program, June 1, 1959 to September 30, 1960," NYO-9071.

elements the bed density is about 70 lb/ft^3 , so, for design purposes, the pressure gradient should be limited to about 56 lb/ft^3 . Since the pressure gradient depends only on the gas pressure, gas flow, and fuel-ball diameter, the limiting heat output per unit of core inlet face area can be expressed in terms of the fuel-ball diameter and the system pressure for a given gas temperature rise. Figure 2.9 is such a plot prepared from Sanderson & Porter data⁴ by adjusting for a gas temperature rise of 800°F (550 to 1350°F) instead of 700°F . Note that the thermal output per unit of core inlet face area can be determined from Fig. 2.9 without stating the core height, since that depends on the linear gas temperature rise. The levitation-limited core diameter for a given total thermal output can be easily determined by using Fig. 2.9. In order to facilitate such estimates, the relationship between the fuel-ball diameter, the levitation-limited core diameter, and the helium pressure is shown in Fig. 2.10 for a thermal output of 800 Mw. For a given core diameter, the core length determines the average power density and the core length-to-diameter ratio. These relations are also shown in Fig. 2.10, together with a scale for the diameter of spherical vessels based on maximum inside diameter for the indicated pressure for a 4-in.-thick shell. The average core power density increases with fuel-ball diameter because higher gas flows are required to levitate beds of larger balls. However, the internal temperature drop and the thermal stress in the fuel increase as the square of the ball diameter (see Fig. 2.4), so the power density is limited by one factor or another to a relatively low value if the core is designed for upflow without levitation.

The above analysis indicates that the principal limitations to be considered in settling on a specific value for the diameter of an upflow core are those imposed by pressure vessel fabrication considerations, flotation of the bed, and thermal stresses in the fuel. The relations developed above were applied to show the effects of these parameters on a single chart. For a given gas system pressure the fuel-wall diameter required to avoid flotation was calculated as a function of core diameter

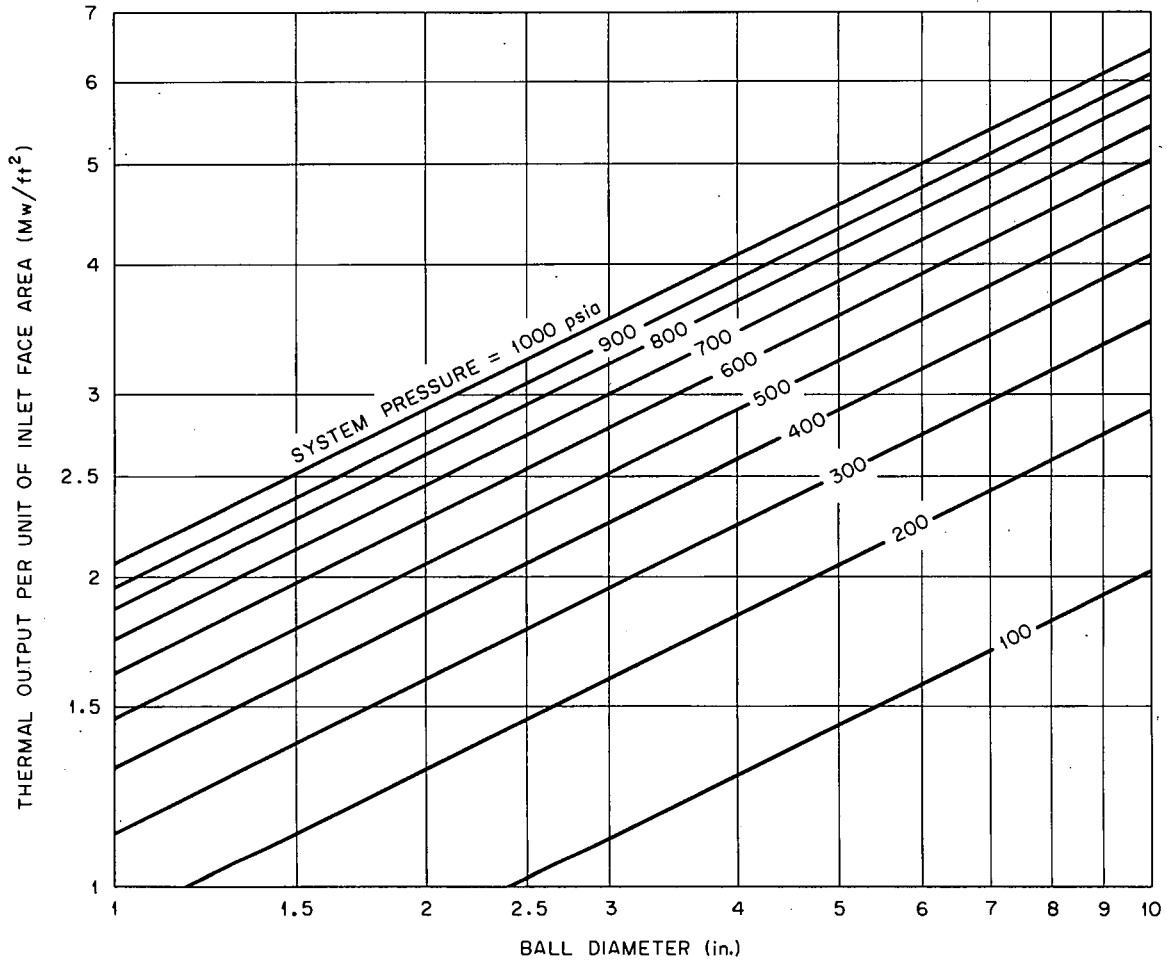
UNCLASSIFIED
ORNL-LR-DWG .54372

Fig. 2.9. Levitation-Limited Power Output Per Unit of Core Inlet Face Area as a Function of Fuel-Ball Diameter and Cooling-Gas Pressure for Axial Upflow Cores. The curves were constructed for a pressure drop equal to 80% of the fuel bed weight per unit of face area and helium inlet and outlet temperatures of 550 and 1350°F, respectively.

UNCLASSIFIED
ORNL-LR-DWG 54373

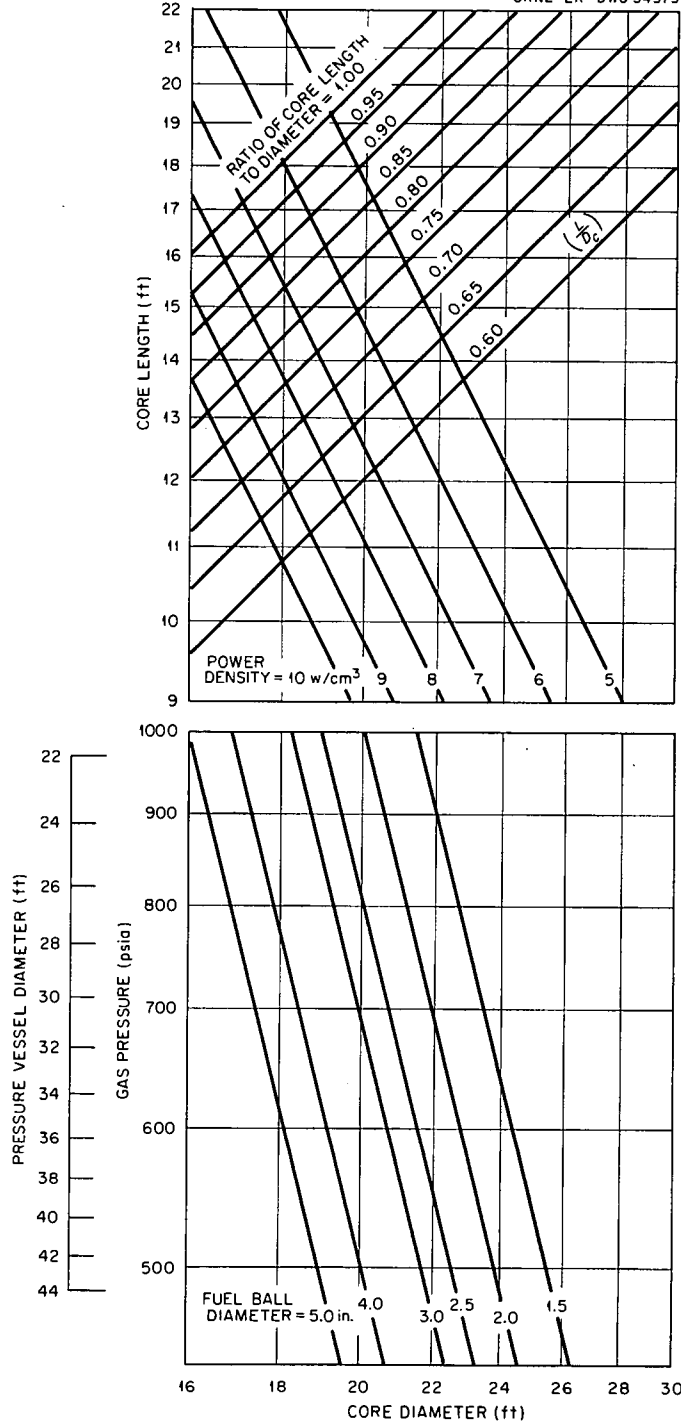


Fig. 2.10. Effects of Fuel-Ball Diameter on Core Diameter and Length, Pressure Vessel Diameter, and Helium Pressure for Levitation-Limited Axial Upflow Cores. The curves were constructed for a pressure drop equal to 80% of the fuel bed weight per unit of face area, 4-in.-thick spherical pressure vessels of maximum inside diameter for the indicated pressure, and helium inlet and outlet temperatures of 550 and 1350°F.

for an 800°F gas temperature rise to give the constant pressure lines of Fig. 2.11. The maximum core diameter for a 4-in.-thick spherical pressure vessel for a core length-to-diameter ratio of 0.7 was then determined for each of the above pressures, and the data were plotted as a dotted line on Fig. 2.11 to indicate the region giving pressure vessels less than 4 in. thick. An additional dotted line showing the limiting fuel-ball diameter as a function of core diameter was then plotted assuming a peak-to-average power-density ratio of 2.0. The constant pressure curves in the region to the right of both this curve and that for a 4-in.-thick pressure vessel have been drawn in solid form to indicate that this region is within the design limitations established above, while the portions of these curves to the left of the dotted lines were dashed to indicate that they fall in a region of questionable feasibility.

After careful study of Fig. 2.11 and similar charts, a 20.7-ft-diam core 12.6 ft high with 2.5-in.-diam fuel spheres and a 700-psi helium system pressure was chosen as giving a well-proportioned axial upflow core. This core length-to-diameter ratio is somewhat less than that for which Fig. 2.11 was prepared, which has the effect of moving the design point to the right and well into the region for good bed stability.

In reviewing these considerations and summarizing, it appears that a 20.7-ft-diam upflow core with 2.5-in.-diam balls is definitely preferable to a 14-ft-diam downflow core. The fuel cycle and pressure vessel costs are lower; the pressure vessel size falls in the region of demonstrated feasibility; the formidable problems of supporting a downflow core are avoided; hazards problems are reduced by greatly improved thermal convection; and, since the pumping power is much lower, the blowers are smaller, simpler, and more easily maintained.

Radial Flow Pattern

The high ratio of pumping power to heat removal characteristic of a high-power-density axial flow core made it important to consider

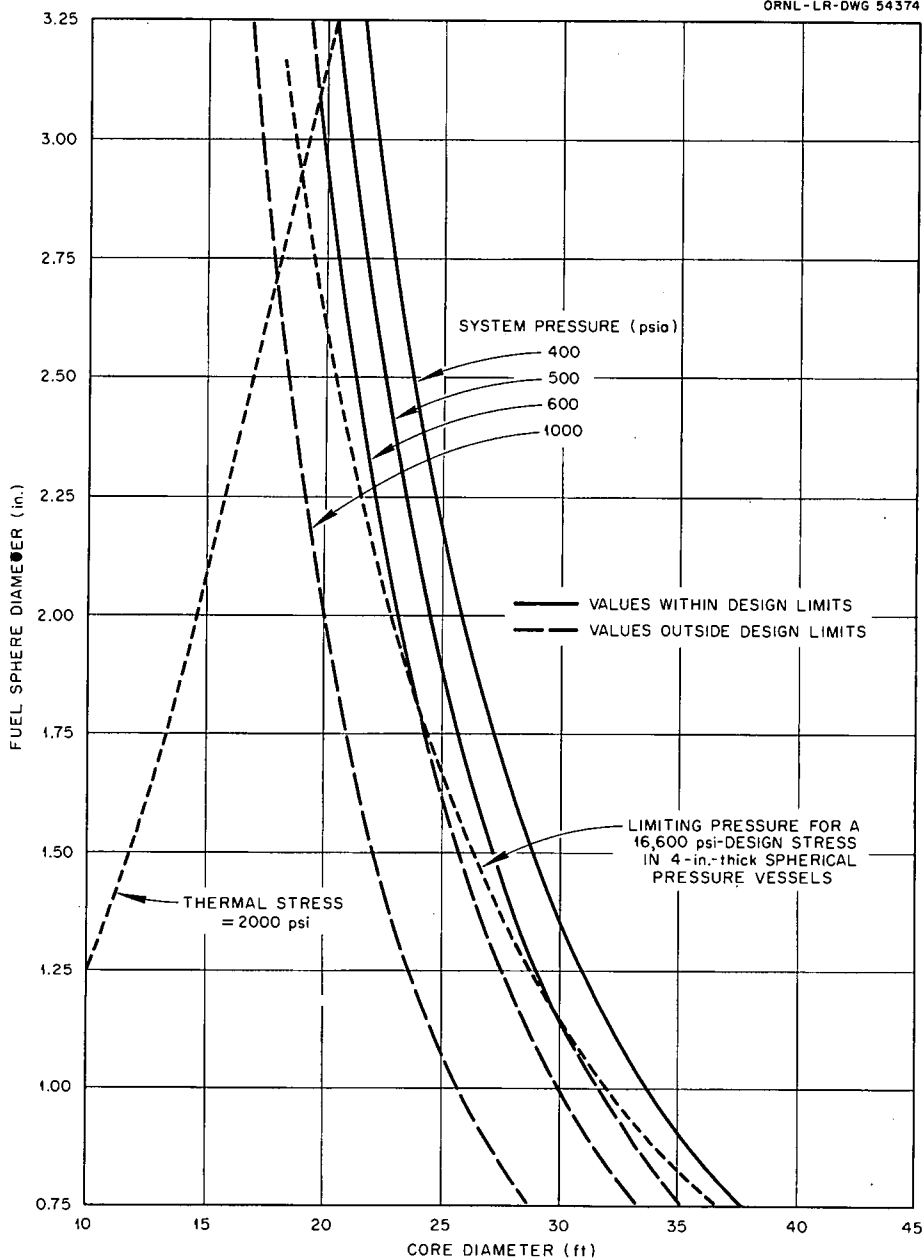
UNCLASSIFIED
ORNL-LR-DWG 54374

Fig. 2.11. Design Chart for Axial Upflow Cores Showing Combinations of Fuel-Ball Diameter, Core Diameter, and System Pressure Which Give Thermal Stresses in the Fuel of Less than 2000 psi and Spherical Pressure Vessels Having Thicknesses Less than 4 in. for 800 Mw and Helium Inlet and Outlet Temperatures of 550 and 1350°F.

other configurations which would increase the effective flow passage area through the high-power-density core. A variety of radial, tandem, and folded flow configurations was considered, but problems of matching the flow distribution to the power distribution made it necessary to reject all except the radial flow core. Inward radial flow appeared less favorable than outward radial flow because a larger central hole was required for the hot exit gas than for the cooler inlet gas. Hence, attention was directed to the outward radial flow core. The construction considered is shown in Fig. 2.12. Cooling gas enters the core axially through a 4-ft-diam passage at the center of the core. Graphite tubes housing the control rods are placed around the perimeter of this inlet passage. The cooling gas flows radially outward through the 3/4-in.-wide gaps between these 5-in.-diam graphite tubes. The pebble bed lies in an annulus between the control rod tubes and a graphite grid at the outer perimeter. The hot gas leaves the reactor through axial ducts in the outer portion of this grid. This configuration not only increases the flow passage area for the cooling gas, but it also reduces the depth of the bed in the cooling-gas flow direction.

One of the important factors in the design of such a core is the effectiveness of the control rods. As shown in Chapter 5, the configuration of Fig. 2.12 gives an adequately effective set of control rods for fuel-bed-annulus thicknesses of up to about 4 ft.

Using the analytical expressions for the pressure drop and heat transfer developed earlier in this section for radial flow, a chart was prepared to facilitate the design study. The relations defined by Eqs. (11), (12), and (13) are shown graphically in Fig. 2.13 for a core internal diameter of 4 ft and core outside diameters of 8, 10, and 12 ft. Two scales for the pumping power-to-heat removal ratio are shown, one for a fuel element diameter of 1.5 in. and one for a diameter of 0.75 in. Preliminary estimates made with the use of Fig. 2.13 show that the core pressure drop with radial flow is reduced drastically,

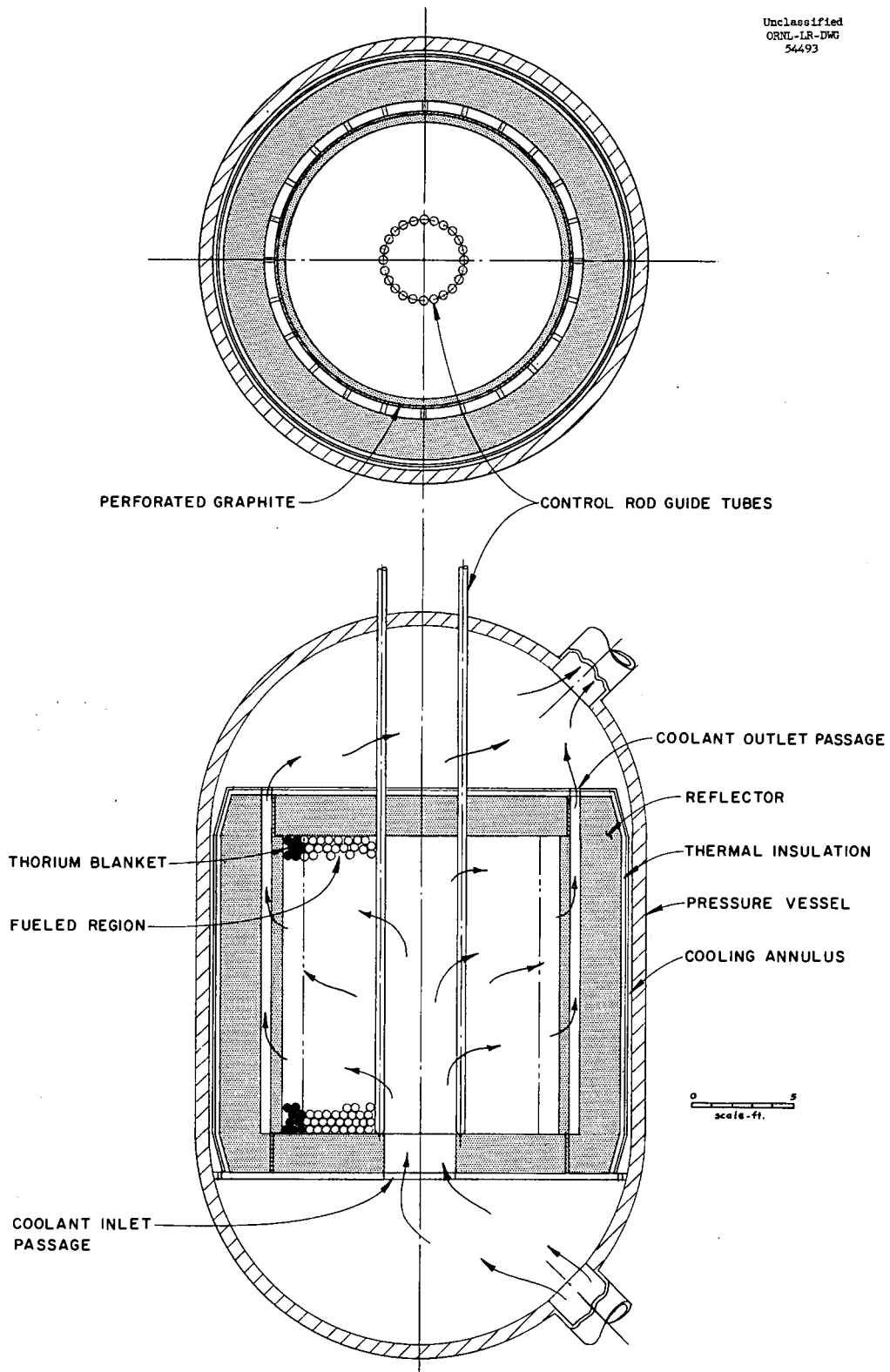


Fig. 2.12. Sections Through an Idealized Radial Outflow Pebble-Bed Reactor Showing the Principal Components.

UNCLASSIFIED
ORNL-LR-DWG-54375

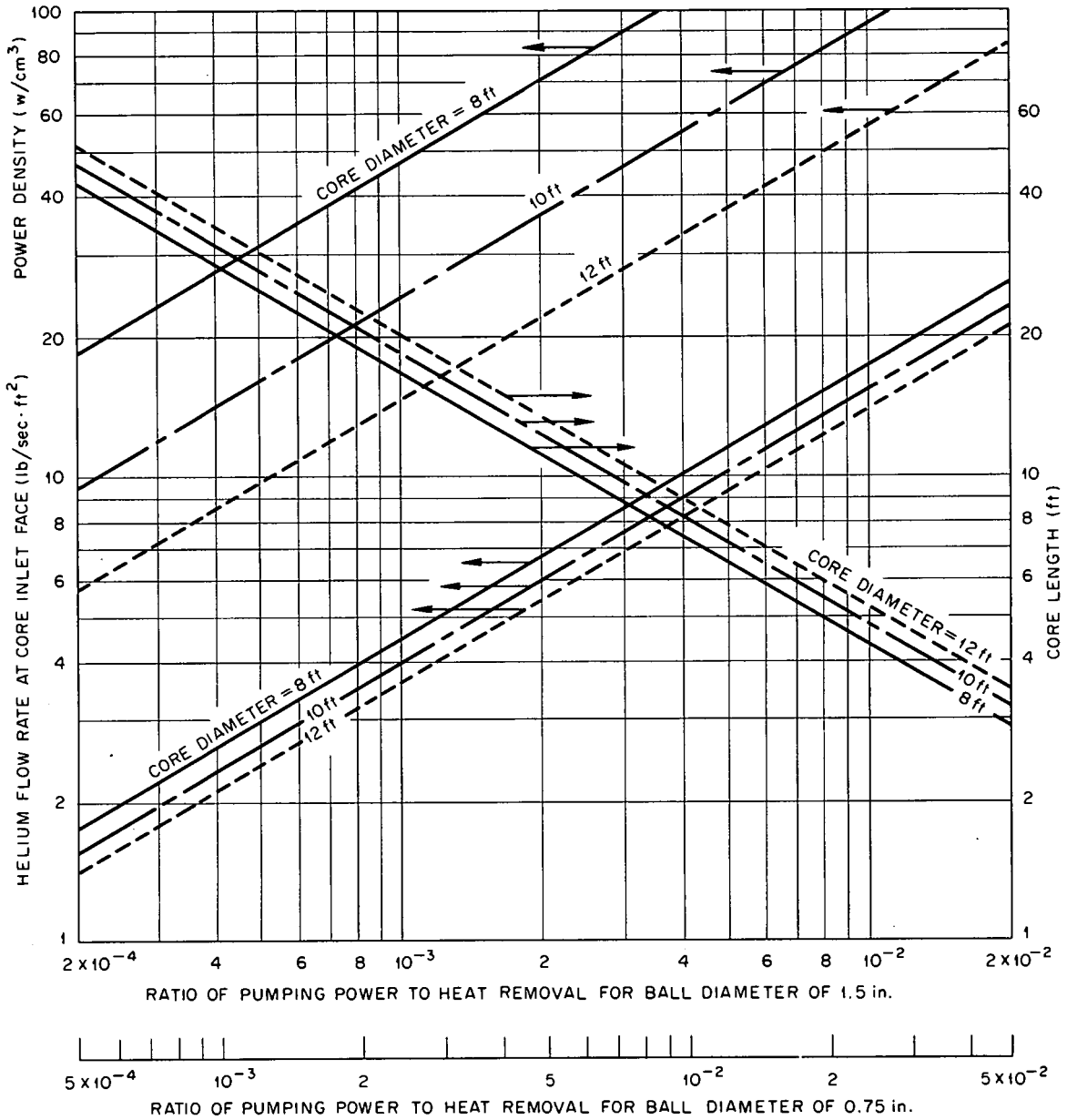


Fig. 2.13. Effects of Ratio of Pumping Power to Heat Removal on the Average Power Density, Helium Flow Rate at the Core Inlet Face, and Core Length for Two Fuel-Ball Diameters and Three Core Outer Diameters for Radial Outflow Cores Having an Inner Diameter of 4 ft, a Power Output of 850 Mw, and Helium Inlet and Outlet Temperatures of 550 and 1250°F.

so the power density is not limited by the economics of pumping. However, if the diameter of the core is no greater than for the axial flow reference case (a necessary condition for inclusion in the same-diameter pressure vessel), the power density in the bed itself must be higher, or the height of the core must be greater for the same total heat generation because of the central hole. Therefore, the radial flow concept favors a high power density and a smaller fuel-ball size than is desirable for the axial flow core. The situation is illustrated in Fig. 2.14, which gives the mass flow rate at the core inlet face, the pressure drop through the core, and the ratio of core pumping power to heat removal vs the core diameter for three power densities for cores with a central opening 4.0 ft in diameter and an output of 850 Mw of heat. As in the case of Fig. 2.7, the gas temperature rise was taken as 700°F. The solid lines for ΔP and W/Q refer to a ball diameter of 1.5 in., and the dotted lines give the corresponding values for 0.75-in. fuel balls. These curves indicate that power densities of more than 10 w/cm^3 are required to keep the height to a reasonable value.

The problem of gas bypassing through the high voidage zones at the core boundaries, discussed in connection with the axial flow concept, is also present with radial flow. Here the problem would be especially bad at the top of the reactor because the balls would not tend to pack tightly against the top reflector.

There are several serious disadvantages inherent in the radial flow concept. The reduction in mass flow per unit of flow passage area as the gas progresses through the bed requires a rather steep radial reduction in power density if excessive fuel temperatures are to be avoided at the core periphery. For example, the radial power distribution shown in Fig. 2.15 was calculated for annular cores of different central hole diameters and thicknesses. As can be seen, the power density at the core periphery for all cases is as high as at the inner edge. The gas flow rate per unit area falls off with increasing radius,

UNCLASSIFIED
ORNL-LR-DWG 54376

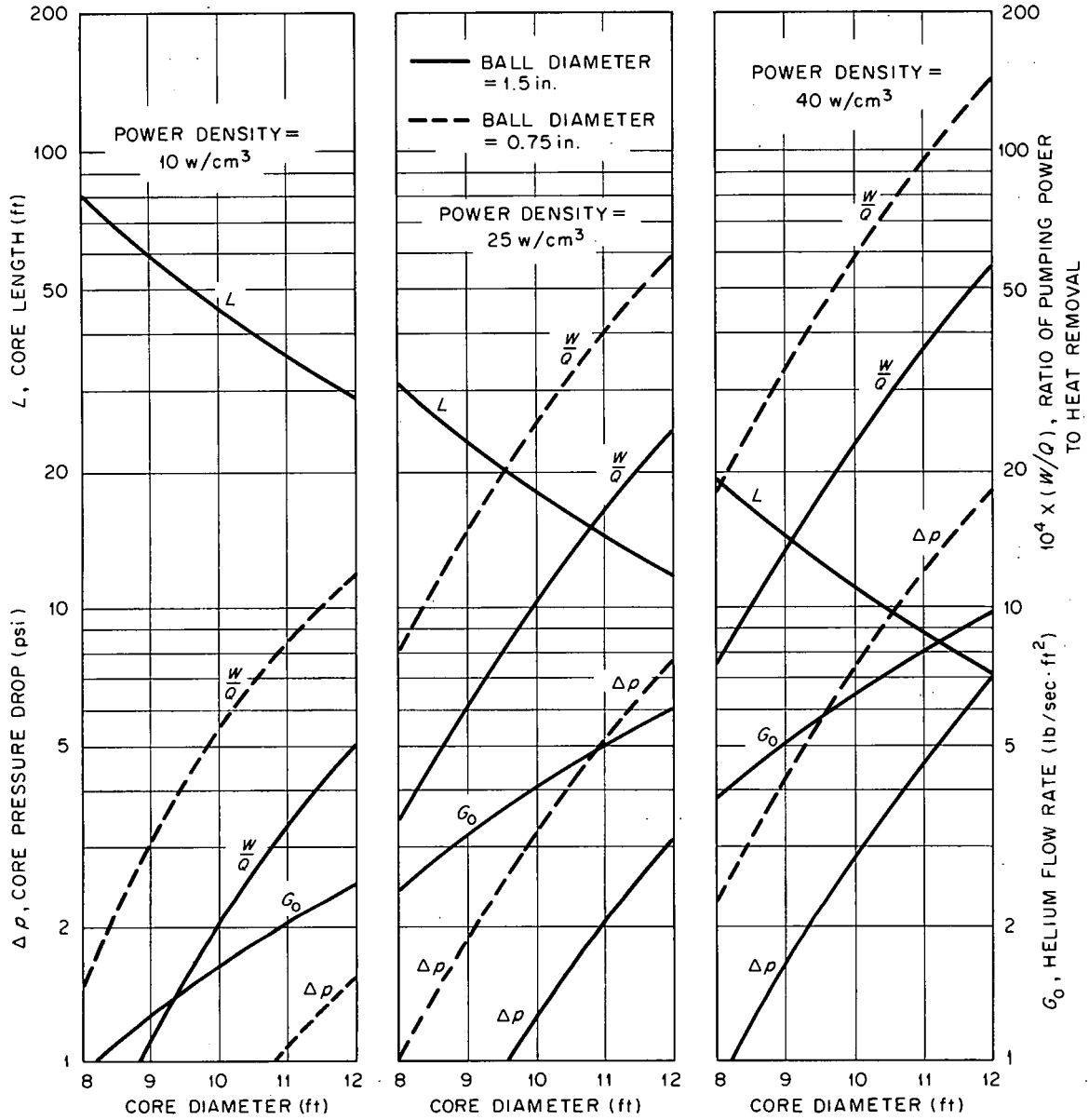


Fig. 2.14. Effects of Power Density, Fuel Sphere Diameter, and Core Outer Diameter on Core Pressure Drop, Core Length, Helium Flow Rate at the Core Inlet Face, and Ratio of Pumping Power to Heat Removal for Radial Outflow Cores Having an Inner Diameter of 4 ft, a Power Output of 850 Mw, and Inlet Temperature Rise of 700°F.

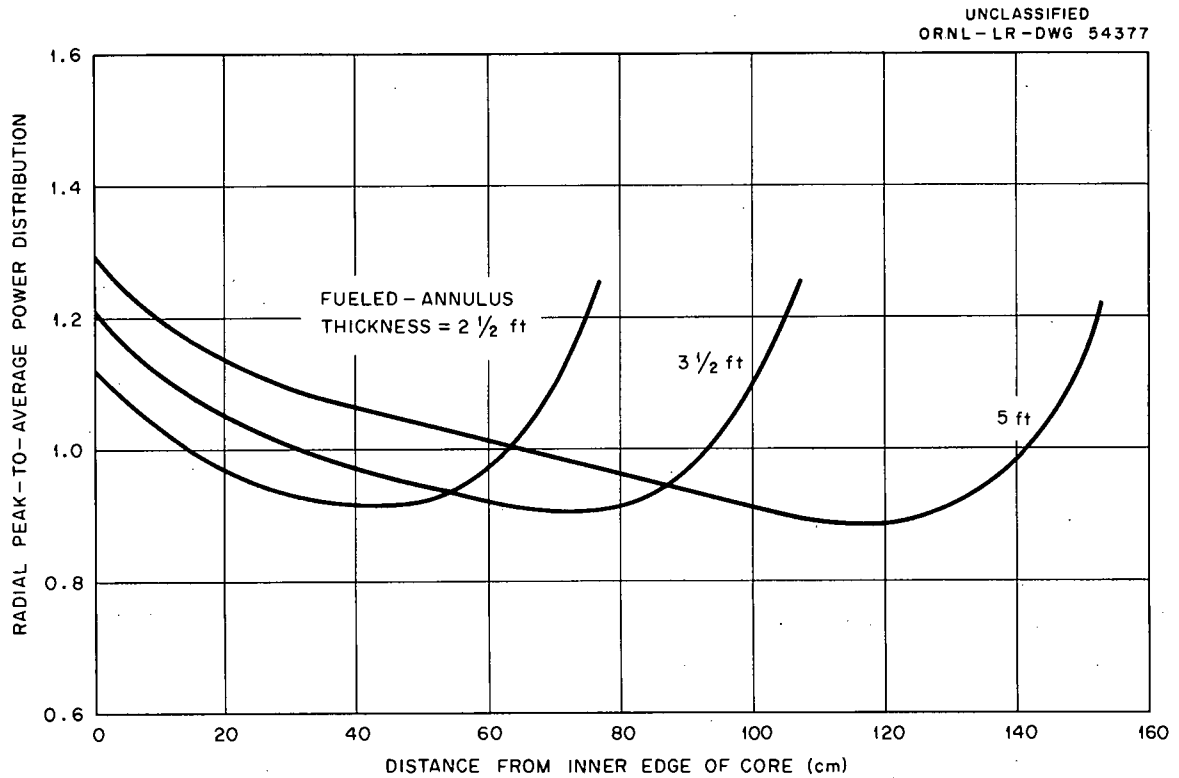


Fig. 2.15. Radial Power Distribution in a Radial Flow Core Having a 4-ft-diam Central Hole and a 3-ft-Thick Reflector.

so the temperature differences between the fuel surface and the gas in the region of the core periphery might well be several times the average difference. With local peak gas temperatures in the range of 1500 to 1800°F; fuel surface temperatures in excess of 2500°F are to be expected. In other words, a mismatch of gas flow and power density as severe as would occur with the power distribution shown in Fig. 2.15 could not be tolerated.

The power density at the perimeter can be reduced by using a thorium blanket in place of a thick reflector. The power distribution shown in Fig. 2.16 was calculated for the same core sizes as used for Fig. 2.15, but the first foot of the reflector was loaded with 10% by weight of thorium oxide. For the largest core ($D_c = 14$ ft), the power density at the core periphery is only 0.7 of the average, but even in this case the temperature difference between the gas and fuel surface at the periphery was estimated to be 1.5 times the average. Conical ends can be used on the core to increase the radial gas velocity near the perimeter and thus relieve these excessive fuel temperatures somewhat. The effectiveness of changing the core shape in this manner can be estimated only by extensive calculations, but the prospects do not appear to be good except for a core having a length-to-diameter ratio less than unity, because making the ends conical would have little effect on the flow at the center for the longer cores.

Another disadvantage of the radial flow concept is inherent in the movement of both the control rods and the fuel at right angles to the gas flow. Operation at power with partial control rod insertion depresses the power density all across the top of the core, with the result that the gas passing through the upper region experiences a smaller temperature rise than the average for the core. In a similar manner, cold gas will bypass through the spent fuel near the bottom. Consequently, the gas in the central region must reach substantially higher temperatures in order to give the desired mixed mean gas outlet temperature, and excessive gas and fuel temperatures are likely to occur in the central part of the reactor. Thus it appears that the

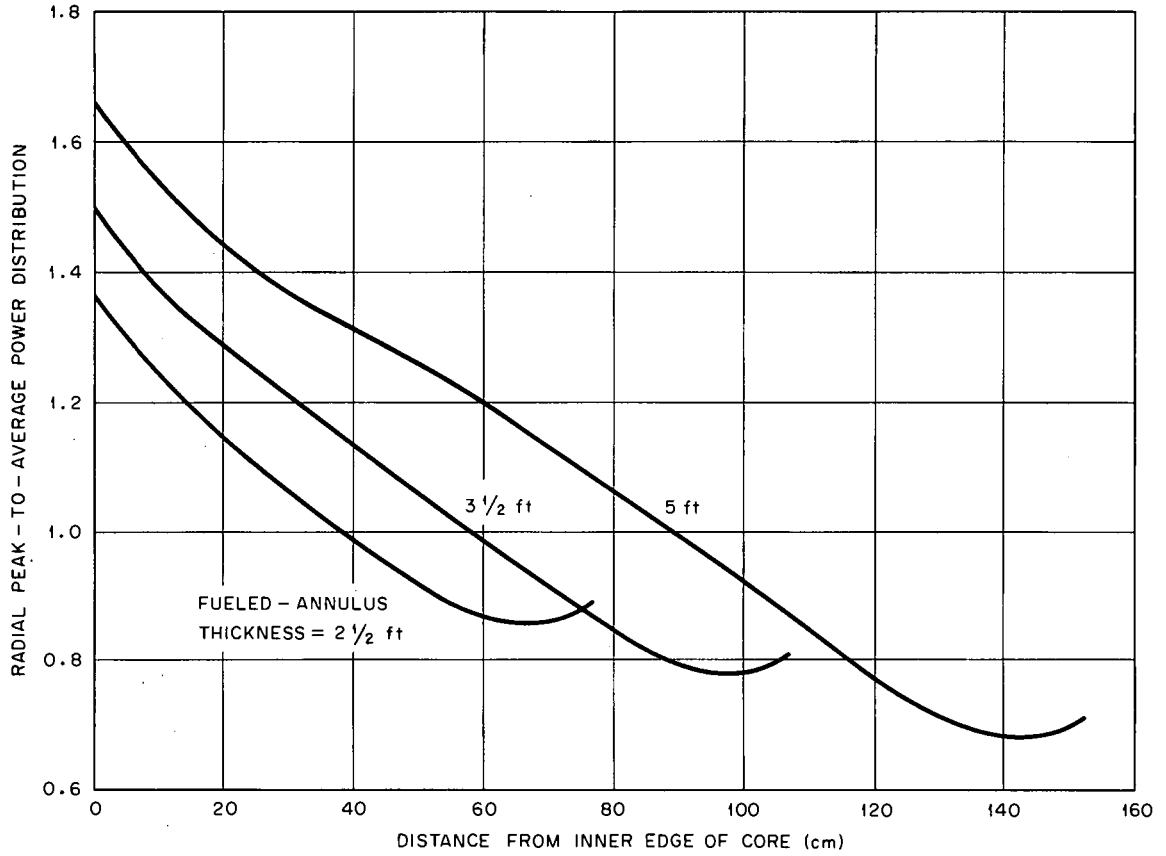


Fig. 2.16. Radial Power Distribution in a Radial Flow Core Having a 4-ft-diam Central Hole, a 1-ft-Thick Blanket Containing 10 wt % ThO₂, and a 2 1/2-ft-Thick Graphite Reflector.

matching of the gas flow to the power distribution will be much less favorable than for axial flow cores.

The graphite structure for the radial flow core is complicated by the necessity for gas passages through the inner and outer circumferential boundaries. Probably the best arrangement evolved is that shown in Fig. 2.12, which utilizes the control rod guide tubes as a bar-grid at the core inlet surface. The neutron economy is not sensitive to the material of the outer grid, since it is outside the thorium blanket. In Fig. 2.12 the outer grid is shown as built up of graphite to avoid the use of steel structure in the highest gas-temperature zone.

The high axial velocity in the central hole of radial flow cores may lead to poor flow distribution and substantial core inlet pressure losses, but time did not permit a careful examination of these problems.

An undesirable characteristic of the radial flow core from the physics standpoint is that the large void at the center leads to severe neutron leakage losses. Preliminary estimates indicate that the core conversion ratio would be only about 0.40 for a 14-ft-o.d. core. This corresponds roughly to the 9.7-ft-diam, 40% void fraction core shown in Fig. 2.2, which indicates that the fuel cycle costs would be so large as to make the radial flow core quite unattractive.

In reviewing the above it appears that poorer neutron economy and higher fuel cycle costs coupled with the more complex fluid flow and construction problems and inherently poor matching of the gas flow to the power distribution make the radial flow core less attractive than the large axial flow core.

Hot Spot Estimates

The hot spot problem for the 20.7-ft-diam, 800-Mw reference design reactor was examined for peak-to-average power density ratios of 1.5 and 2.0 using the method described in the PBRE study.³ The significant temperatures and temperature differences are shown in Table 2.1 and may be compared directly with the corresponding values for the PBRE (Table 10.1 of ref. 3).

Table 2.1. Factors in a Simplified Hot Spot Temperature Estimate

Core diameter = 20.7 ft
 Fuel ball diameter = 2.5 in.
 Reactor power = 800 Mw
 Helium inlet temperature = 550°F
 Helium outlet temperature = 1350°F

	Temperature (°F) Based on Peak-to-Average Power Density of 2.0 in Hot Zone	Temperature (°F) Based on Peak-to-Average Power Density of 1.5 in Hot Zone
Average film temperature drop for entire core	126	126
Average film temperature drop for hot zone	250	190
Film drop in wake of a closely packed cluster in hot zone	550	415
Temperature drop within an average ball uniformly cooled (average power density assumed)	235	235
Same as above except for peak power density in hot zone	470	350
Average gas temperature in hot zone	1100	1100
Peak gas temperature in hot cluster	1400	1400
Hot-ball surface temperature	1950	1815
Hot-ball internal temperature	2420	2165

2.34

The gas and ball-surface temperatures are essentially the same for the PBR and PBRE designs, but the internal ball temperatures differ markedly for the same power-density ratios. The average gas temperature in the hot zone is about 70°F higher for the large reactor because an outlet gas temperature of 1350°F was chosen rather than 1250°F, but the higher central ball temperatures result mainly from using a fuel thermal conductivity of 8 Btu/hr·ft²·°F/ft instead of the value of 15 Btu/hr·ft²·°F/ft assumed in the PBRE study. The lower value was chosen after recent discussions with Dragon project personnel indicated that the conductivity of fueled graphite after severe irradiation may be only 7 or 8 Btu/hr·ft²·°F/ft.

In Table 2.1 the estimated temperature drop within the fuel has not been adjusted upward for irregularities in heat transfer coefficient over the ball surface, as was done for the PBRE design, because a recent analysis has shown that the ball central temperature is not much affected by surface temperature irregularities (see Chapter 7).

Credit was not taken in Table 2.1 for the temperature flattening resulting from gas radial mixing, but this will probably be small at the center of the core. On the other hand, no allowance was made for radial mismatch of flow and power density.

Calculation of the actual peak-to-average power density ratio for this reactor requires a detailed investigation of the effect on the flux profile of partial control-rod insertion and of progressive fuel burnup toward the core bottom. These calculations could not be made for the present study, but it became apparent that the ratio would be between a value of 1.5 for the most optimistic case (no control rod insertion and uniform fuel burnup) and the value of 2.0, which was calculated for the PBRE. The hot-spot analysis was therefore carried out for both cases, as shown in Table 2.1, to show the ranges within which the various temperatures and temperature drops would lie. The peak fuel temperature will not be less than about 2150 to 2200°F, and if it should actually turn out to be close to 2400°F, the use of alumina-coated UO₂ fuel particles in the graphite matrix is precluded

because of the reaction of alumina with graphite to form aluminum carbide. Uranium carbide particles pyrolytically coated with carbon should withstand temperatures higher than 2500°F, and, if used, should relieve the hot-spot problem.

Comparison of Design Problems of Spherical and Prismatic Fuel Element Reactors

The numerous complex relations set forth earlier in this section indicate the many limitations imposed on the designer of a pebble-bed reactor. It is important to recognize that these restraints are more restrictive than is the case for similar reactors employing tubular or prismatic fuel elements of the same basic material. In such reactors the fuel elements might be in the form of rods, tubes, plates, axially finned tubes, or the like. In any case, the designer has the option of varying the effective flow passage diameter and the fuel element thickness independently so that the fuel element can be proportioned to give the desired heat transfer characteristics both internally and externally. Further, the tubular or prismatic fuel elements give an aerodynamically cleaner configuration and hence much lower pumping power losses for a given core size. As an illustration, a series of tubular fuel element cores was compared with a similar series of pebble-bed reactors for core diameters in the range from 10 to 35 ft. Figure 2.17 shows the effects of core diameter on the ratio of pumping power to heat removal, the fuel element thermal stress, and the fuel element internal temperature drop. In each case the reactor length was determined first for the pebble-bed reactor, and the tubular fuel element core was made to have the same length. Note the markedly lower pumping power, thermal stress, and internal temperature for the tubular fuel elements at any given core diameter.

The prismatic or tubular fuel element core has the advantage that it permits reducing the void fraction to 0.14 or 0.25 to yield an important improvement in the conversion ratio and a reduction in the

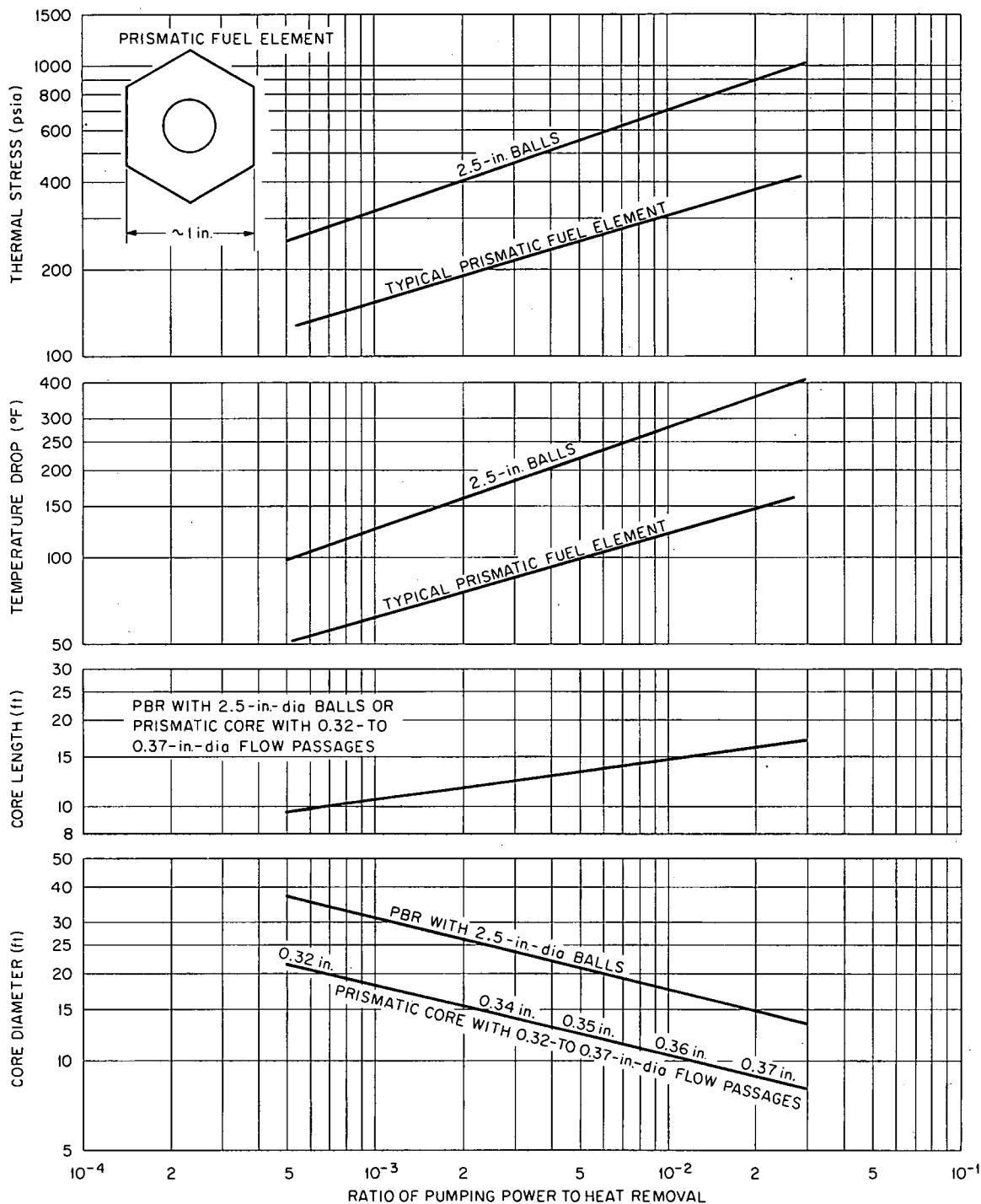


Fig. 2.17. Comparison of Core Diameters, Thermal Stresses, Internal Temperature Drops, and Pumping Power Requirements for Spherical and Tubular Graphite-Uranium Carbide Fuel Elements Using the Void Fraction, Core Length, and Cooling-Gas Temperature Conditions Best Suited to an Axial Upflow Core.

fuel cycle costs. The savings indicated by Fig. 2.2 are more than enough to justify the capital charges for a quite elaborate fuel-handling machine.

An additional advantage offered by a prismatic or tubular fuel element core is that the flow distribution across the inlet face can be varied by orificing the core inlet or outlet or by varying the diameter of the coolant flow passages through the fuel elements. In either case, better matching of the coolant flow to the power-density distribution can be obtained than would be possible in a pebble-bed core, so the peak fuel element surface temperature should be substantially lower for a given core outlet gas temperature. Further, a thorium blanket could be employed to reduce neutron leakage losses while still maintaining a good match of power density and gas flow.

If, as seems likely from the limited data available, the inner layers of the reflector will have to be replaced from time to time because of graphite shrinkage cracking, a service machine will be required for a pebble-bed reactor. Preliminary studies indicate that such a machine has much in common with a fuel-handling machine suitable for prismatic or tubular fuel elements.

3. REACTOR DESIGN

The major features and principal dimensions of the reactor are, as established in the preceding chapter, a 20.5-ft-diam, 12.4-ft-high, upflow core, with a 3-ft-thick reflector and a spherical pressure vessel. Many of the more important details are shown in the layout of Fig. 3.1, and some of the design problems are discussed in the following paragraphs.

The reactor is enclosed within a 32-ft-diam, 4-in.-thick, pressure vessel of type SA-212, grade B, carbon steel. Two separate steam generators and two blowers are provided as indicated. The control rods are uniformly distributed through the core and are actuated by drive units at the top. Seven large access tubes at the base are provided for servicing and fuel removal. The precepts from which this design was evolved are presented in the report on the PBRE.¹

Graphite Structure

The graphite reflector provided over the top and bottom of the core, as well as around the sides, to protect the pressure vessel from fast-neutron damage is 3 ft thick. The outer 2 in. of this graphite is borated to inhibit gamma heating in the pressure vessel and ease the shielding problem, particularly in the vicinity of ducts where thermal neutrons and gamma-ray streaming would present serious problems.

As was the case for the PBRE, graphite-shrinkage cracking considerations strongly influenced the design of the reactor. A 1-ft-thick layer of unfueled graphite balls is provided around the outer perimeter of the core to protect the graphite blocks in that region sufficiently so that they will not require replacement. A similar arrangement might be used for the top and bottom reflectors if the entire core were loaded and discharged in a single batch. Since one

¹"Preliminary Design of a 10-Mw(t) Pebble-Bed Reactor Experiment," ORNL CF-60-10-36, November 1, 1960, chaps. 3 and 4.

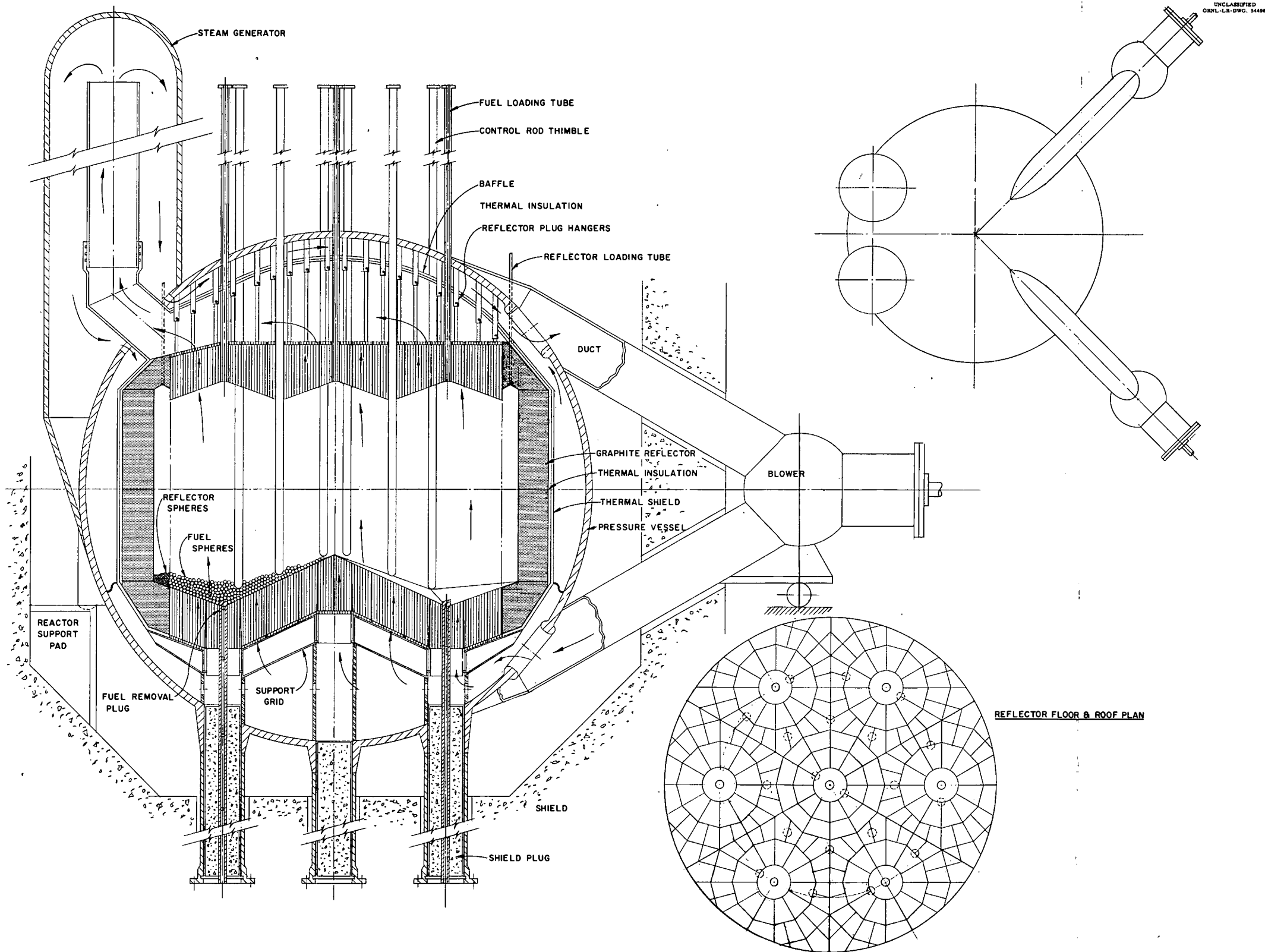


Fig. 3.1. Pebble-Bed Reactor.

of the objectives of the design is to permit refueling in small increments, this arrangement is not feasible. Several designs for the graphite structure at the top and bottom of the core were considered. The most promising of these appeared to be one using closely packed cylindrical graphite rods with their axes parallel to that of the core. The close-packed spacing provides a flow passage area for gas to enter and leave the core that is equal to approximately 9% of the gross face area of the core. By making use of relatively small-diameter rods, perhaps 2 in., it appears that the stresses in the rods set up by variations in shrinkage from the tip to the base can be kept sufficiently low so that the rods should have a life of at least six years. The shrinkage problem can be alleviated by boring a tapered hole into the core face end of each rod. Further analysis will be required to determine the extent to which this hole can be shaped to reduce the shrinkage stresses, but it is possible that the stresses can be kept to low values.

The structure contemplated to support the rods in the top and bottom reflectors consists of steel grids to which the graphite rods would be attached by threaded studs. Figure 3.2 shows a sketch of the proposed design.

The rod clusters would be made in sizes and shapes such that they could be removed through a 28-in.-diam servicing-access tube. The pattern contemplated is shown in the section at the lower right of Fig. 3.1. A rod cluster in the lower reflector would be replaced by extending arms radially from the service ram into the grid at the base. The cluster would then be raised to lift it from its socket in the reactor support grid, moved radially inward over the ram, and then withdrawn through the service tube. Somewhat similar operations would be carried out for removal of the graphite in the top reflector. In the layout this graphite is shown suspended by hangers attached to sockets suspended from the top of the pressure vessel. The attachment envisioned would be effected by inserting the rod cluster into position, inserting the hanger rod into its socket at the top, and then rotating the hanger rod to lock it in place with a bayonet joint.

Unclassified
ORNL-LR-DWG
54495

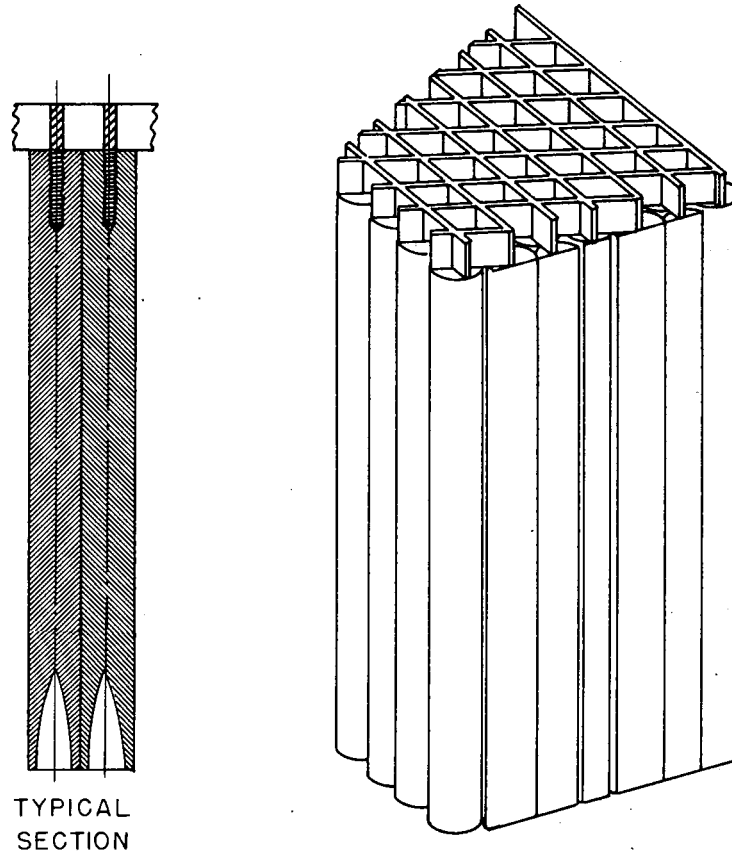


Fig. 3.2. Arrangement of Graphite Reflector Floor and Roof Plug.

Steel Support Structure

The reactor assembly has been designed to be supported at three points, one between the two steam generators and two under the blowers, all three being in the same horizontal plane. The supports at the blowers will be on rollers to provide for thermal expansion without the use of bellows in the ducts. The blowers are fairly well isolated from the core by shielding. The line-of-sight paths from the core into the blower cell pass through the 3-ft-thick reflector, a 1-in.-thick skirt, and the 4-in.-thick pressure vessel, and the radiation must penetrate the 2-in.-thick ducts twice, both times obliquely. Eight hours after shutdown, this gives a gamma dose from the core of roughly 50 mr/hr at the blowers, which is an acceptable value.

The reactor core support grid is divided into seven segments, each of which is supported independently by one of the access tubes at the base of the reactor. The weight load introduced into the pressure vessel in this fashion is less than 0.5% of the pressure load, so the consequent bending stresses in the pressure vessel should not be serious. If they should prove to be appreciable, they could be relieved by modifying the pressure vessel shape so that it would be slightly ellipsoidal, rather than spherical. The support grid, access tubes, and pressure vessel will all be at the reactor inlet gas temperature.

The steel skirt around the outer perimeter of the reflector and the liner over the hot gas plenum at the top of the core are isolated from the hot region by a 2-in.-thick layer of thermal insulation and are cooled either by gas returning from the steam generators to the blowers or by gas being discharged from the blowers into the core inlet plenum region. Similarly, a liner in each of the steam generators isolates the steam generator vessel wall from the hot gas region, and cool gas from the core inlet plenum circulates vertically upward through the space between this liner and the vessel. The heat added to this gas is less than 0.01% of the total power generated. In fact, the temperature losses through 4 in. of thermal insulation on the shell

exterior are roughly equal to the heat flowing through the 2 in. of thermal insulation to the steam generator vessel liner, so the temperature rise in the cooling gas for the pressure vessel wall will be much less than 50°F. Forced circulation of gas between the liner and the pressure vessel is believed essential, however, to insure that the entire pressure envelope will be held at a uniform temperature so that thermal stresses in the pressure envelope will be negligible.

The gas in the core inlet plenum is isolated from the gas returning from the steam generator by a diaphragm between the outer perimeter of the core support structure and the pressure vessel. Differential thermal expansion should not be a problem, but the diaphragm should be made sufficiently flexible to accommodate distortion in the support structure under changes in the weight load from the core-empty to the core-full condition.

The penetrations in the main pressure vessel for the blower ducts pose a gas-flow problem because of the limited space available. The gap between the rounded flow nozzle inlet for these penetrations and the vessel liner was made equal to one-quarter of the inside diameter of the nozzle, so the flow passage area at no point is less than the area of the hole in the pressure vessel. The pressure loss associated with this arrangement should not be more than one-half of a dynamic head, since the change in flow passage area is not great for the duct leading to the blower. For the return gas flow, the arrangement can be made to approximate a flat-plate diffuser.

As in the PBRE design,¹ means would be provided for hydraulically isolating the blowers from the reactor to permit decontaminating them prior to servicing. Inflatable rubber bladders seem to be the most promising arrangement for effecting this hydraulic isolation. Several other ducting configurations were considered but were rejected because of factors such as interference with access tubes at either the top or the bottom of the reactor.

Ball Flow

The large-diameter core poses serious design problems in making provisions for fuel handling. In order to obtain a reasonably uniform ball flow distribution across the core, it seems to be necessary to make use of at least six ball inlet and discharge positions, and a substantial slope toward one or another of these positions must be provided over the entire top and bottom faces of the core. If this is not done, there might be local relatively "dead" zones where fuel balls might dwell for excessive periods. Concern for this latter factor led to the use of control rod tubes which do not extend to the face of the bottom reflector, since otherwise the balls might lodge at the base of one of the tubes instead of flowing as desired.

Control Rods

Twenty-two 8-in.-diam access tubes are provided at the top of the reactor for control rods. Graphite tubes, 6 in. in diameter and $3/4$ in. thick, are inserted into the core through these access tubes to provide passages in the pebble bed for the control rods. The control rods will consist of stainless steel tubes containing boron carbide and will be operated by control rod drives similar to those planned for the EGCR. It is expected that these graphite tubes for the control rods will require replacement every few years because of graphite shrinkage cracking.

Steam Generators

The steam generators are placed close together to minimize bending moments in the pressure vessel and possible buckling of the pressure vessel wall under seismic loads. A single steam generator would be preferable from the support standpoint, but two vessels are used to facilitate identification of a steam leak. Further, two smaller vessels may make it possible to fabricate the steam generators in the shop and ship them as units for installation at the site, since the weight of each should be less than 200 tons.

4. PLANT LAYOUT

The design for a modern high-temperature steam power plant now under construction was adapted for use with the pebble-bed reactor in order to facilitate the design and to make comparisons with coal-fired plants as direct as possible. Modifications were made in the flow sheet to accommodate the blower drive turbines, and the feedwater heating system was modified to give a feedwater inlet temperature well matched to the reactor cooling-gas temperatures.

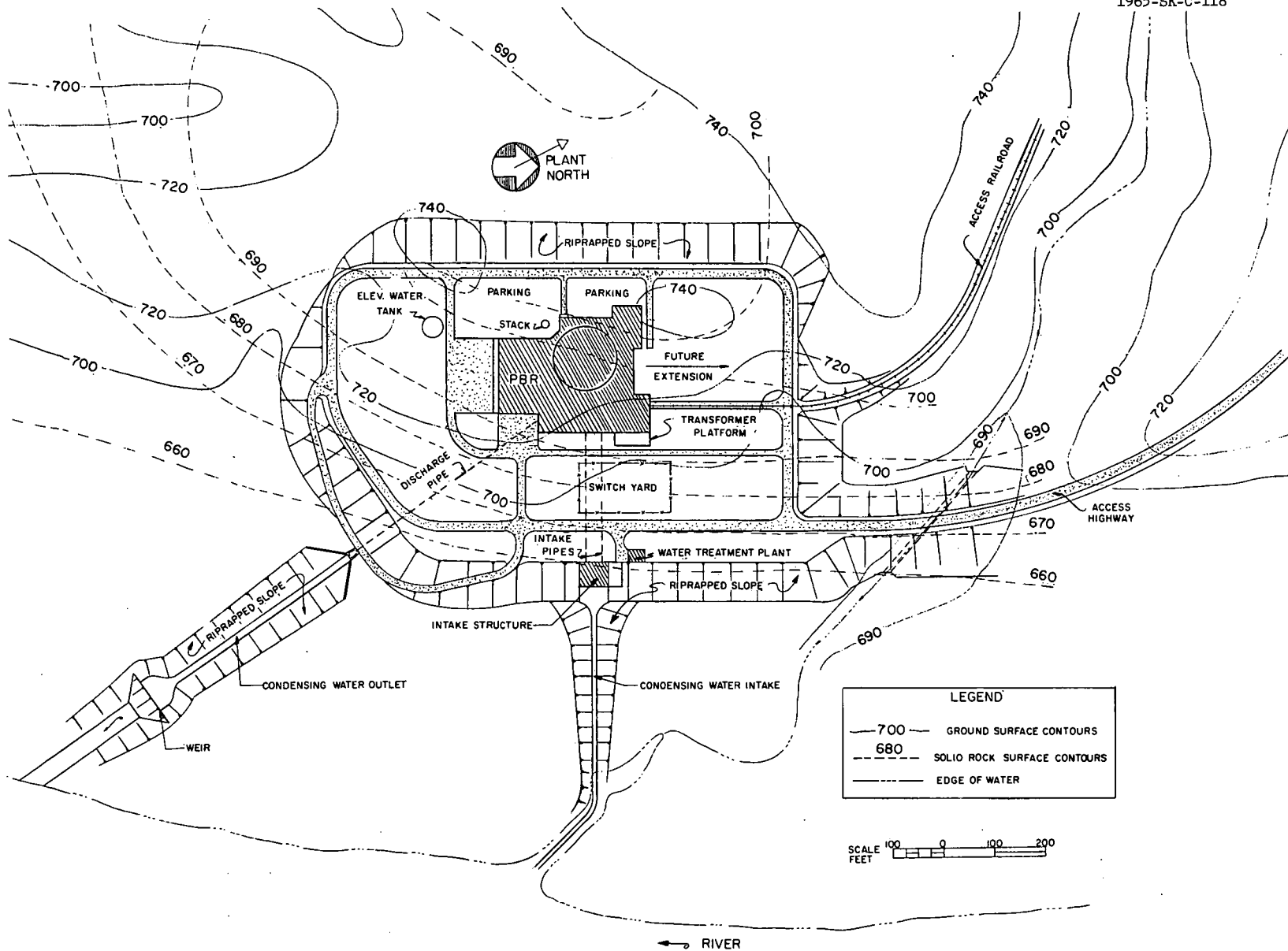
Site

For convenience, the Yellow Creek site used in the GCR-2 study¹ of 1958 was chosen for design purposes. At the site, loose soil (clay, sand, silt, and gravel) covers an irregular layer of weathered limestone up to 7 ft thick, which, in turn, covers a sound formation of thin-bedded, fissile, varicolored shale. This sound shale is found at an elevation of approximately 680 ft on the river side of the powerhouse and at an elevation of 710 ft on the west side of the service bay.

The elevation of the river can be expected to fluctuate between a minimum level of 675 ft and a maximum probable flood (regulated) of 718 ft. The normal fluctuation is much less than this. The general topography of the site is indicated by the contour lines on the general plan, Fig. 4.1.

Representative river temperatures are: maximum, 84°F; minimum, 41°F; and average, 62°F. The flow averages approximately 23 000 ft³/sec, and the minimum flow can be regulated, as required, from a dam that is situated one mile upstream. Prevailing winds are from the southwest, and representative ambient air temperatures are: maximum, 103°F; minimum, 10°F; average, 60°F.

¹"The ORNL Gas-Cooled Reactor," ORNL-2500, April 1, 1958.



4.2

Fig. 4.1. Plot Plan for Pebble-Bed Reactor.

The site is sufficiently remote from heavily populated areas to be acceptable, and yet it is well located at a central point in the TVA grid, particularly with reference to Alcoa and Oak Ridge. The nearest incorporated towns are approximately 23 miles distant, and the load centers are about 40 to 60 miles from the plant site.

Design Data

The principal performance and dimensional data for the plant are presented below:

Power Generation

Thermal output, Btu/hr	2.73×10^9
Thermal output, Mw	800
Gross electrical output, Mw	347
Net electrical output, Mw	330
Gross thermal efficiency, %	42.7
Net thermal efficiency, %	40.6

Fuel Elements

Sphere diameter, in.	2.5
Maximum thermal stress (for ideal rigid body), psi	1300
Sphere surface, ft^2/ft^3 of fuel	28.7
Sphere surface, ft^2/ft^3 of core (39% voidage)	17.5
Number of spheres per ft^3 of core	129
Average power density in fuel, w/cm^3	10.7
Average surface heat flux, $\text{Btu}/\text{hr}\cdot\text{ft}^2$	35 800
Graphite thermal conductivity, $\text{Btu}/\text{hr}\cdot\text{ft}^2$ ($^\circ\text{F}/\text{ft}$)	8
Maximum fuel surface temperature, $^\circ\text{F}$	2000
Maximum fuel internal temperature, $^\circ\text{F}$	2200
Fractional fission-product release rate (R/B)	10^{-4} to 10^{-5}

Reactor

Core	Cylindrical, axial upflow
Core diameter, ft	20.7
Core height, ft	12.4
Core inlet face area, ft^2	336
Core average power density, w/cm^3	6.6
Reflector	1 1/4 in. of graphite balls plus fixed graphite

4.4

Total reflector thickness, ft	3.0
Core fuel feed positions	One in center, six on 7.3-ft-radius circle
Reflector feed positions	Twelve on 10.8-ft-radius circle
Fuel removal positions	Six on 7.3-ft-radius circle
Diameter of core plus reflector, ft	26.7
Core density, g/cm ³	1.0
Machined weight of fixed graphite, tons	288
Weight of unfueled graphite balls, tons	27
Weight of fueled graphite balls, tons	134
<u>Pressure Vessel</u>	
Shape	Sphere
Outside diameter, ft	32.1
Inside diameter, ft	31.4
Thickness, in.	4.0
Material	Type SA-212, grade B, carbon steel
Working pressure, psia	700
Design stress, psi	16 600
Maximum temperature, °F	600
Volume, ft ³	31 000
Gross vessel weight, including core supports, thermal barriers, nozzles, and insulation, lb	~500 000
<u>Coolant System Characteristics</u>	
Gas	Helium
Working pressure, psia	700
Flow through core, lb/sec	763
Flow to steam generators, lb/sec	868*
Reactor inlet temperature, °F	550
Reactor outlet temperature above core, °F	1350
Mixed mean gas temperature to steam generator, °F	1250
Number of inlet pipes	2
Number of outlet pipes	2
Cool pipe inside diameter, ft	3.5
Mean coolant velocity in cool pipe, ft/sec	194
Diameter of ports to blower ducts, ft	3.0
Mean coolant velocity in ports, ft/sec	255
Diameter of hot gas port to steam generator, ft	3.25
Mean coolant velocity in hot gas port, ft/sec	337
Total volume occupied by coolant, ft ³	30 000

*The bypass flow through the unfueled ball layer lining the reflector is about 14% of the flow through the core.

Circuit pressure drop, psi	12.0
Pressure drop through core only, psi	3.8
Specific heat of coolant, Btu/lb.°F	1.24
System pressure losses in terms of ratio of pumping power to heat removal	
Core	0.003
Ducts	0.003
Steam generator	<u>0.004</u>
Total	0.010

Coolant Blowers

Number	2
Type	Single-stage, centrifugal
Blower drives	Steam turbines
Compression power, Bhp	5400
Adiabatic efficiency, %	70
Turbine power, Bhp	7700

Steam Generator

Type of generator	Once-through
Number of generators	2
Shell height between heads, ft	60
Shell height including heads, ft	75
Shell outside diameter, ft	8.5
Shell thickness, in.	~2.25
Gas inlet inside diameter, ft	3
Steam pressure, psi	2450
Steam pressure at throttle, psi	2400
Steam temperature at high-pressure stage, °F	1050
Reheat temperature, °F	1000

General Layout

The general layout of the plant is shown in Figs. 4.2 and 4.3. The largest and most important element of the system, the reactor building, is located at the center. The other facilities are located for convenience relative to the reactor and to each other.

The turbine generator unit is located immediately adjacent to the reactor building in order to minimize the lengths of steam piping required, particularly for the reheater. The turbine building is located on the river side of the plant to give a good layout for the condenser

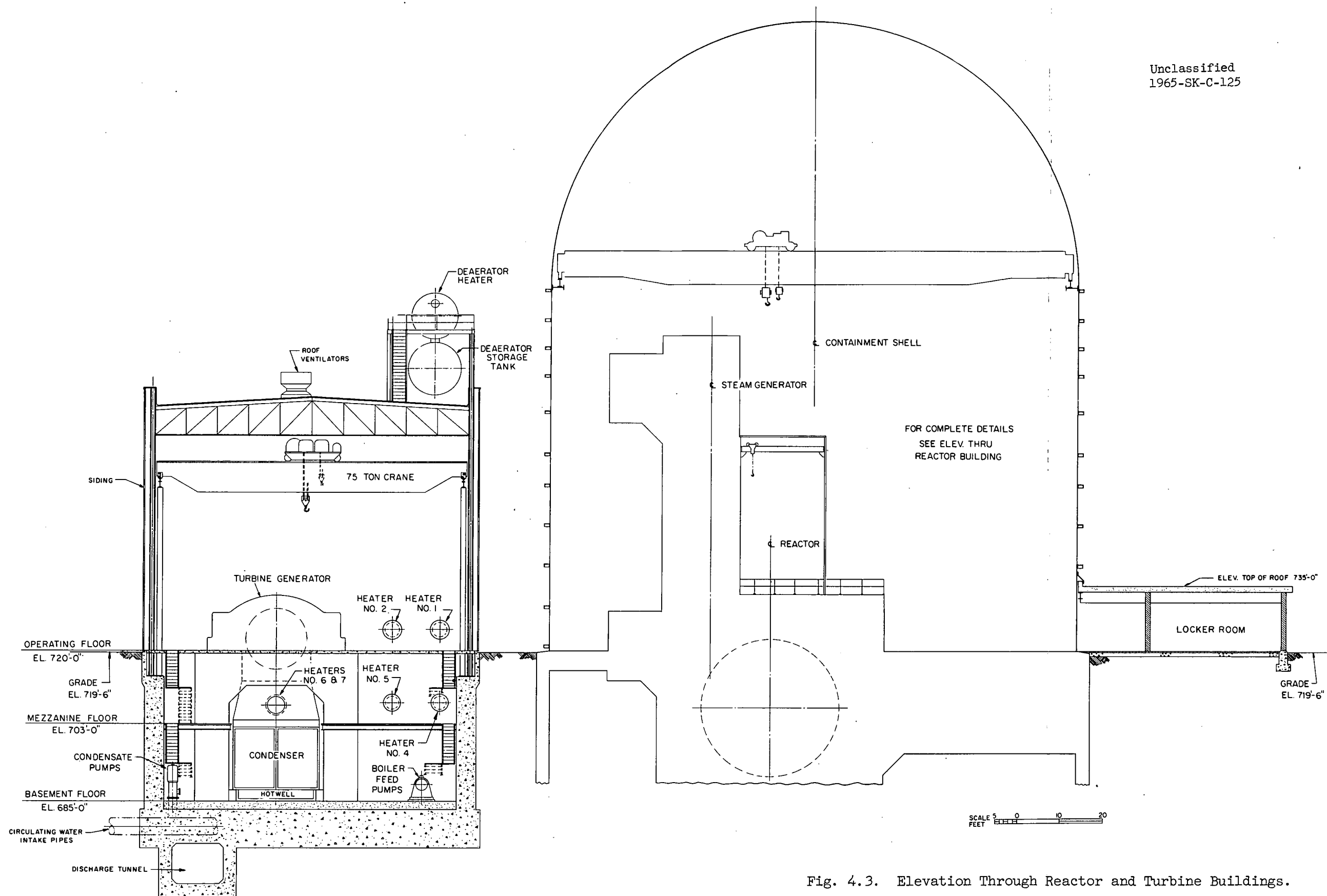


Fig. 4.3. Elevation Through Reactor and Turbine Buildings.

cooling-water system. The feedwater pumps, feedwater heaters, and other components of the steam system are also located in this bay.

The control room is located at the north end of the plant adjacent to the reactor containment shell and the turbine generator bay. This arrangement provides a good view of the turbine generator bay, and minimizes the length of instrumentation lines both to the reactor and to the turbine generator. Offices and other facilities for personnel are located adjacent to the control room or on the floor above it.

The machine shop is located at the south end of the turbine bay. The large equipment lock to the reactor containment shell opens into a reactor service area adjacent to the machine shop. The stack, with its filters and related core equipment, is located to the west of the reactor building.

Reactor Building

The reactor and its associated equipment are enclosed in a pressure-tight containment shell 122 ft in diameter and 221 ft high. A vertical section through this building is shown in Fig. 4.4, and a set of horizontal sections are shown in Figs. 4.5 through 4.8. The layout generally follows that used for the PBRE, with the lower portion modified to reduce the height of the reactor building, as suggested in the PBRE report.² As in the PBRE, to facilitate decontamination, metal-lined rooms enclose all flanged joints for the contaminated-gas-system pressure envelope. These rooms are the blower rooms, the service area below the reactor, the hot-fuel-storage vaults, and the control-rod drive region on top of the reactor.

Helium Storage

The quantity of contaminated helium for which storage capacity must be provided is about 25 times that for the PBRE, so transfer of the major portion of the gas by simple blowdown to intermediate pressures would require excessive storage volumes. Accordingly, the transfer system utilizes a pair of booster compressors (one serving as a spare) that raise the storage pressure to twice the reactor residual pressure

²"Preliminary Design of a 10-Mw(t) Pebble-Bed Reactor Experiment," ORNL CF-60-10-63, November 1, 1960, chap. 21.

Unclassified
1965-SK-C-119

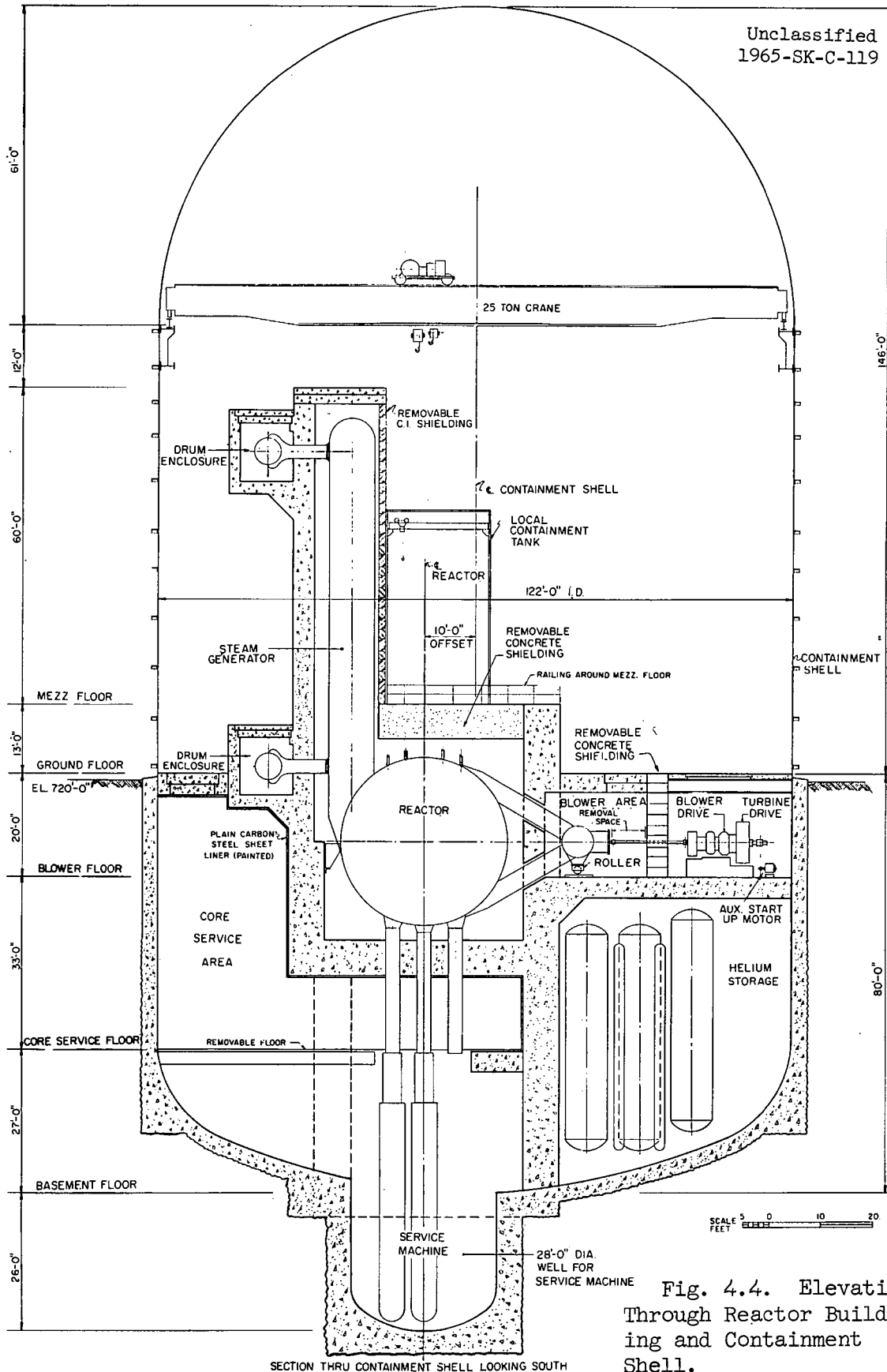


Fig. 4.4. Elevation Through Reactor Building and Containment Shell.

SECTION THRU CONTAINMENT SHELL LOOKING SOUTH

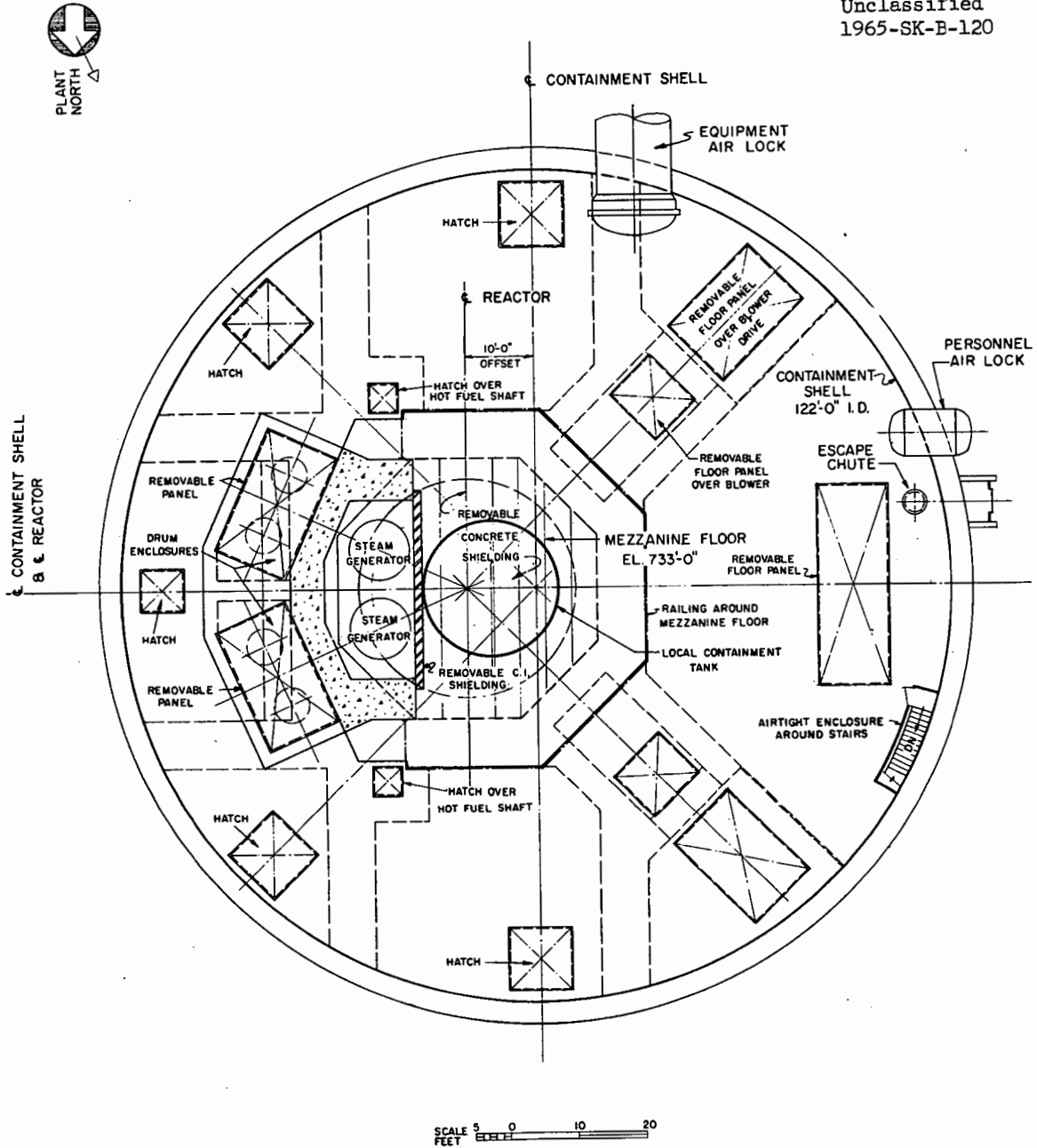
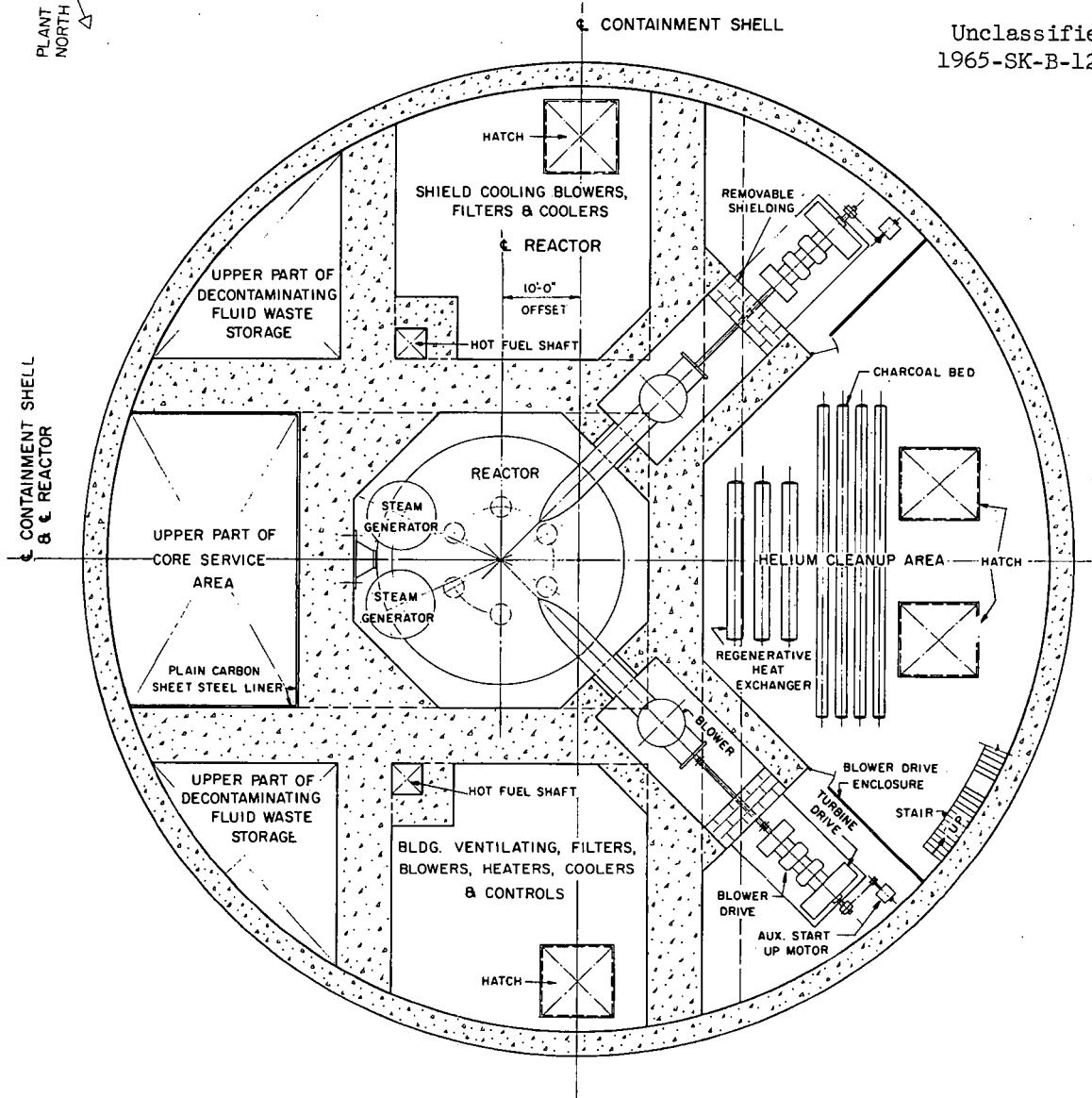


Fig. 4.5. Ground Level Plan of Reactor Building.



Unclassified
1965-SK-B-122



SCALE 5 0 10 20
FEET

Fig. 4.6. Plan View of Blower Floor Level.

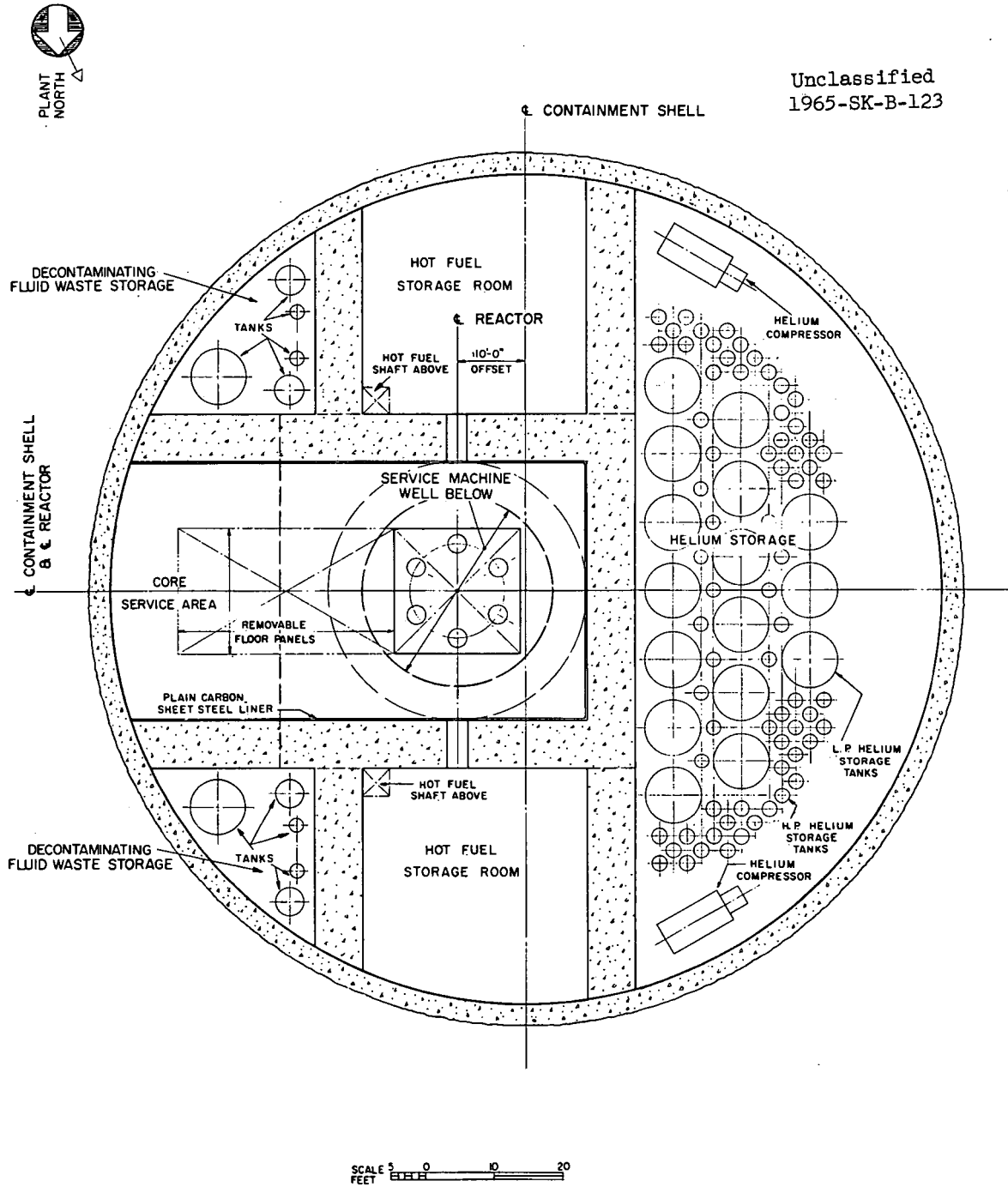
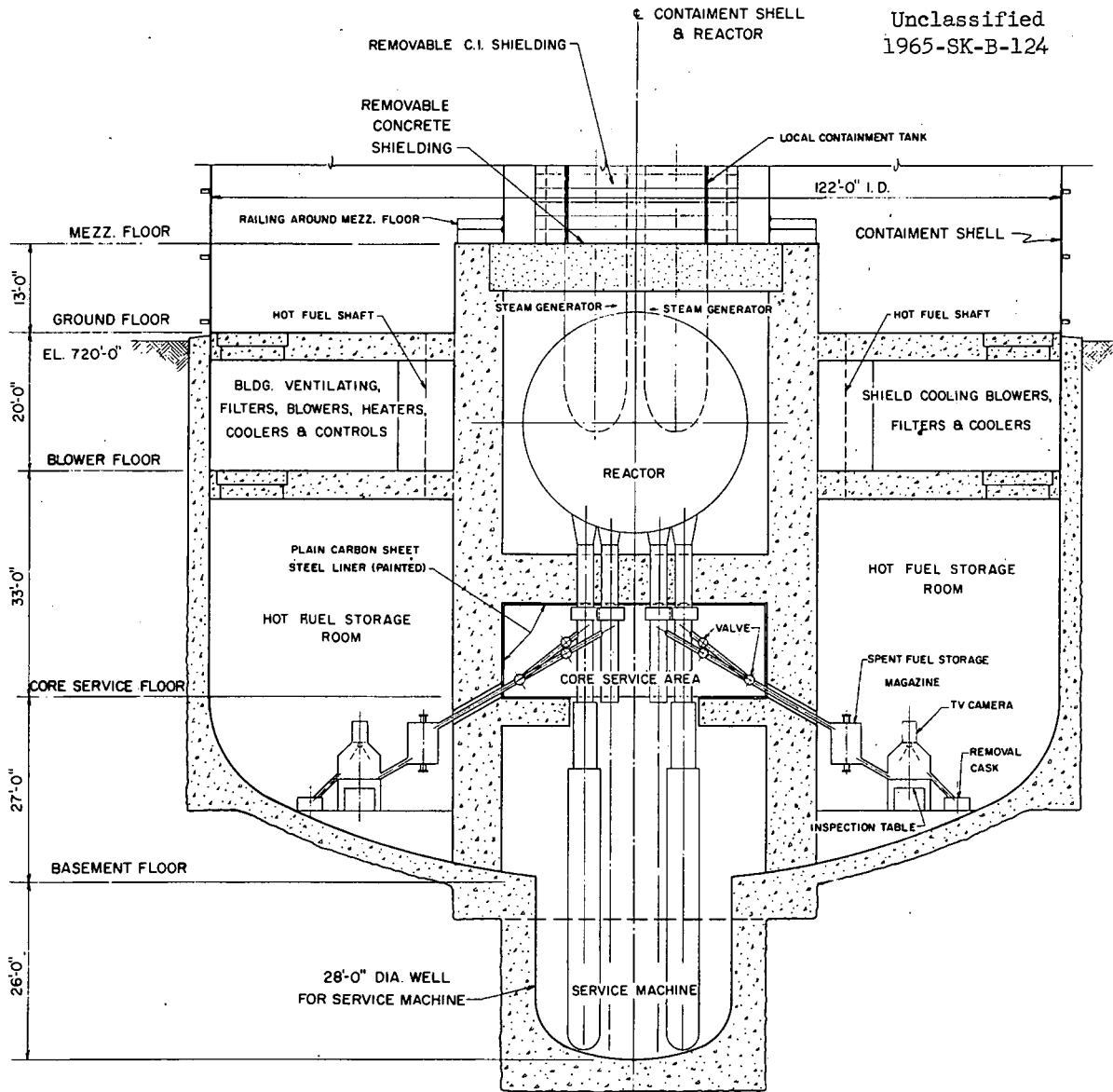


Fig. 4.7. Plan View of Core Service Area.

Unclassified
1965-SK-B-124



PARTIAL SECTION THRU CONTAINMENT SHELL LOOKING EAST

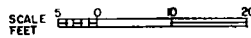


Fig. 4.8. Elevation Through Spent-Fuel Storage Rooms.

at each stage. In this way the storage volume is reduced to about one-half that otherwise required. The gas is stored at 11 different pressures from 1000 psia down to 31 psia, leaving a residual reactor pressure that is slightly above atmospheric. An additional storage capacity of 7500 ft³ is provided for evacuation to well below atmospheric pressure. With 500-hp pumps capable of handling 1000 ft³/min, the total transfer time required to draw the reactor system pressure down to about atmospheric pressure is about 1 hr, which is a reasonably short time for reducing the reactor pressure in the event of a leak.

The same transfer pumps will be used to recharge the reactor system, but the time required will be a little longer. The tanks required for the storage system, the different pressure levels, and the approximate floor area assigned to the storage system in the containment shell are shown in Table 4.1.

Table 4.1. Helium Storage Requirements

Tank Diameter and Length (ft)	Number of Tanks	Floor Area (ft ²)	Storage Pressure (psia)	Storage Volume (ft ³)
2 x 40	70	630	1000	2 500
			700	3 500
			500	2 500
8 x 43	12	1200	350	3 500
			250	2 500
			175	3 500
			125	2 500
			87.5	3 500
			62.5	2 500
			43.8	3 500
31.2	2 500			
8 x 43	4	400	~20	7 500
Total		2200		40 000

Helium Circulation

The flow passage areas in the system are designed to give adequate thermal-convection circulation for removing afterheat in the event of a forced outage of both blowers. Since the blowers are driven by steam generated in the closely coupled reactor and steam generator system, it is believed, however, that the steam-turbine drives give the blowers an exceptionally high degree of reliability.

Servicing Equipment

The servicing area beneath the reactor is intended to serve for the fuel-discharge equipment and maintenance operations inside the reactor pressure vessel, such as replacement of the moderator. Any one of the seven 28-in.-i.d. access tubes at the bottom of the reactor can be served by either of the two ram assemblies mounted on a turntable beneath the service area. These rams are similar to the ram described in the PBRE report.³ Two rams are provided in the full-scale plant to facilitate major servicing operations in the reactor and to provide an arrangement in which one ram can be used to extricate the other if it becomes jammed in the reactor core. A variety of heads for the ram can be stored in the service area. The heads will include one for removing the shield plug from its access tube, special tools for servicing the fuel drain equipment, and special heads for removing the segments of the bottom and top reflector. Two Robots⁴ will operate in the service area to maintain the fuel-drainage equipment, assist in mounting special heads on the rams, move special ram heads from storage to positions over the rams, move casks into position in the vicinity of the rams, and similar operations. The service-machine equipment would normally be operated remotely from the main reactor control room.

³Ibid., chap. 15.

⁴Ibid., Fig. 15.1, chap. 15.

Viewing Provisions

Television cameras attached to periscopes can be inserted into the core through the access tubes provided for the control rods, as well as through those for servicing. These should give an excellent means for viewing a major operation, such as replacement of the graphite reflector.

Most, if not all, maintenance on the service-machine rams and drive assemblies can be carried out in situ using conventional contact-maintenance procedures. In order to facilitate removal of a ram and drive assembly, a small canyon is provided in the bottom of the reactor building at the left of the well for the service machine (see Fig. 4.4). Removal of a ram-drive assembly would require special rigging operations, but clearances are adequate to permit removal through the hatch in the ceiling over the service area to the left of the reactor.

Decontamination

Tanks for storing contaminated fluid used in equipment decontamination operations are located in the lower portion of the reactor building, as shown in Fig. 4.7. In view of the large sizes of the heat exchanger, reactor, and blowers, the tank capacity was based on the premise that decontamination operations would be carried out by spray rather than by bath operations. Six tanks are provided to store various types of decontaminating fluid and wash water. The pumps for handling the decontaminating fluid are located in the room housing the helium-purification equipment.

Ventilating System

The interior of the reactor building is to be maintained slightly below atmospheric pressure by means of a blower that exhausts through filters to the stack. Both the air inlet and the air discharge ports will be sealed automatically in the event of an accident.

The shield is cooled by a recirculating-air system, with filters and a cooler. The same blowers and filters will handle the air from

the service area, the blower vaults, and the enclosure around the control-rod drives so that leakage of contaminated gas will not result in dispersal of activity around the building. A small blower will discharge from this system through filters to the stack to hold the system pressure a few inches of water below the pressure in the rest of the containment shell.

The blower drive turbines are included within the gas-tight enclosure surrounding the blowers to avoid a seal on the quill shaft between the blower and the drive turbine. However, shielding is provided between the blower and turbine so that the radiation dose level at the turbine will be below 6 mr/hr at all times.

5. REACTOR PHYSICS

Three basic core arrangements were considered in this study. A few summary comments are made below concerning the first two of these, and the results of a somewhat more detailed study of the third are presented.

The reactor designed for radial gas flow is characterized by a large central channel for the inlet gas stream, surrounded by an annular core region. Radial power distributions in cores of various annular thicknesses are given in Chapter 2 for the case in which the core is surrounded by a graphite reflector (Fig. 2.15) and for the case in which the core is surrounded by a thorium-graphite blanket (Fig. 2.16). The reactor with the thorium-graphite blanket is preferable to the one with a pure graphite reflector because of the better matching of power generation distribution with gas velocity distribution. It would be desirable to locate the control devices for this reactor at the interface between the central gas passage and the core annulus. In this position the control rods would not create hot spots by perturbing the gas flow patterns as they would if located within the core. The results of calculations which show the total amount of control which might be obtained in this manner are presented in Fig. 5.1. The calculations were based on a complete annulus of B_4C , and the flux depression resulting from streaming down the central gas passage was neglected. The effect of each of these approximations is to overestimate the available control. The indication from Fig. 5.1 is that a core no larger than 3 to 5 ft in annular thickness could be controlled without the complication of control rods in the core itself.

In comparison with the axial-flow reactors, to be discussed below, the radial-flow reactor suffers from the disadvantage of a considerably lower core conversion ratio. This characteristic arises from a combination of the streaming down the central gas passage, the greater outward radial leakage caused by the central gas passage, and the greater outward radial leakage caused by the presence of thorium in the reflector.

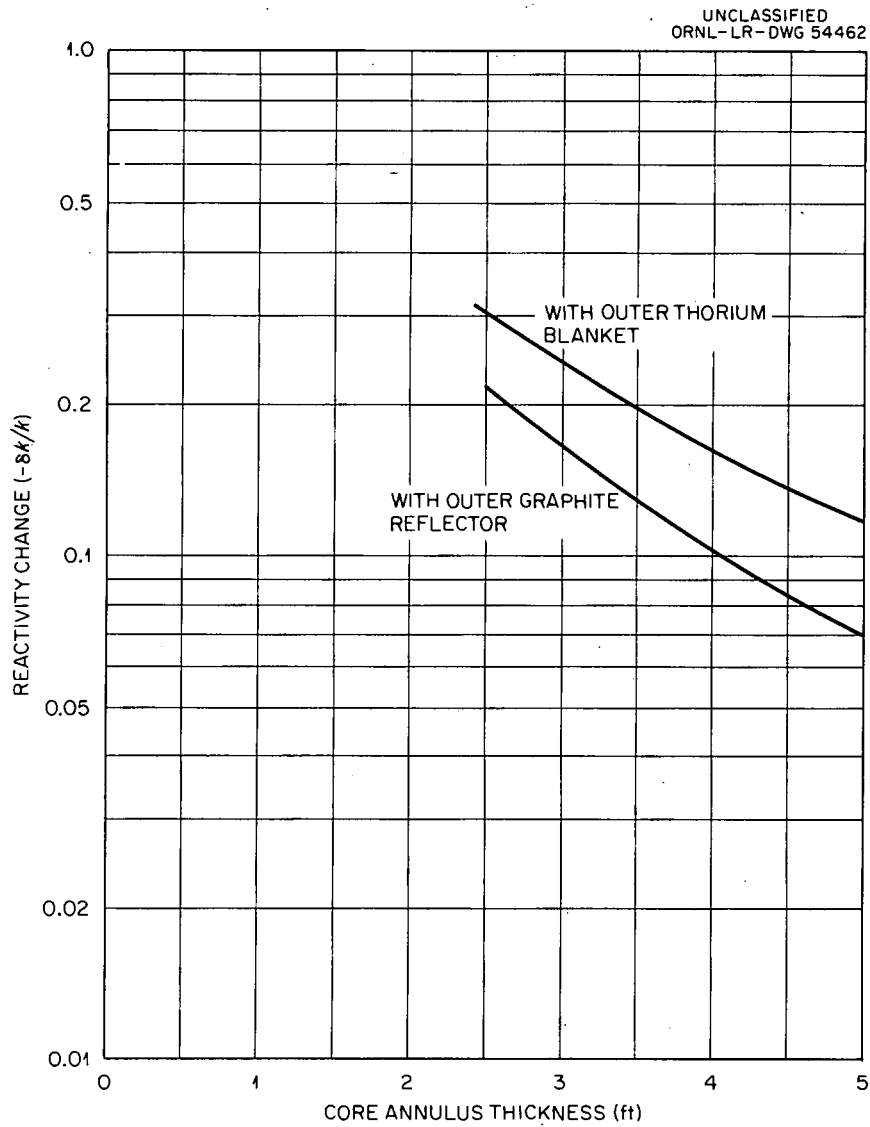


Fig. 5.1. Reactivity Control from B_4C Annulus at Inner Surface of PBR Core with Radial Gas Flow.

As a consequence, it is found that the fission cross section decreases more rapidly with burnup and that the axial power distribution has a greater peak-to-average ratio for a given terminal burnup than is the case in the axial-flow reactors. In addition, the available reactivity-limited burnup will be reduced. The decrease in conversion in the core is not all lost because some conversion occurs in the thorium of the blanket. It appears likely, however, that the additional complexity of design required to provide for reprocessing a fertile blanket, together with the cost of the blanket reprocessing, would come close to offsetting the value of the U^{233} recovered from the blanket. To the extent that the smaller size of the fuel balls allows a higher peak power density in this core, some of the disadvantages of the power distributions mentioned above might be minimized.

An approximate radial power distribution is given in Fig. 5.2 for a reactor with axial downflow of the coolant gas, an average power density in the core of about 25 w/cm^3 , a core diameter of 13 ft, and a 2.75-ft-thick graphite reflector. The effects of control rods in the core have been neglected. The power distribution appears to match the gas flow distribution reasonably well, although it would be necessary to analyze more carefully the discontinuous nature of the details of the power distribution next to the core wall. The core conversion ratio is higher than with the radial flow core, since there is no central gas passage and no thorium in the reflector. However, the conversion ratio is less than with the larger core to be discussed below.

The third type of reactor, and the one studied in more detail, has axial upflow of the coolant gas. A core diameter of 20.7 ft is required to assure that the gas flow at the design pressure does not cause levitation of the bed of fuel balls. A core height of 12.4 ft is required to obtain a thermal output of 800 Mw at an average core power density of 6.6 w/cm^3 .

An initial carbon-to- U^{235} ratio of 4000 was chosen, corresponding to an initial specific power of 1280 kw/kg. This value has not been

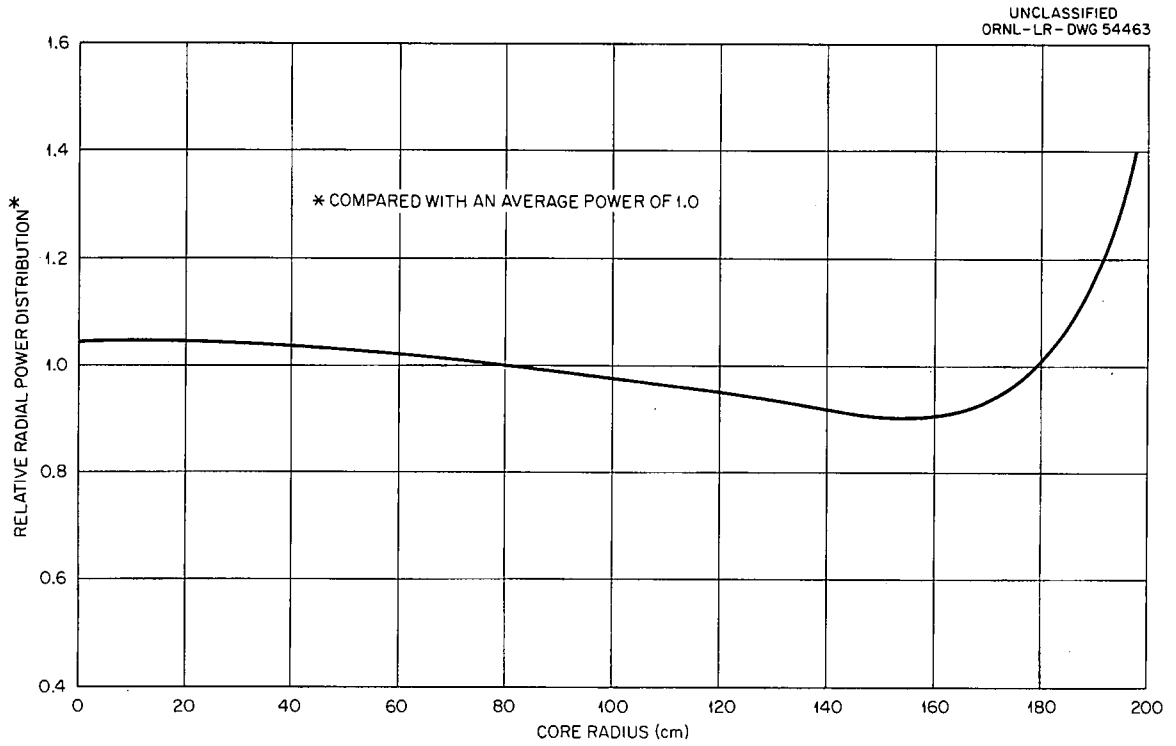


Fig. 5.2. Relative Power Distribution for a PBR Core 13 ft in Diameter with Axial Downflow of Coolant Gas and a 2.75-ft-Thick Graphite Reflector.

optimized, although it is believed that the optimum is not far from the value chosen. A complete analysis would have to balance such factors as uranium inventory cost, fuel fabrication cost, required override for peak xenon concentration, cost of recovering uranium from the spent fuel, and the effect of the moderator ratio on the effective cross sections which affect the conversion ratio. There are still considerable uncertainties regarding the unit costs for fuel fabrication and uranium recovery that reflect, in part, uncertainties in the processes to be used, and, in part, a lack of reliable cost data for large-scale processes involving contaminated systems. For this reason, a detailed analysis of the fuel cycle cost would lead to a somewhat ambiguous result.

Criticality calculations were made (with a 27-group one-dimensional diffusion code) to determine the thorium concentration in the core. Doppler-broadened effective thorium resonance integrals were computed for this purpose from the resonance parameters. The calculations give an initial thorium-to-U²³⁵ ratio of 18.1.

A neutron balance is given below for the hot, fresh core with equilibrium xenon and samarium poisoning, but no other fission products, and no buildup of heavy isotopes.

	<u>Neutron Absorptions per Source Neutron</u>
Core	
Graphite	0.0130
U ²³⁵	0.5094 ($\bar{\eta} = 1.96$)
Th ²³²	0.3845
Xe	0.0212
Sm	0.0067
Reflector graphite	0.0148
Escapes	
Radial	0.0138
Axial	0.0212
Shim control rod	0.0154
Total	<u>1.0000</u>

It may be seen from these numbers that the initial conversion ratio is 0.75. Reactivity lifetime calculations have not been made for the system. It was felt that an analysis of the economic optimum for burnup would be subject to the same uncertainties of unit costs that were mentioned in connection with the optimization of specific power. In addition, a calculation of an economic optimum is not definitive in the absence of data concerning the physical capability of the fuel balls to withstand radiation damage, since the latter factor may well turn out to be the one which limits the reactivity lifetime. However, a few qualitative observations may be made regarding lifetime. The poisoning effect of low-cross section fission products and the loss in reactivity from burnup of U^{235} will be offset initially by the higher fission cross section and higher $\bar{\eta}$ of the U^{233} . It is to be expected that the high conversion ratio of the system will allow burnups of from 1.0 to 2.0 fissions per initial fissionable atom before the reactivity finally decreases to an objectionable point.

The moderator temperature coefficient, resulting almost entirely from the change in the ratios of the effective cross sections, was computed by the multigroup method for the initial loading of U^{235} . A value of $-2.4 \times 10^{-5}/^{\circ}\text{F}$ was obtained. The fuel temperature coefficient was obtained by comparing the effective thorium resonance integrals obtained from the resonance parameters and taking into account the Doppler-broadened self-shielding at two different temperatures. A value of $-1.4 \times 10^{-5}/^{\circ}\text{F}$ was obtained. Adding these two contributions, the over-all initial temperature coefficient is $-3.8 \times 10^{-5} (\delta k/k)/^{\circ}\text{F}$.

Requirements for reactivity control during operations will come from the temperature coefficient, the fission-product accumulation, and the fuel burnup. The poisoning from low-cross section fission products, heavy isotope buildup, and fuel depletion depend upon the fuel lifetime selected. The other requirements are summarized below:

	<u>$\delta k/k$</u>
Moderator temperature coefficient	0.0238
Fuel temperature coefficient	0.0179
Equilibrium xenon	0.0315
Equilibrium samarium	0.0106
	<u> </u>
Total	0.0838

The control system consists of 20 B_4C poison rods, each 4 in. in diameter. The rods travel vertically through the length of the core. Two central rods are located 1 ft from the center of the core, have a combined worth of 0.013 $\delta k/k$, and are to be used for regulating and for shim control of fuel burnup. A circle of 8 equally spaced rods is placed 4 ft from the center of the reactor, and 10 rods are 7 ft from the reactor center. These 18 rods have a combined worth of 0.098 $\delta k/k$, and would serve to overcome the temperature defect and the equilibrium xenon poisoning and to provide a shutdown margin of safety of 0.025 $\delta k/k$. Each of the control rods travels through a 5-in.-i.d., 6.5-in.-o.d. graphite sleeve. When the core has reached an equilibrium fuel distribution, compensation for fuel burnup would be by periodic partial refueling (insertion of fresh fuel balls at the top of the core and removal of spent fuel balls from the bottom), with the two central shim rods serving to provide control between refuelings. During initial operations, prior to the establishment of an equilibrium fuel distribution, there will be somewhat larger changes in reactivity resulting from the accumulation of samarium, other stable fission products, and heavy isotopes. It is anticipated that these would be compensated for by appropriate periodic changes in the height of the fuel bed, combined if necessary with the use of a burnable poison. The amount of reactivity control available by changing the bed height is given in Fig. 5.3. The use of a decreased bed height to control reactivity is particularly appropriate to the first few months of operation, since it is likely that the reactor would operate for a period of time at reduced power levels while the operating characteristics of the system were being studied. The value of the reactivity

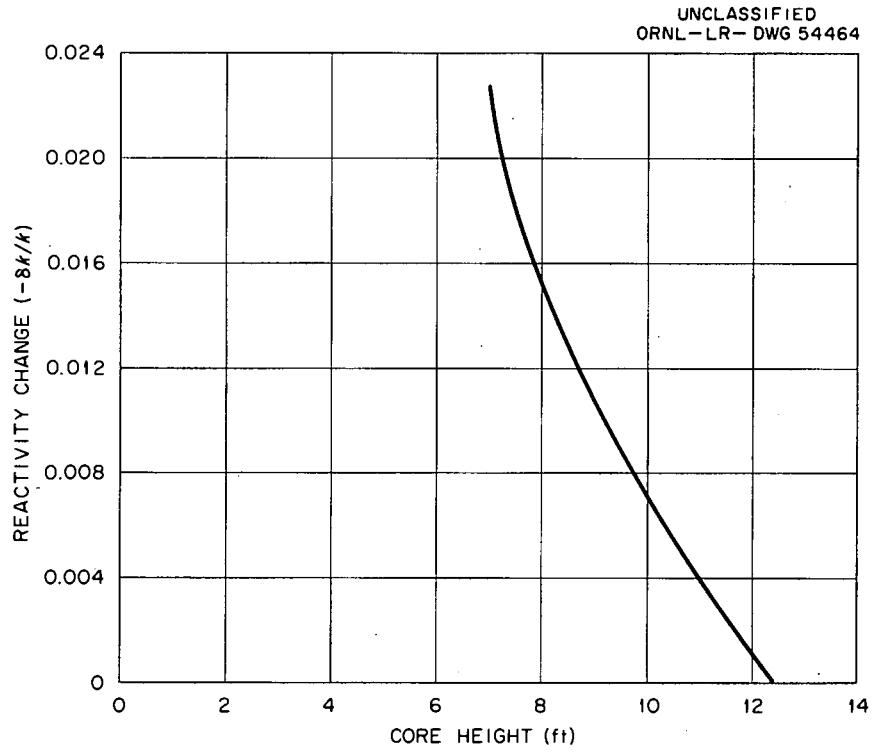


Fig. 5.3. Change in Reactivity with Core Height Based on a Height of 12.4 ft.

control needed to balance the moderator temperature coefficient (0.0213) was computed for the initial conditions of pure U^{235} fuel. As the U^{233} builds up, the moderator temperature coefficient will decrease because of the difference in energy dependence between the U^{235} and U^{233} cross sections. A core in which the U^{235} had all been replaced by U^{233} would have a k_{eff} at room temperature only 0.0039 greater than at operating temperature.

No provision has been made in the control system for overriding the peak xenon poisoning which will occur several hours after a shutdown. It was assumed that scheduled shutdowns and shutdowns from equipment failure would normally be of such duration that the xenon concentration would fall below its equilibrium value before startup was attempted and that the control instrumentation could be made sufficiently reliable so that instrument shutdowns would be infrequent. This latter assumption should be investigated in detail in the final design of the reactor, since some of the currently operating reactors experience rather frequent unscheduled shutdowns caused by instrument failures. If it should be necessary to override the peak xenon poisoning, an additional $0.043 \delta k/k$ would have to be provided in the form of control rods which would remain inserted during normal operations. There would be a corresponding decrease of 0.056 in the conversion ratio and a probable decrease in the fuel lifetime.

In order to protect the graphite moderator structure at the side of the core from radiation damage, a 12-in.-thick layer of unfueled graphite balls is inserted between the core and the "permanent" graphite structure. The unfueled graphite balls flow with the fuel balls and some are removed with each refueling. The fast neutron flux is shown in Fig. 5.4 as a function of radial position. A factor of 7.4 reduction in the fast flux occurs across the 12 in. of unfueled balls.

The heating rates in the inner portions of the reflector are shown in Fig. 5.5. The neutron heating was computed from the fluxes of the one-dimensional multigroup calculation and the scattering

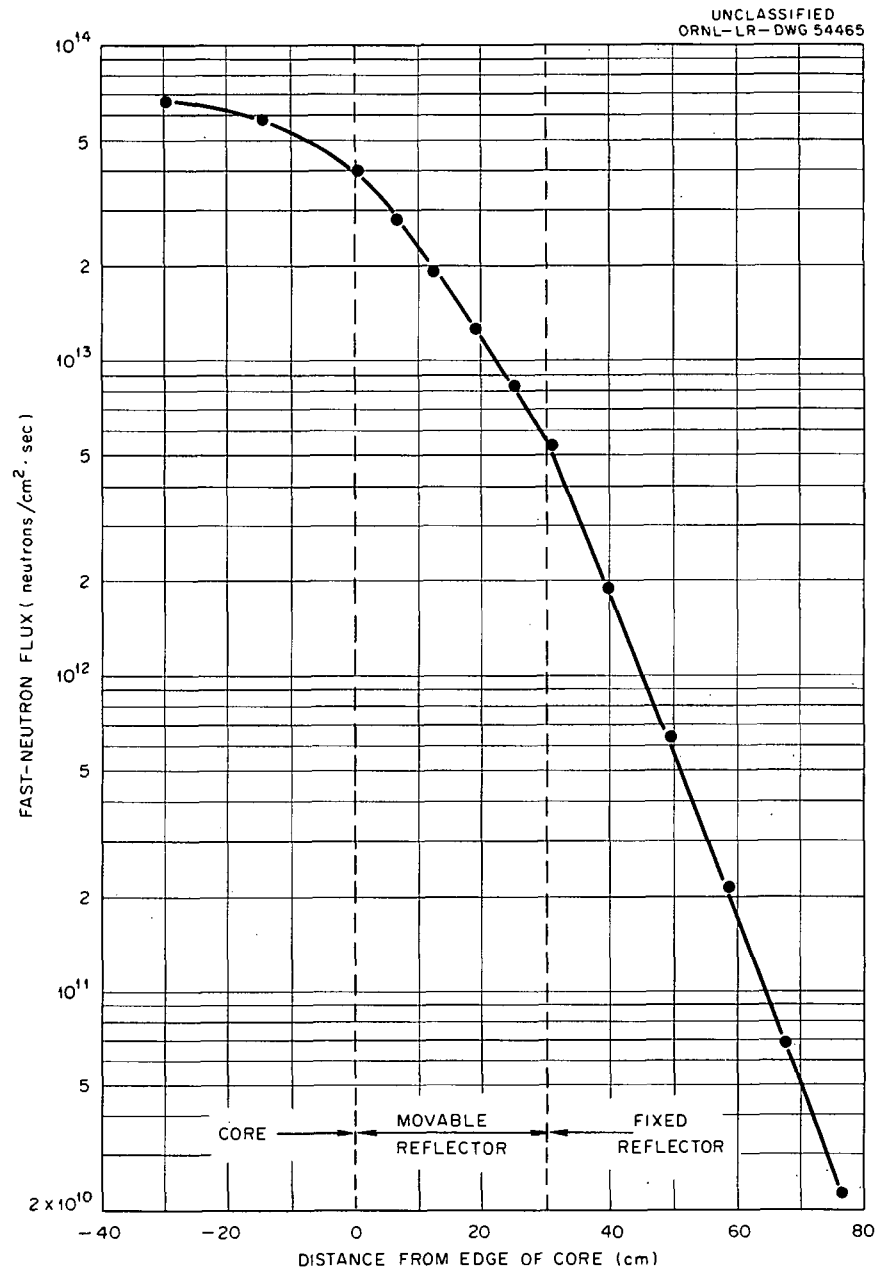


Fig. 5.4. Fast-Neutron Flux ($E > 0.1$ Mev), Distribution as a Function of Radial Position for an Axial Upflow Core.

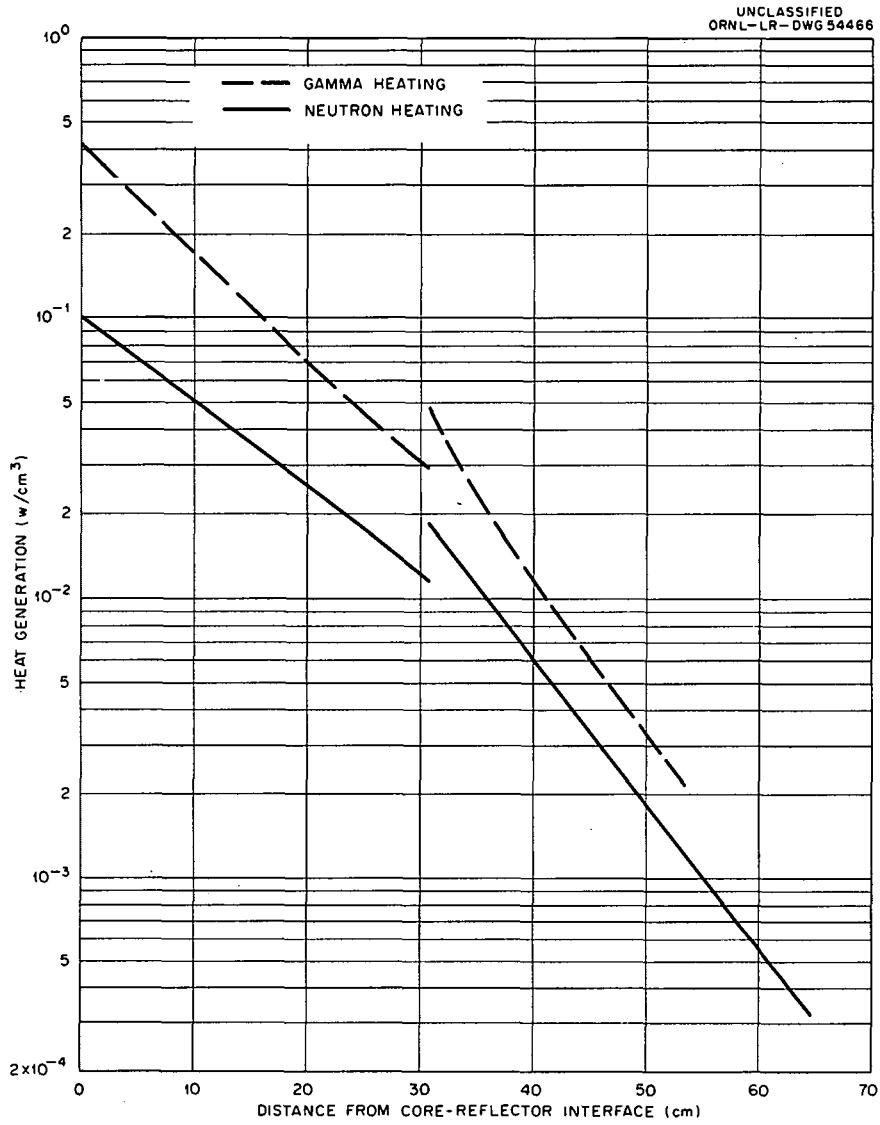


Fig. 5.5. Heating in Inner Portions of Reflector of Axial Upflow Core.

cross sections. The gamma heating was computed by summation of contributions from a six-group space-dependent source distribution. The points of discontinuity occur at the interface between the movable reflector and the fixed reflector because of the higher density of the fixed reflector.

A two-dimensional horizontal cross section of the power distribution in the core is given in Fig. 5.6. The plot is calculated for a normal operating condition of complete insertion of the two central control rods and complete withdrawal of the remaining control rods. The power distribution is normalized to an average value of 1.0.

The mean generation time for prompt neutrons was computed by perturbation theory. The fluxes and adjoint fluxes were determined by a one-dimensional four-group calculation. A value of 0.3×10^{-3} sec was found.

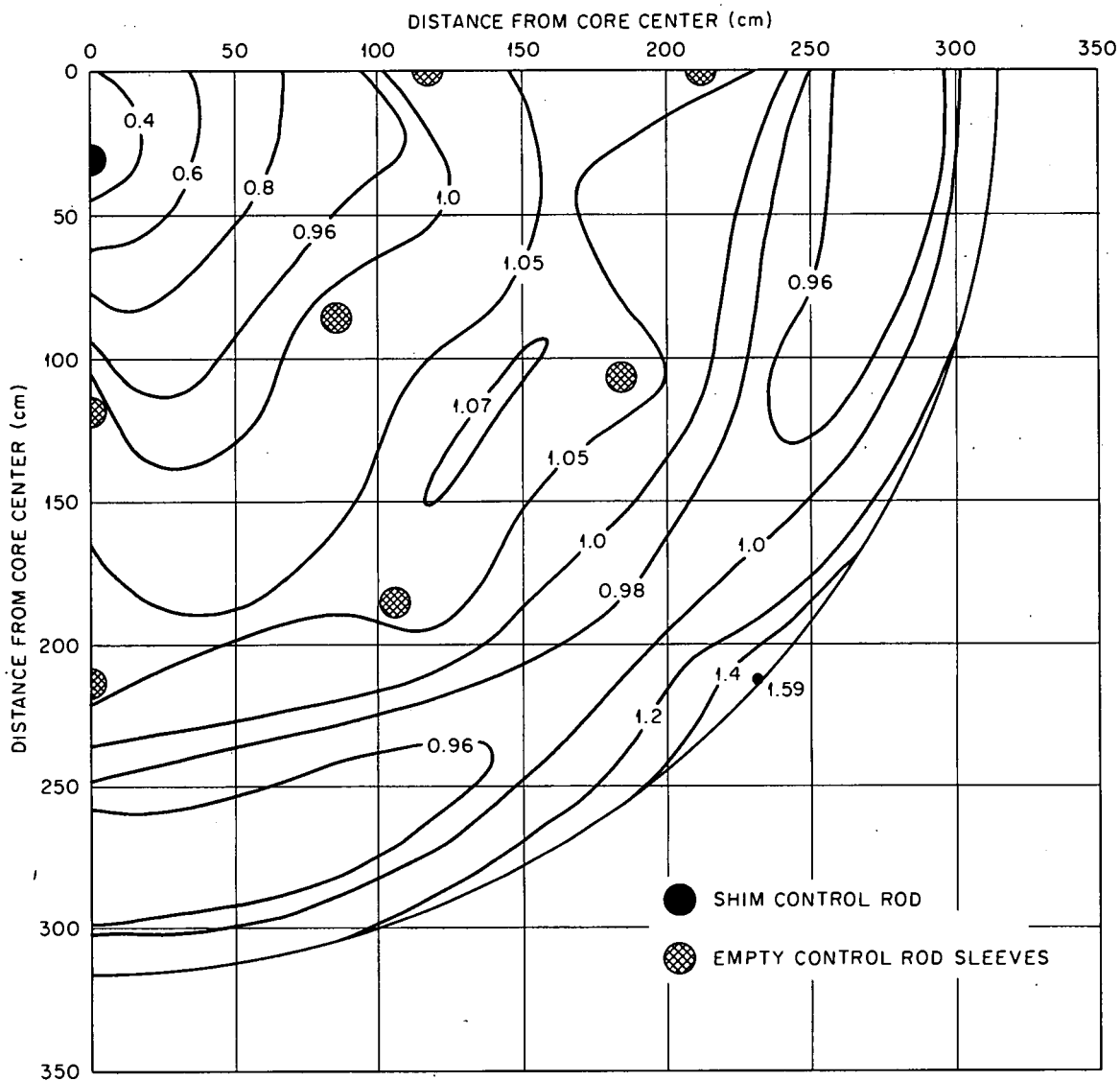


Fig. 5.6. Core Power Distribution Relative to an Average Power of 1.0.

6. FUEL ELEMENT FABRICATION

The available experimental data pertaining to the ability of graphite-matrix fuel elements to withstand the mechanical, chemical, and nuclear effects imposed in reactors of the pebble-bed type were presented and discussed in the PBRE report.¹ The data indicated the need for impervious coatings on the individual fuel particles to provide the degree of fission-product retention required. In addition, if the hot fuel spheres would be exposed to air as the result of a rupture in the primary coolant system, oxidation-resistant coatings on the spheres would be required to prevent sustained combustion. Sphere surface coatings also may be required to prevent mass transfer of carbon by impurities in the helium. Consideration of all the operating requirements, therefore, requires a fuel sphere consisting of coated fuel particles dispersed in a graphite matrix with an oxidation-resistant sphere surface coating.

The materials under consideration for coating fuel particles are Al_2O_3 and BeO for UO_2 - ThO_2 particles and pyrolytic carbon for UC_2 - ThC_2 particles. The oxide systems have the advantage that the UO_2 - ThO_2 mixtures are less expensive and easier to handle than the UC_2 - ThC_2 particles. However, both Al_2O_3 and BeO react with graphite above approximately 2500°F, even in the absence of radiation. If irradiation lowers the threshold temperature for this reaction, only marginal protection would be afforded by oxide coatings of the PBR fuel elements. Since the reaction between the oxides and graphite proceeds rapidly at temperatures well below the normal application temperature for Si-SiC (3200-3300°F), this coating, which is the most promising surface coating for graphite protection known at the present time, could not be used on spheres fueled with Al_2O_3 - or BeO -coated particles. The combination of pyrolytic-carbon-coated UC_2 - ThC_2 particles and

¹"Preliminary Design of a 10-Mw(t) Pebble-Bed Reactor Experiment," ORNL CF-60-10-63, November 1, 1960, chap. 8.

graphite would be in chemical equilibrium and, therefore, not temperature limited by chemical reactions, either during reactor operation or during sphere surface-coating operations.

Based on the above considerations, the most promising PBR fuel ball would contain pyrolytic-carbon-coated UC_2 - ThC_2 fuel particles and would be coated with Si-SiC. Many problems must be solved, of course, before this concept can be proved to be feasible for reactor operation.

One of the most serious problems is the complete lack of high-temperature, high-burnup, irradiation test data on pyrolytic-carbon-coated fuel particles. Data obtained by neutron activation followed by postirradiation annealing indicate excellent fission-gas retention.¹ The effect of fission-fragment and fast-neutron damage on coating permeability could be very serious, however, and must be evaluated in high-temperature irradiation tests.

Mechanical and physical properties must be determined as a function of temperature, fabrication procedure, and irradiation. Graphite oxidation and carbon-mass-transfer must be thoroughly investigated, the type and quality of sphere coatings required must be determined, and inspection methods for quality control must be developed.

Fabrication Costs

The process for fabricating fuel spheres of the PBR type may be divided into four general areas: (1) preparation of spheroidal fuel particles, (2) coating the fuel particles, (3) blending the fuel particles with graphite and fabricating spheres, and (4) surface coating the fueled spheres. Experience in each of these areas has been limited to the processing of relatively small batches. Considerable extrapolation is required, therefore, to project the present experience to the fabrication of the more than one-half million fueled spheres required for the PBR.

Estimates of the cost for the preparation of large quantities of spheroidal particles range from \$0.30/g to \$1.00/g. These figures

are based on 100 kg of UC_2 particles but should be reasonably valid for UC_2 - ThC_2 mixtures. Thorium dicarbide is reported to be more reactive than UC_2 , however, and may require special handling before coating.

The coating of UC_2 particles in the size range 100 to 200 μ was estimated to cost \$0.24 to \$0.30/g. These estimates are based on 30 to 50 μ of pyrolytic carbon on 100 kg of the particles. Increasing the quantity from 100 kg to 14 000 kg would probably lower the unit cost, but increasing the coating thickness to about 80 to 100 μ would offset this decrease. The present cost for coating UC_2 particles in gram lots is approximately \$1.30/g.

The graphite spheres are loaded with 0.50% UO_2 plus 9.61% ThO_2 , or 0.48% UC_2 plus 9.32% ThC_2 , by weight. Fuel sphere fabrication, including blending, molding, and baking, was estimated to cost \$0.75 to \$1.50/sphere for 20 000 spheres, 1.5 in. in diameter. Increasing the lot size to 600 000 spheres would decrease the unit cost. This decrease, however, may be offset somewhat by the increased cost of fabricating the larger 2.5-in.-diam spheres.

Costs for coating 20 000 1.5-in.-diam spheres with Si-SiC were estimated to be \$1 to \$4/sphere.¹ Increasing the sphere diameter to 2.5 in. would not be expected to increase the unit coating cost significantly.

The estimated fabrication costs for PBR fuel elements containing 23.2 g of UC_2 - ThC_2 per sphere may be summarized as follows:

UC_2 - ThC_2 spheroidal particles at \$0.30-\$1.00/g	\$ 6.96-\$23.20
Coating particles at \$0.24-\$0.30/g	5.57- 6.96
Fabricating fueled spheres	0.75- 1.50
Coating spheres	1.00- 4.00
Total	<u>\$14.28-\$35.66</u>

It may be seen that the major proportion of the cost lies in the preparation and coating of the particles. For the most part, the

development of spheroidal carbide particles is still in the experimental stage; the present uncertainties in the fabrication processes are reflected in the wide variation in the estimated cost.

7. STRESS ANALYSIS OF FUEL ELEMENTS

Stress Analysis of Uncoated Fueled Graphite
Spheres With Uniform Heat Removal

The temperature distributions in the fuel balls will induce compressive stresses in the radial direction and tensile stresses in the tangential directions. The maximum tensile stresses will occur at the surfaces. Since graphite is weak in tension, these are the limiting quantities, and the maximum allowable sphere diameter for a given heat generation rate depends upon the ultimate tensile stress. Although the thermal strains produce tensile stresses at the surface of a sphere, the hydrostatic pressure loading provides a mitigating factor, since compressive stresses result from this source.

As a first approximation in the stress analysis, the spheres were assumed to be solid, homogeneous bodies with uniform internal heat generation and uniform surface cooling. The material was assumed to be an ideally elastic, isotropic, fueled graphite. The temperature is thus a function only of the radius, r , and is given by

$$T - T_s = \frac{A_0}{6k} (b^2 - r^2) \quad , \quad (1)$$

where

- T_s = surface temperature,
- A_0 = power-generation rate,
- b = outside radius,
- k = thermal conductivity.

The general equation for the tangential stress is¹

$$\sigma_t = \frac{\alpha E}{1 - \nu} \left(\frac{2}{b^3} \int_0^b Tr^2 dr + \frac{1}{r^3} \int_0^r Tr^2 dr - T \right) \quad . \quad (2)$$

¹S. Timoshenko and J. N. Goodier, "Theory of Elasticity," p. 418, McGraw-Hill, New York, Second Edition, 1951.

The maximum stress is found by substituting Eq. (1) into Eq. (2) and integrating from $r = 0$ to $r = b$. Thus

$$\sigma_{t_{\max}} = \frac{\alpha A_0 E b^2}{15(1 - \nu)k}, \quad (3)$$

where

- α = thermal coefficient of expansion,
- E = elastic modulus,
- ν = Poisson's ratio.

The limiting power generation rate as a function of the outside diameter, D , and the ultimate tensile stress is obtained from Eq. (3):

$$A_0 = \frac{60(1 - \nu)k}{\alpha E} \frac{\sigma_{\text{ult}}}{D^2}. \quad (4)$$

A value of 8 Btu/hr·ft·°F for the thermal conductivity appears to be reasonable. However, the value varies with fuel loading, fast-neutron exposure, temperature, and the amount of graphitization. For this reason, four different values of k were used in the analysis. The values used for the constants in Eq. (4) are the following:

$$\begin{aligned} \sigma_{\text{ult}} &= 1500, 2000, \text{ and } 2500 \text{ psi} \\ \alpha &= 3 \times 10^{-6} \text{ in./in.}\cdot\text{°F} \\ E &= 1.5 \times 10^6 \text{ psi} \\ \nu &= 0.3 \\ k &= 4, 8, 12, \text{ and } 15 \text{ Btu/hr}\cdot\text{ft}\cdot\text{°F} \end{aligned}$$

The choice of these values will be discussed later. The results of the analysis are given in Figs. 7.1 and 7.2. The allowable power generation rate as a function of the ball diameter is shown in Fig. 7.1, with the values of thermal conductivity listed above as parameters. The effect of ultimate tensile stress is indicated in Fig. 7.2.

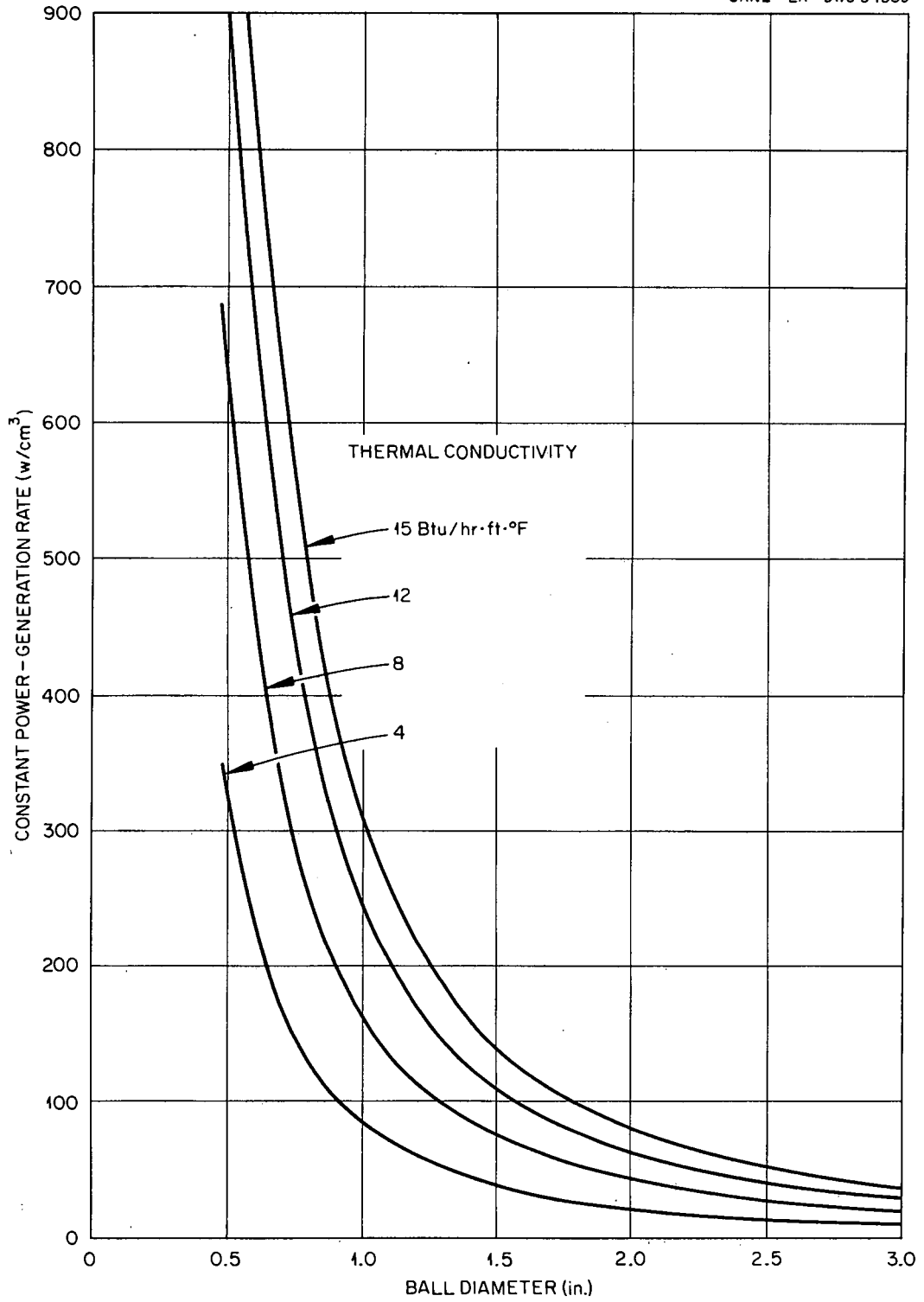


Fig. 7.1. Rupture Curves for Ultimate Tensile Stress of 1500 psi in Fuel Balls.

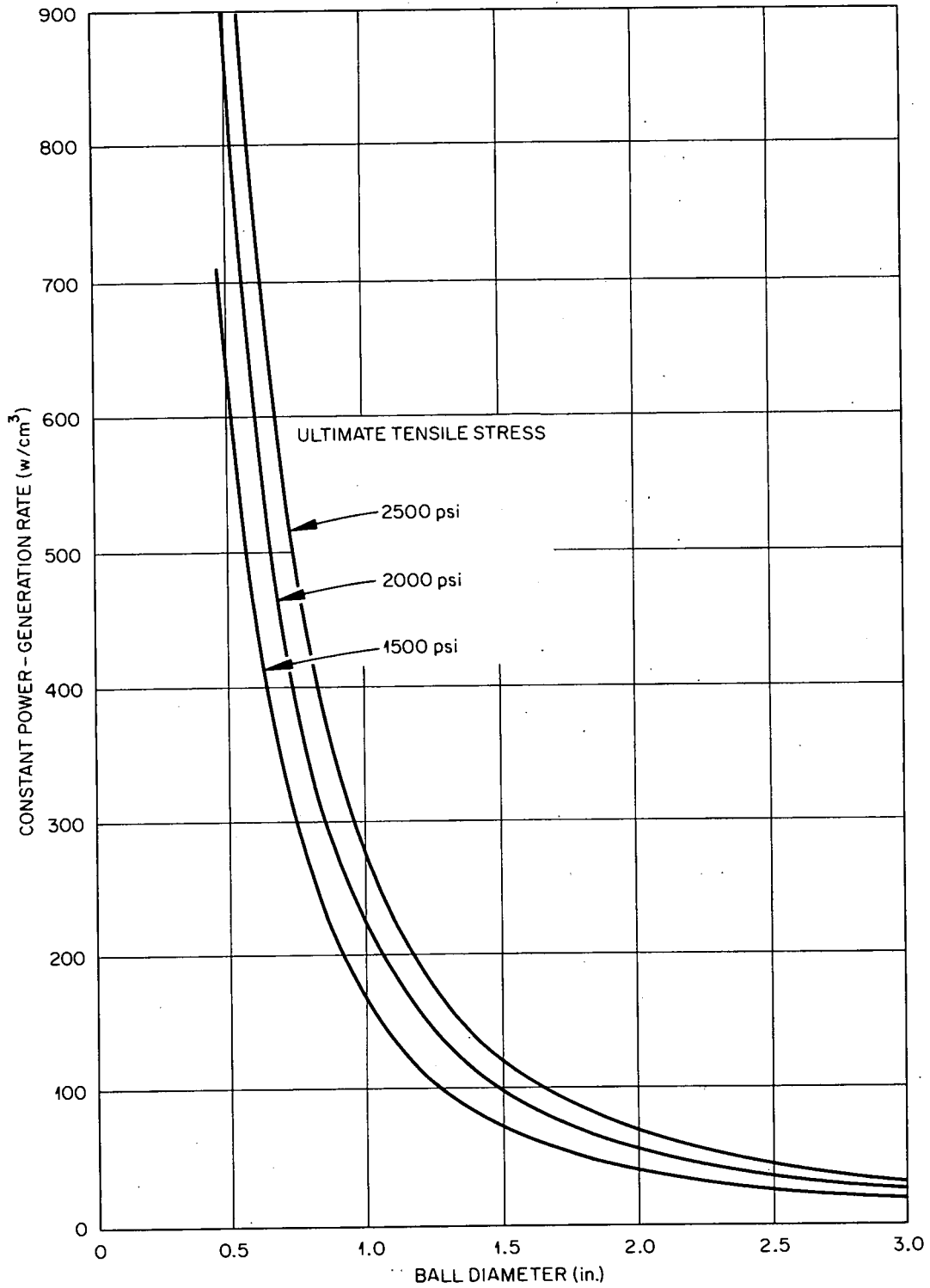
UNCLASSIFIED
ORNL-LR-DWG 54390

Fig. 7.2. Rupture Curves for Indicated Ultimate Tensile Stresses in Fuel Balls with a Thermal Conductivity of 8 Btu/hr·ft·°F.

If credit can be taken for the compensating effect of external pressure on the graphite balls, Eq. (3) becomes

$$\sigma_{t_{\max}} = \frac{\alpha A_0 E b^2}{15(1 - \nu)} - p ,$$

where p is coolant pressure. The allowable power generation rate, from Eq. (4), becomes

$$A_0 = \frac{60(1 - \nu)k \sigma_{\text{ult}} + p}{\alpha E D^2} .$$

For a system pressure of 700 psi, the effect is the same as taking $\sigma_{\text{ult}} = 2200$ psi instead of 1500 psi, as in the previous equation.

Effect of Thermal Stresses Caused by a Nonuniform Heat Transfer Coefficient Over the Surface of a Sphere with Uniform Internal Heat Generation

Since the fuel spheres will be stacked in the cavity which forms the fuel region of the reactor, contact between adjacent elements and the coolant flow distribution will result in a nonuniform surface heat flux for each sphere. This gives rise to temperature distributions in the spheres which are functions of the three space coordinates. The stress analysis of a solid sphere with this type of temperature distribution represents a complex thermoelastic problem. However, an approximate value for the maximum stress in each sphere may be obtained by considering the difference between the mean temperature of a body and the temperature at a point on the surface. Here it is assumed that the maximum stress is in the tangential direction at the surface.

The tangential stress for a temperature distribution with radial dependence only is given by Eq. (2). Since the mean temperature of that portion of a sphere within the radius r is

$$[\bar{T}]_r = \frac{3}{r^3} \int_0^r T(r) r^2 dr, \quad (5)$$

the tangential stress at any point becomes

$$\sigma_t = \frac{2\alpha E}{3(1-\nu)} \left\{ [\bar{T}]_b + \frac{1}{2} [\bar{T}]_r - \frac{3}{2} T(r) \right\}. \quad (6)$$

The maximum tangential stress at the surface is

$$\sigma_{t_{\max}} = \frac{\alpha E}{1-\nu} \left\{ [\bar{T}]_b - T(b) \right\}. \quad (7)$$

Equation (7) may therefore be used to obtain approximate maximum stress magnitudes for the case of nonuniform surface heat flux. Thus

$$\sigma_{t_{\max}} \approx \frac{\alpha E}{1-\nu} \left\{ [\bar{T}]_b - T_{\min} \right\}. \quad (8)$$

The temperature distribution in balls with a uniform internal heat generation rate and a nonuniform film heat transfer coefficient over the surface was calculated for several cases using the generalized heat conduction code for the IBM-704 computer.² The following assumptions were made:

1. Each stacked fuel ball in the PBR has an average of seven contact points with the adjacent balls.³
2. The contact points are uniformly distributed over the ball surface.
3. The heat transfer coefficient is a minimum at the contact point and increases with distance from this point.
4. The values for the heat transfer coefficient are symmetrical with respect to the contact point.

²T. B. Fowler and E. R. Volk, "Generalized Heat Conduction Code for the IBM-704 Computer," ORNL-2734 (Oct. 16, 1959).

³Unpublished Canadian research on heat transfer in packed bed of balls.

If the heat transfer coefficients for all contact points are equal, the typical section to be analyzed can be approximated by that portion of the sphere subtended by a 90-deg cone angle from the ball center, with the axis of the cone passing through the contact point. The condition of symmetry about the axis reduces the problem to a two-dimensional heat-conduction analysis of a sector of a circle with a central angle of 45 deg. The following boundary conditions apply: (1) no heat flow at the two boundaries formed by the radii and (2) a variable heat transfer coefficient for the spherical surface. The constants selected for the problem were:

Thermal conductivity	10 Btu/hr·ft·°F
Heat generation in the ball	50 kw/liter
Ball diameter	1.5 in.

The bulk gas temperature was assumed to be constant over the ball surface and equal to zero, for convenience in the calculations.

The temperature distributions represented in Figs. 7.3a, b, and c are for an average film heat transfer coefficient of 610 Btu/hr·ft²·°F. Figures 7.3a and b are for ratios of the average to the minimum film heat transfer coefficient of 2 and 3, respectively. The data presented in ref. 3 were used as a guide in selecting these ratios. Figure 7.3c represents the temperature distribution for a uniform film heat transfer coefficient of 610 Btu/hr·ft²·°F. The temperatures given are all in °F above the reference bulk coolant temperature. Figures 7.4a, b, and c represent the results of similar calculations for an average film coefficient of 305 Btu/hr·ft²·°F. The mean temperature for the complete sphere in each case was obtained by summing the products of each local temperature and its incremental volume and dividing by the sum of the incremental volumes. The mean temperature is given in each figure.

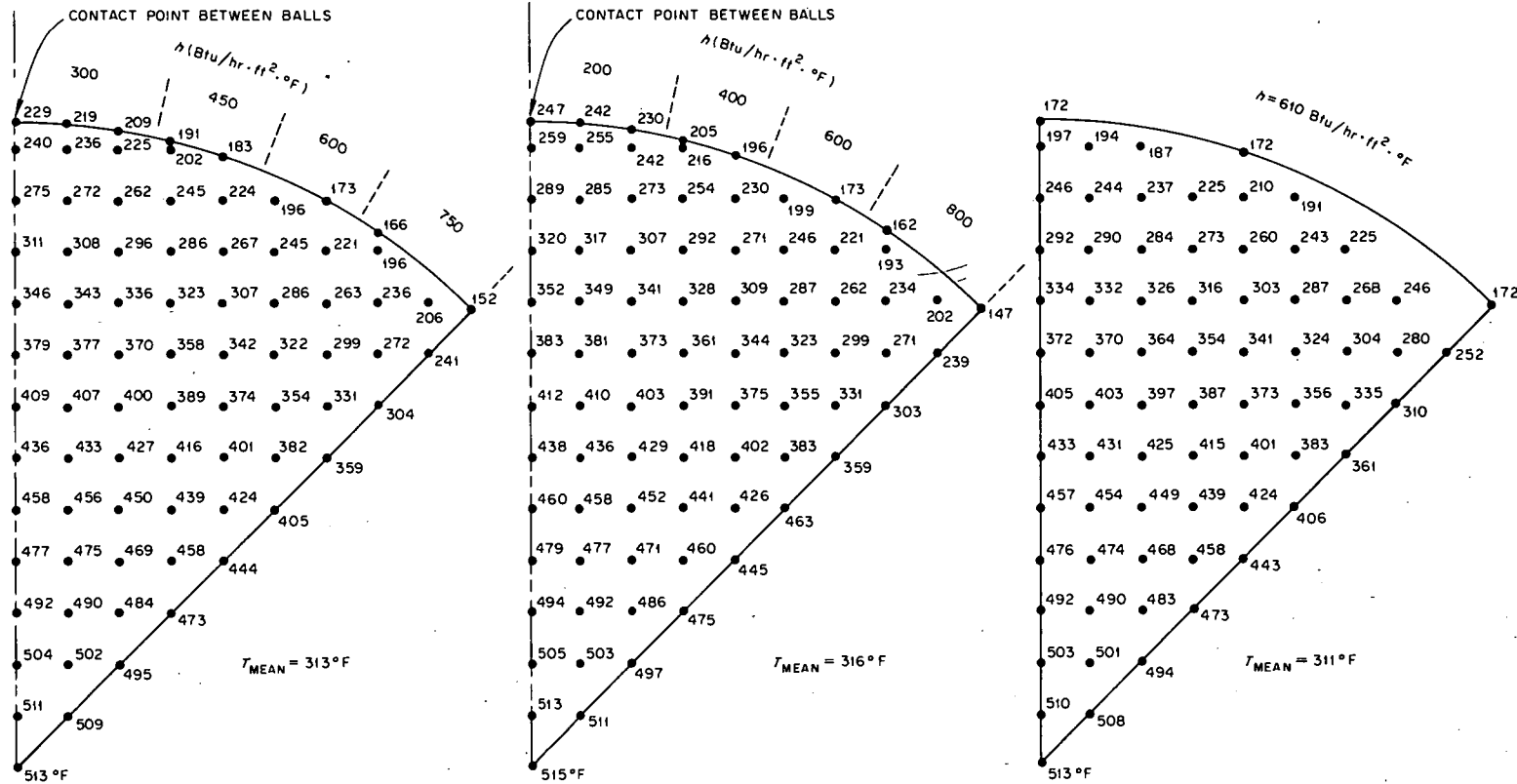
The following material properties were assumed for the graphite balls:

$$E = 1.5 \times 10^6 \text{ psi}$$

$$\nu = 0.3$$

$$\alpha = 3.0 \times 10^{-6} \text{ in./in.}\cdot^\circ\text{F}$$

NOTE: NUMBERS GIVE TEMPERATURE DROP, T (°F), FROM POINT IN BALL TO BULK FREE STREAM TEMPERATURE.



(a) LOCAL FILM COEFFICIENT

$$\frac{h_{AV}}{h_{MIN}} \cong 2$$

(b) LOCAL FILM COEFFICIENT

$$\frac{h_{AV}}{h_{MIN}} \cong 3$$

(c) UNIFORM FILM COEFFICIENT

Fig. 7.3. Temperature Distribution in Fuel Ball Based on an Average Film Coefficient, h , of 610 Btu/hr·ft²·°F, a Heat Generation Rate of 50 kw/liter, a Ball Thermal Conductivity of 10 Btu/hr·ft·°F, and a Ball Diameter of 1.5 in.

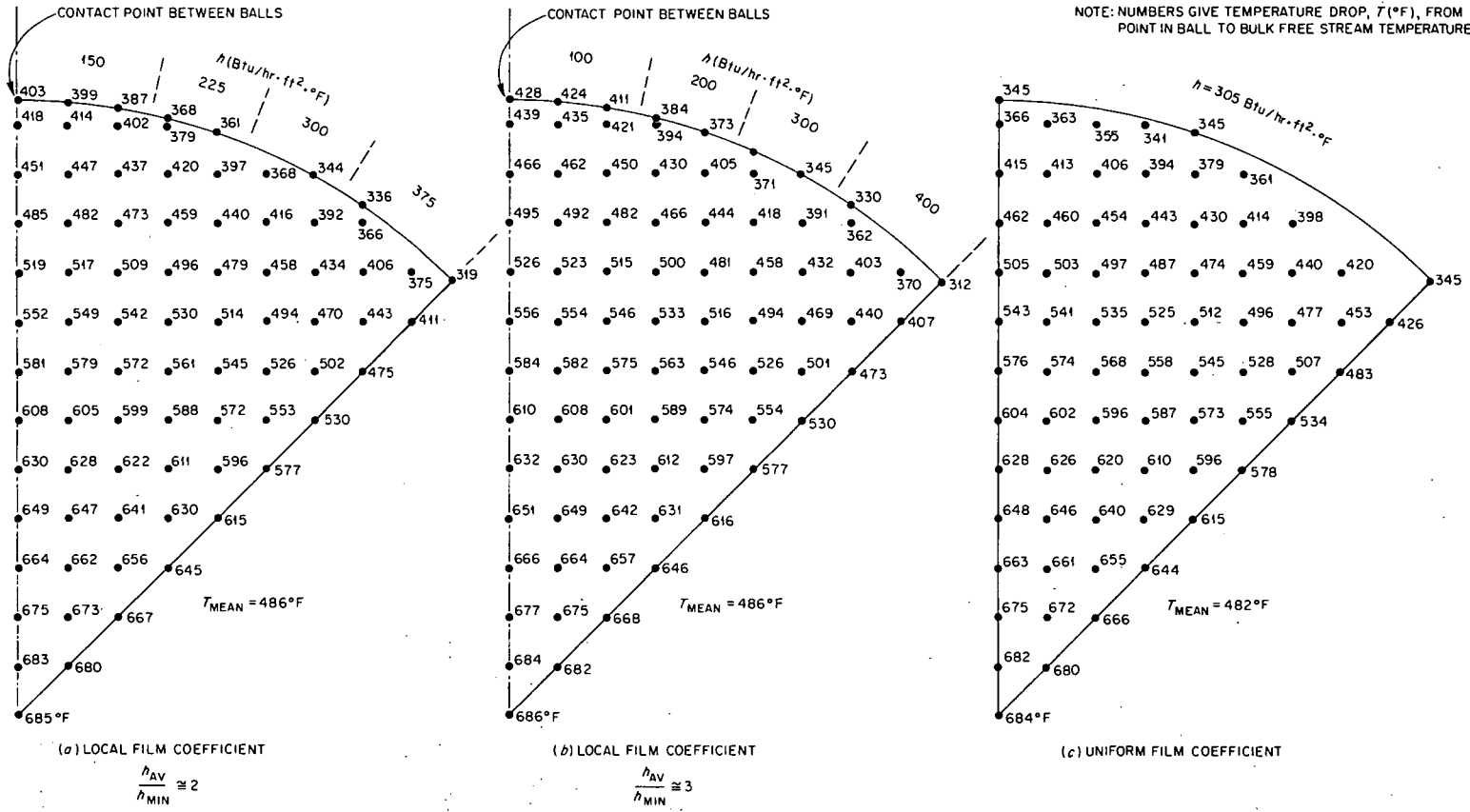


Fig. 7.4. Temperature Distribution in Fuel Ball Based on an Average Film Coefficient, h , of 305 Btu/hr.ft².°F.

Table 7.1 gives the calculated stresses for each of the six cases corresponding to Figs. 7.3 and 7.4 and the percentage increases in maximum stress over the stresses for the case of a uniform heat transfer coefficient.

Table 7.1. Comparison of Maximum Calculated Thermal Stresses, σ_{\max} , in Balls With Uniform and Nonuniform Heat Transfer Coefficient

Case	σ_{\max} (psi)	Increase in Thermal Stress Over That for Uniform Film Coefficient
3a	1035	15.8
3b	1090	21.6
3c	895	
4a	1075	21.9
4b	1120	27.0
4c	880	

It may be concluded that varying the film coefficient over the ball surface while keeping its average value constant does not alter the ball center temperature; only the temperatures near the surface are affected. The maximum surface temperature for a variable heat transfer coefficient is from 20 to 40% higher than for a uniform heat transfer coefficient. It may also be concluded that the maximum thermal stress is increased by 15 to 30% for the assumed conditions.

Properties of Fueled Graphite

The physical and mechanical properties of graphite vary widely from one grade to another. They also vary widely from specimen to specimen and even within the same specimen. In addition to these variations, most of the properties are dependent on such factors as temperature, the type of coke, the type of binder, the amount of graphitization,

the method of fabrication, and the orientation of the grains. In nuclear applications the fast-neutron exposure, as well as the irradiation temperature, affects the properties. When fueled graphite is considered, the effects of the fuel must be taken into account. Thus, it becomes extremely difficult to obtain data from the literature that are directly applicable to a particular situation.

The PBR fuel elements are molded graphite spheres containing uranium and thorium. Because of the temperature limitations of surface coatings, the final baking temperatures of the spheres may be below the temperature range required for complete graphitization. Thus, the spheres may be only partially graphitized. A literature search reveals that the data most applicable to the PBR fuel elements are the results of research by the Los Alamos Scientific Laboratory,^{4,5} the National Carbon Company,^{6,7,8} the Hanford Laboratories,⁹ and North American Aviation, Inc.¹⁰ The following discussion of the applicable physical and mechanical properties is taken from these references.

⁴P. Wagner et al., "Some Mechanical Properties of Graphite in the Temperature Range 20 to 3000°C," Second United Nations International Conference on the Peaceful Uses of Atomic Energy, 7, 379 (1958).

⁵Leon Green et al., "Mechanical Property Measurements on Pure and Uranium-Loaded Graphites at Elevated Temperatures," Report No. 1537, Aerojet-General Corporation (Dec. 23, 1958).

⁶W. P. Eatherly et al., "Physical Properties of Graphite Materials for Special Nuclear Applications," Second United Nations International Conference on the Peaceful Uses of Atomic Energy, 7, 389 (1958).

⁷L. M. Currie et al., "The Production and Properties of Graphite for Reactors," Proceedings of the International Conference on the Peaceful Uses of Atomic Energy, 8, 451 (1955).

⁸"Summary Report - Phase 1, Graphite-Matrix Nuclear Fuel Elements," Vol. 1, National Carbon Company (Dec. 27, 1959).

⁹R. E. Nightingale et al., "Damage to Graphite Irradiated Up to 1000°C," Second United Nations International Conference on the Peaceful Uses of Atomic Energy, 7, 295 (1958).

¹⁰Richard E. Durand et al., "Effect of Reactor Irradiation on the Thermal Conductivity of Uranium Impregnated Graphite at Elevated Temperatures," NAA-SR-836, North American Aviation, Inc. (Aug. 15, 1954).

The linear coefficients of thermal expansion, α , in the temperature range of interest are reported in refs. 4 and 5 for several grades of uranium-impregnated molded graphite manufactured at Los Alamos. Normal UO_2 was added to yield grades of finished material with the uranium concentrations given in Table 7.2. The test specimens were machined with their long axes parallel to the grains (perpendicular to the molding-pressure vector), so the values reported are for a direction parallel to the grains. Table 7.3, taken from data given in ref. 5, gives the results of thermal expansion measurements on these specimens.

Table 7.2. Fuel Content of Graphite Used in Los Alamos Tests

Specimen Identification	Fuel Content (wt %)	Volume Concentration of Uranium (g/cm^3)
CK	0	0
LDH	6.7	0.125
LDC	13.1	0.250
LDP	39.0	0.350

Table 7.3. Average Coefficients of Linear Thermal Expansion, α , for Pure and Uranium-Loaded Graphite Specimens

Specimen	Fuel Content (wt %)	Temperature Range ($^{\circ}\text{F}$)	α (in./in. $\cdot^{\circ}\text{F}$) $\times 10^{-6}$
CK	0	68-1922	1.32
		2372-4352	2.67
LDH	6.7	68-1922	1.61
		2372-4352	2.70
LDC	13.1	68-1922	2.19
		2372-4352	2.22
LDP	39.0	68-1922	2.50
		2372-4352	2.31

The coefficient of thermal expansion for use in the thermal stress calculations of the PBR fuel elements would be between the values given in Table 7.3 because the temperature will be approximately 2000°F. It appears, however, that the amount of graphitization was higher for the graphite specimens listed than would be expected in the fueled spheres for the PBR. Since α decreases slightly with the amount of graphitization, a value of 3×10^{-6} in./in.·°F was used in the PBR stress calculations.

The most applicable thermal conductivity data are given in refs. 4, 9, and 10. The values of thermal conductivity listed in Table 7.4 were taken from ref. 4 and are for the unirradiated Los Alamos graphite specimens discussed above. The measurements were made in a direction parallel to the grains:

Table 7.4. Thermal Conductivity of Pure and Uranium-Loaded Unirradiated Graphite Specimens at 2000°F

Specimen	Fuel Content (wt %)	Thermal Conductivity (Btu/hr·ft·°F)
CK	0	14.5
LDH	6.7	15.0
LDC	13.1	13.8

Reference 8 gives the room-temperature thermal conductivity of unirradiated UO₂-graphite compacts and unirradiated ThO₂-graphite compacts. Since the data are for room temperature, they are not directly applicable to the PBR fuel elements. The data do indicate, however, that the effect on the thermal conductivity of a given amount of ThO₂ in the graphite is approximately the same as the same amount of UO₂.

The thermal conductivity of graphite is reduced by fast-neutron exposures up to approximately 5000 Mwd/AT.¹¹ Above this value a near-saturation state is reached. The amount of reduction is highly dependent on the temperature at which the graphite is irradiated. Data are presented in refs. 9 and 10 that indicate the amount of reduction in thermal conductivity as a function of exposure and irradiation temperature. The ratio of thermal conductivity for unirradiated unimpregnated graphite to the thermal conductivity of irradiated uranium-impregnated graphite is given in ref. 10 as a function of exposure and irradiation temperature. The uranium-impregnated graphite contained 0.018 g/cm³ of uranium, and the thermal conductivities were measured at the irradiation temperature. The data indicate that, when saturation exposures are reached, the thermal conductivity is reduced by a factor of approximately 2 for the temperature range expected in the PBR fuel balls. Table 7.5 gives the factors by which the room-temperature thermal conductivities are reduced for several unfueled graphite specimens, as reported in ref. 9.

¹¹One megawatt day per adjacent ton is defined as the amount of reactor radiation received by a sample in the Hanford reactors during the time required for the ton of uranium adjacent to the sample to generate one megawatt-day of fission energy.

Table 7.5. Reduction Factors for the Room-Temperature Thermal Conductivity of Graphite Irradiated At Various Temperatures

Grade	Irradiation Temperature (°F)	Reduction Factor for Exposure of 1000 Mwd/AT	Reduction Factor for Exposure of 3000 Mwd/AT
CSF	86	31.7	41.3
CSF	752	4.1	5.5
CSF	932	3.2	4.0
TSGBF	1382		2.0

Assuming that fueled graphite behaves similarly to unfueled graphite and that the effect of irradiation on the thermal conductivity measured at high temperatures is approximately the same as the effect on thermal conductivity measured at room temperature, the data in Table 7.5 substantiate the results given in ref. 10 and again indicate that the thermal conductivity in the PBR fuel elements will be decreased by a factor of not more than 2 during fuel element lifetime. Based on the value of 15 Btu/hr·ft·°F from Table 7.4, the value after irradiation will be approximately 8 Btu/hr·ft·°F. This value may be slightly high because of incomplete graphitization.

The tensile strengths of the Los Alamos fueled and unfueled graphite specimens are given in ref. 4, and the applicable data are summarized in Table 7.6. The values are for a direction parallel to the grains. Although it is not apparent in Table 7.6, the data presented in ref. 4 do not indicate any obvious relationship between ultimate strength and uranium content up to 0.35 g/cm³ of uranium. The strength of graphite increases with irradiation, and the modulus of elasticity increases in approximately the same proportion. When elastic thermal stress calculations are made and the calculated stresses are compared with the stress required for rupture, the ratio is essentially independent of the accumulated dose. Hence, the net effect of irradiation may be neglected. A similar situation exists because of graphitization, since both the

Table 7.6. Ultimate Tensile Strengths of Pure and Uranium-Loaded Graphites

Specimen	Fuel Content (wt %)	Ultimate Tensile Strength (psi)	
		At Room Temperature	At 1832°F
CK	0	1500	2100
LDH	6.7	1500	1800
LDC	13.1	1700	1800
LDP	39.0	1500	1550

modulus of elasticity and the strength decrease with the amount of graphitization. In accordance with these observations, the ultimate tensile strengths and moduli of elasticity for the unirradiated graphite specimens listed were considered to be applicable. The strength of the PBR fuel elements was therefore assumed to be within the range of 1500 to 2500 psi.

The data given in ref. 5 do not indicate any obvious relationship between the modulus of elasticity and the uranium content in fueled graphites. In this study a value of 1.5×10^6 psi was used.

Discussion of Results

On the basis of available physical properties, rupture-elongation data, and the present knowledge concerning graphite behavior, it must be concluded that failure can occur as a result of large steady-state thermal stresses. The probability of failure depends on the ability of the graphite to withstand deformation without rupture.

Early attempts were made at Oak Ridge to correlate calculated graphite thermal stresses with fracture without success.^{12,13} The tests were run using specimens made from KS graphite and from graphitized and non-graphitized uranium impregnated graphite (5 wt % U). The maximum stress conditions that could be obtained with the equipment used did not cause thermal rupture. The maximum temperature for each specimen was maintained at 2500°F. The maximum calculated thermal stress for the KS graphite specimens, using room-temperature properties, was 3090 psi. The maximum calculated stresses in the uranium-impregnated samples tested were 2930 psi for the graphitized specimens and 3420 psi for the nongraphitized specimens.

¹²A. R. Crocker, "Thermal Stress Tests of KS Graphite," NEPA 1125-EXR-2 (July 19, 1949).

¹³A. R. Crocker, "Thermal Stress Tests on 5% Uranium Impregnated Graphite," NEPA 1369-EXR-7 (September 1949).

These calculated stresses are above the room-temperature ultimate strengths for the materials tested. However, these stresses were probably overestimated, since isotropic behavior of the material was assumed and materials properties were chosen that result in high stress predictions. No conclusions can be drawn regarding the thermal-rupture criterion, since the actual stresses were probably within the range of the ultimate stresses reported.

In establishing a thermal-rupture criterion, it should be remembered that a basic difference exists between thermal and mechanical stresses. The strain is the controlling factor in the first case, and the stresses are induced by the strains according to some stress-strain relationship. In the latter case, the stresses within the body are those required to maintain equilibrium between internal forces and applied loads. Thus, the load is the controlling factor, and, for a simple member, the stress is obtained directly from the applied loads by the use of statics. A uniaxial tensile test provides one example. An accurate prediction of thermal rupture from uniaxial tensile data thus depends upon the validity of the assumed relationship between stress and strain.

Graphite is an anisotropic material that exhibits both nonlinear elastic and plastic deformation before fracture. Thus, if thermal stresses are calculated using linear, elastic theory and the modulus (or moduli) of elasticity at zero strain, the calculated values will be higher than the actual stresses. Conversely, the calculated strains may not be conservatively calculated, and caution must be used to insure that the rupture strains are given proper recognition.

The rupture curves for PBR fuel balls were derived by ignoring irradiation effects upon mechanical properties and the probability that creep will occur. This course was taken because, as mentioned above, the strain is the controlling factor in thermal stresses and the integrity of a body depends upon its ability to absorb strain. The changes in material behavior due to irradiation alter the stress-strain relationships, but no increase in rupture strain has been reported.

From the data presently available, it is apparent that the uncertainty in the thermal conductivity values equals or exceeds the uncertainty associated with the ultimate tensile strength values. This fact suggests that primary emphasis should be placed upon accurately determining this quantity as a function of irradiation and the other factors which have significant influence. In addition, a test program should be initiated to provide thermal-rupture data which will form a basis for making accurate theoretical predictions. On the analytical side, mathematical models should be developed for accurately evaluating both elastic and plastic behavior of bodies made from anisotropic materials.

8. STEAM GENERATORS

The basic design requirements for a steam generator suitable for operation with a gas-cooled pebble-bed reactor power plant were outlined in the PBRE report¹ and are summarized below:

1. The steam generator unit must be capable of producing high-temperature high-pressure steam.
2. The reliability of the steam generator is of paramount importance.
3. It must be possible to block off tubes from a point outside the shield in the event of tube leaks.
4. The design should enhance removal of afterheat by natural convection.
5. The design should be such as to minimize plant gas piping and shielding requirements.
6. The unit should be readily fabricable.

The 330-Mw(e) reactor system incorporates two steam generators, each 8.5 ft in outside shell diameter and approximately 70 ft high. The units are located as shown in Figs. 3.1 and 4.4. The use of two units eases the problems of leak detection and makes possible the isolation of a unit in the event of a tube failure.

A once-through steam generator was selected to minimize the number of tube penetrations through the heat exchanger shell. In addition, a once-through design permits a higher feedwater temperature to the steam generator than is possible with a recirculating unit, and this, in turn, is reflected in a higher plant thermal efficiency. A limitation, perhaps not generally recognized, on gas-cooled reactor power plants involves the requirement for reducing return gas temperatures to values normally below the optimum feedwater temperatures for the most modern steam power plants. In the present design the feedwater temperature to the steam generator is 400°F, whereas a comparable conventional plant operating at similar conditions would employ additional feedwater heaters

¹"Preliminary Design of a 10-Mw(t) Pebble-Bed Reactor Experiment," ORNL CF-60-10-63, November 1, 1960, chap. 12.

and might operate with feedwater temperatures well in excess of 500°F. This limitation on maximum feedwater temperature, because of minimum gas temperature requirements, results in a lower thermal efficiency.

General Considerations for Steam Generator Design

The exterior shell geometry and the size of the steam generator unit were significantly influenced by basic boundary conditions of the reactor plant. The conditions most closely affecting the steam generator design were (1) the decision to employ an integral pressure envelope for the steam generator and the reactor vessel, (2) the steam generator height required to achieve natural convection for decay-heat removal, (3) requirements for access room and control-rod space on the top of the reactor vessel, and (4) the limitation on the steam generator height imposed by the overhead crane, containment shell considerations, and structural stability under lateral shaking forces.

The design selected is shown schematically in Fig. 8.1. Gas from the reactor core is directed through an entrance nozzle to the central circular upflow pipe of the steam generator. At approximately two-thirds of the vessel height, the gas passes through a transition piece to a square section containing the reheater of the generator unit. At the top of the vessel, turning vanes reverse the gas flow downward around the outside of the reheater shroud and into the main tube annulus. The gas is directed parallel to the superheater, boiler, and economizer tubes and countercurrent to the tube-side flow. Cool gas from the core inlet is directed up the cooling annulus between the shell and a layer of thermal insulation designed to maintain shell temperatures below 600°F. The annulus gas discharges into the main helium stream at the top of the steam generator unit.

The decision to employ an upflow core and limit the core pressure drop to prevent core levitation reduced the ratio of core pressure drop to total system drop. The maximum permissible system pressure drop was selected for good removal of afterheat by thermal convection. The

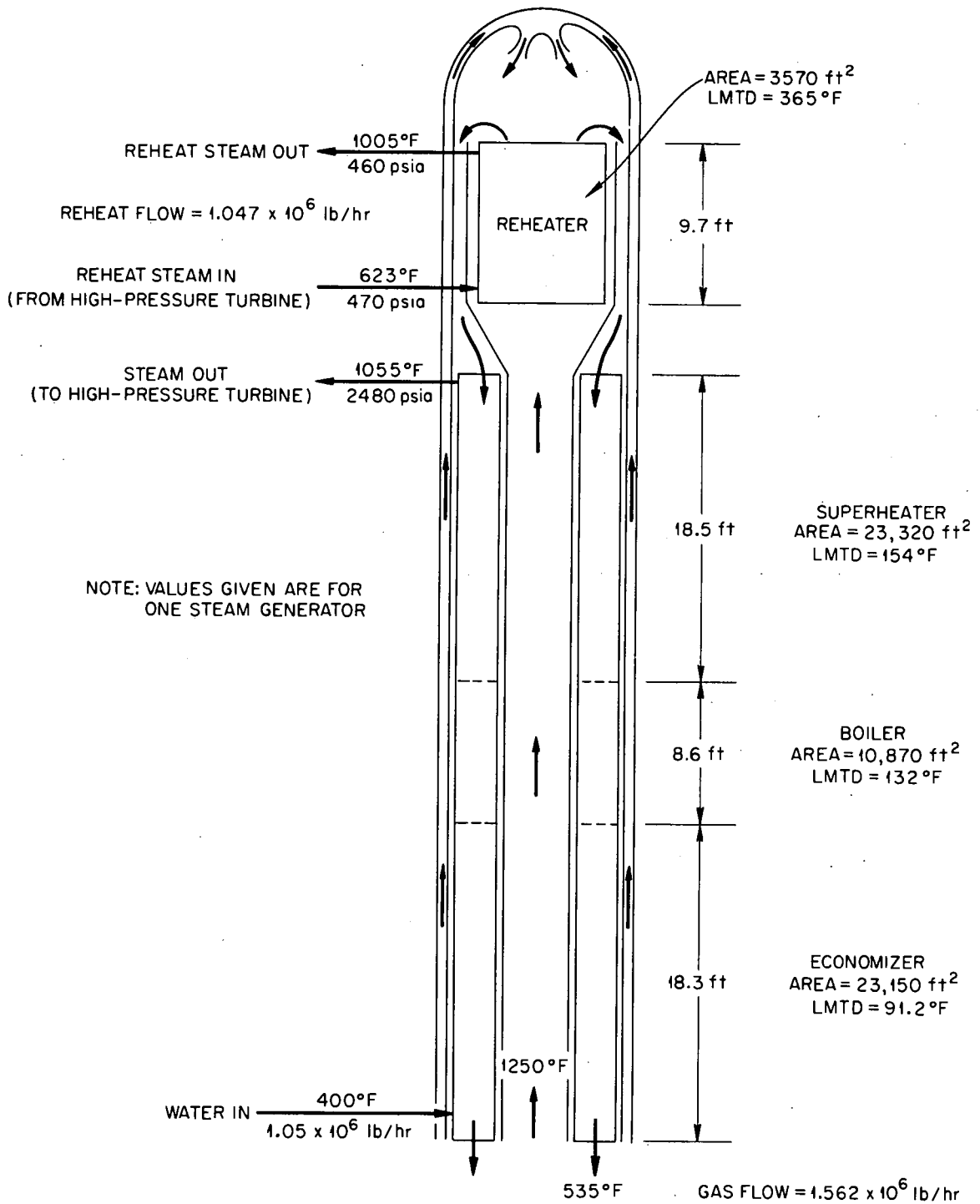


Fig. 8.1. Schematic Diagram of Steam Generator.

reduction in pressure losses in the core permitted a more liberal pressure drop in the steam generator while still keeping the over-all reactor system pressure drop below the limiting value for adequate thermal convection. The steam generator was designed so that the gas pressure drop would not exceed 50% of the total system drop.

Steam and Gas Conditions in the Steam Generator

Table 8.1 and Figs. 8.1 and 8.2 summarize the pressures and temperatures of the fluids entering and leaving the steam generator. The requirement of the added heat from the blowers necessitates a gas temperature of 535°F leaving the steam generator to achieve a 550°F core inlet temperature. The two turbine drives for the blowers utilize approximately 300 000 lb/hr of steam between the superheat and reheat steam pressures. The discharge steam from the drive turbine and the high-pressure turbine generator discharge steam mix and return to the reheat section of the steam generator.

Table 8.1. Gas and Steam Conditions in Steam Generator.

Helium	
Flow per generator, lb/hr	1.56×10^6
Inlet temperature, °F	1250
Outlet temperature, °F	535
Pressure drop, psi	9
Steam	
Flow per generator, lb/hr	1.05×10^6
Feedwater inlet temperature, °F	400
Feedwater inlet pressure, psia	2550
Superheated steam outlet temperature, °F	1055
Superheated steam outlet pressure, psia	2480
Reheater inlet temperature, °F	623
Reheater outlet temperature, °F	1005
Reheater inlet pressure, psia	470
Reheater outlet pressure, psia	460

UNCLASSIFIED
ORNL-LR-DWG 54428

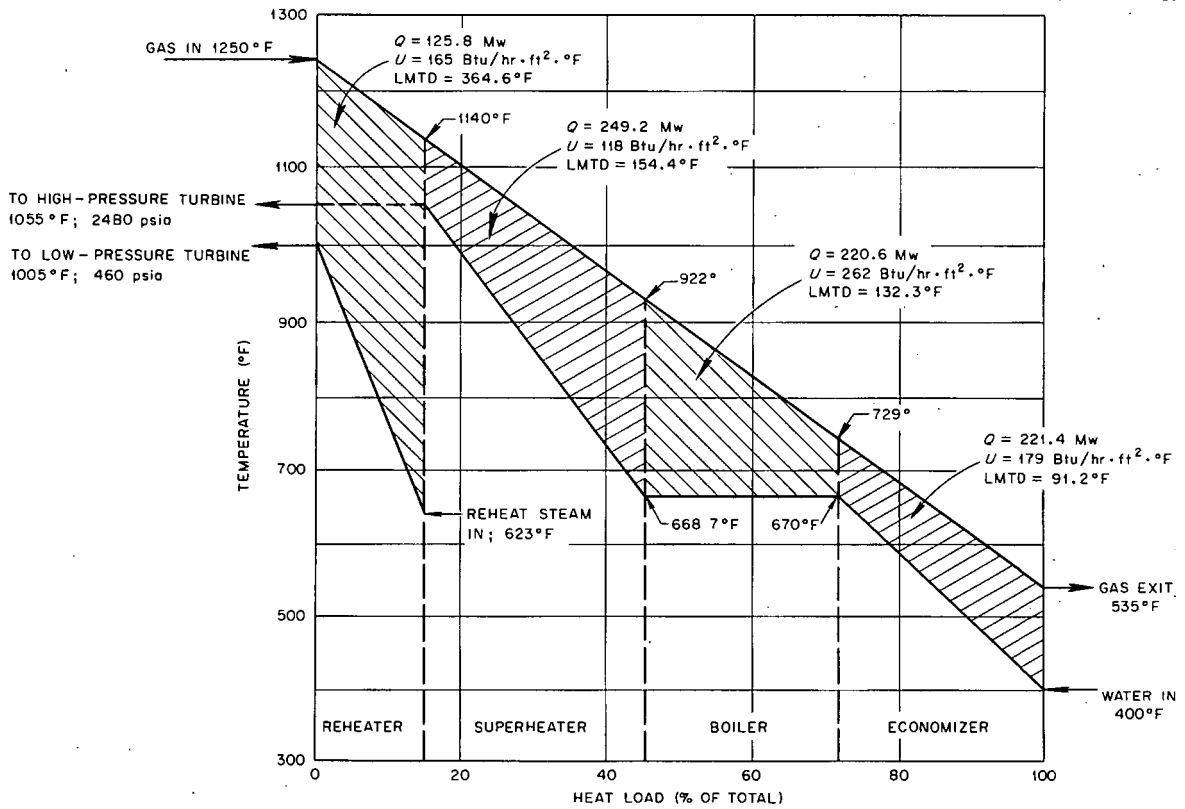


Fig. 8.2. Helium-Steam Temperature Diagram for PBR Steam Generators.

Steam Generator Geometry

The favorable heat transfer properties of helium and the high mass velocities permissible through the steam generator make extended surfaces of doubtful value. An analysis of the heat exchanger performance under a number of design conditions indicated that a unit utilizing bare tube surfaces could be designed to meet the necessary performance requirements. Accordingly, no extended surface tubing is used in the proposed design. Specific design parameters for the steam generator are given in Table 8.2.

Water enters the feedwater drum at 400°F and passes into the shell through 1 3/4-in.-diam feeder lines. These feeder lines terminate in 6-in. spherical headers serving 61 tubes 5/8 in. in diameter arranged in a hexagonal tube bundle, as indicated in Fig. 8.3. Time has not permitted the development of a suitable layout, and therefore the tubes are vertical within the heat exchanger. They terminate at the top in spherical steam headers identical to the lower feedwater headers. The superheated steam passes from the spherical steam headers through collector tubes to the superheater drum. The proposed design utilizes approximately 7700 tubes 5/8 in. in diameter. Approximately 125 header and shell-wall penetrations are required at the entrance to the economizer section and a like number at the superheater exit. Tubes near the inner and outer peripheries that cannot be accommodated in the hexagonal tube bundles are fed by special headers.

Thermal expansion loops on the feedwater line and superheater tubes are provided in the primary section of the steam generator. The tube bundles are hung from support cradles on the expansion loops in the superheater section. The support cradles are, in turn, tied to the vessel wall. Thus the individual tube bundles are free to move independently in a vertical direction and are permitted limited relative lateral motion before contacting adjacent bundle spacers. The tube bundle spacers are tied to apex points of the hexagonal bundle.

Table 8.2. Design Data for One Once-Through Steam Generator

	Economizer, Boiler, and Superheater Section	Reheater Section
Flow scheme	Axial counterflow of gas outside tubes	Cross flow
Tube outside diameter, in.	0.625	1.75
Tube inside diameter, in.	0.400	1.62
Tube material	Carbon steel in economizer, low-alloy Cr-Mo steel in boiler, high-alloy stainless steel in superheater	High alloy stainless steel
Number of tubes	7700	200
Tube spacing and arrangement	Equilateral pitch, 0.875 in. on centers	Transverse spacing, 2.5 in.; longitudinal spacing, 1.875 in. (staggered)
Upflow pipe diameter, ft	3.25	
Dimensions of tubed sections, ft	3.25, i.d.; 7.58, o.d.	5.25 square
Tube length, ft	45.5	50
Straight height of each section, ft	18.3, economizer; 8.6, boiler; 18.5, superheater	9.7
Estimated over-all shell height, ft	70-75	
Gas mass velocity, lb/sec.ft ²	22.8	50.1
Shell-side area (total, 61 000), ft ²	23 200, economizer; 10 900, boiler; 23 300, superheater	3580
Water-side mass velocity, lb/sec.ft ²	43.4	98.7
Log mean temperature difference, °F	91.2, economizer; 132, boiler; 154.4, superheater	~365
Heat load (total = 1.39×10^9), Btu/hr	3.78×10^8 , economizer; 3.76×10^8 , boiler; 4.25×10^8 , superheater	2.15×10^8
Heat load as percentage of total load, %	27.1, economizer; 27.0, boiler; 30.5, superheater	15.4
Gas-side heat transfer coefficient, Btu/hr.ft ² .°F	330	652
Tube-side heat transfer coefficient, Btu/hr.ft ² .°F	708, economizer; 5000, boiler; 334, superheater	293
Heat flux (outside area), Btu/hr.ft ²	16 300, economizer; 34 500, boiler; 18 200, superheater	60 000
Over-all heat transfer coefficient, Btu/hr.ft ² .°F	179, economizer; 262, boiler; 118, superheater	165

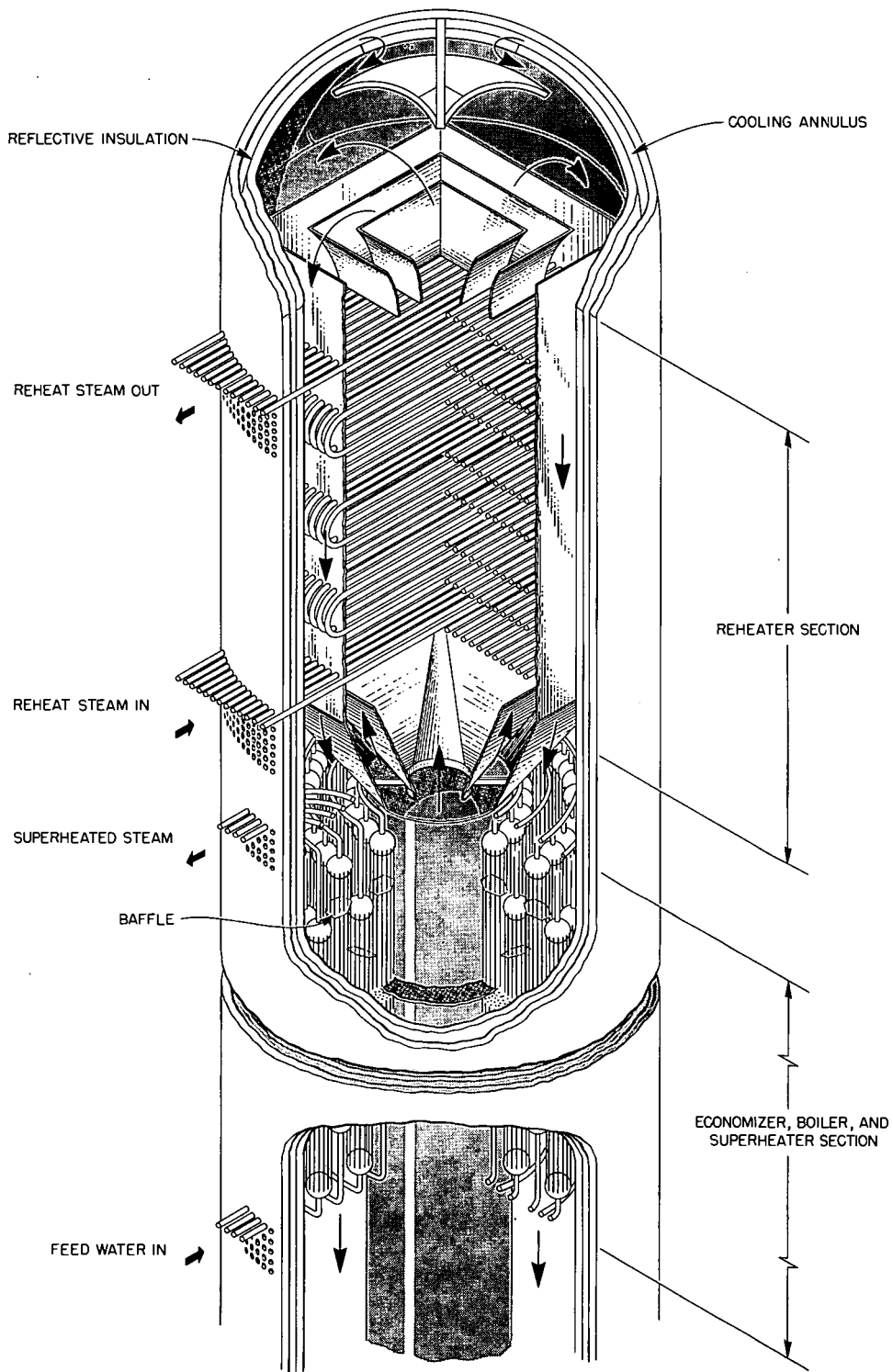


Fig. 8.3. Sketch of PBR Steam Generator.

In order to avoid the complication of an additional header system or an excessive number of shell penetrations, the reheater section is designed as a serpentine coil, as shown in Fig. 8.3. The reheater section is housed in a 5.3-ft square shroud with the serpentine tubes of the reheater section supported from the hemispherical dome. Reheat steam from the high-pressure turbine enters the reheat section through a bank of eight rows of tubes having 25 tubes per row. Thus 200 tube wall penetrations are required at each end of the reheat section. Gas from the upflow pipe passes through the transition piece to the reheat section. Guide vanes are required in the transition piece to prevent localized high-impingement gas velocities and poor gas flow distribution across the reheater tubes.

It is estimated that approximately 4 ft of shell height will be required for accommodating thermal expansion loops and interior headers on each end of the primary section. Approximately 2 to 3 ft will be required for the upflow transition piece. The over-all steam generator shell height is estimated to be 70 to 75 ft.

Some modifications in the design may be required to achieve boiling stability in the steam generator, but time did not permit analysis of this aspect. The use of vertical tubes in the boiler region gives a distinct advantage from this standpoint.

Leak Detection and Maintenance Procedures

The use of two steam generators separately housed permits the incorporation of moisture-detectors in the exit gas stream leaving each unit. Upon an indication of a tube leak in a steam generator unit, the reactor would be shut down and the water and steam lines to the failed unit blocked off. Repair would be accomplished by entering the header drum and plug welding the feeder line to the tube bundle containing the failed tube. Thus repair of the failure of a single heat exchanger tube would render inoperative 61 heat exchanger tubes or 0.39% of the total reactor steam generator capacity.

It is important in the heat exchanger design to consider the effect of an inoperative tube bundle on over-all unit performance. The presence of plugged-off tube bundles would normally result in a stream of un-cooled gas passing the entire length of the primary tube section. To prevent channeling of this nature, spacer baffles are provided in each tube bundle, as shown in Fig. 8.3. These baffles divert the gas flow to adjacent tube bundles and alleviate the problem of hot channeling.

The pressure gradient between the steam and helium system will result in steam leakage from the once-through boiler into the gas system and gas leakage into the reheater under design conditions. In the event of a tube failure, the reactor would be shut down and the steam and gas system pressures reduced in such a way as to maintain a small pressure difference between them. Contaminated helium could thus be prevented from entering the steam system in order to avoid a need for decontamination.

9. BLOWERS AND DRIVES

Two single-stage centrifugal blowers will be used to circulate helium through the reactor. The design operating conditions are:

Flow rate per blower	434 lb/sec 100 750 cfm
Suction temperature	535°F
Required head	6800 ft 12.2 psi
Pumping power per blower	4000 kw

These blowers, in contrast to those required for the PBRE,¹ are high-volume-flow low-head units and will probably be of a mixed-flow design. As a compromise between specific speed and size the following compressor design was established:

Impeller outside diameter	48 in.
Rotative speed (maximum)	3000 rpm
Specific speed	1250
Estimated over-all efficiency	70%

The compressors also serve as two of the three support points for the reactor vessel. A design to accomplish this is shown in Fig. 9.1. Use is made of a vertical shear web welded to the inlet and outlet pipes and a portion of the compressor casing along the midplane of these components. This plate transfers the weight load to a roller to allow for thermal expansion of the reactor vessel and ducts. The compressor is driven by a splined quill shaft to provide for the associated movement of the compressor.

¹"Preliminary Design of a 10-Mw(t) Pebble-Bed Reactor Experiment," ORNL CF-60-10-63, November 1, 1960, chap. 13.

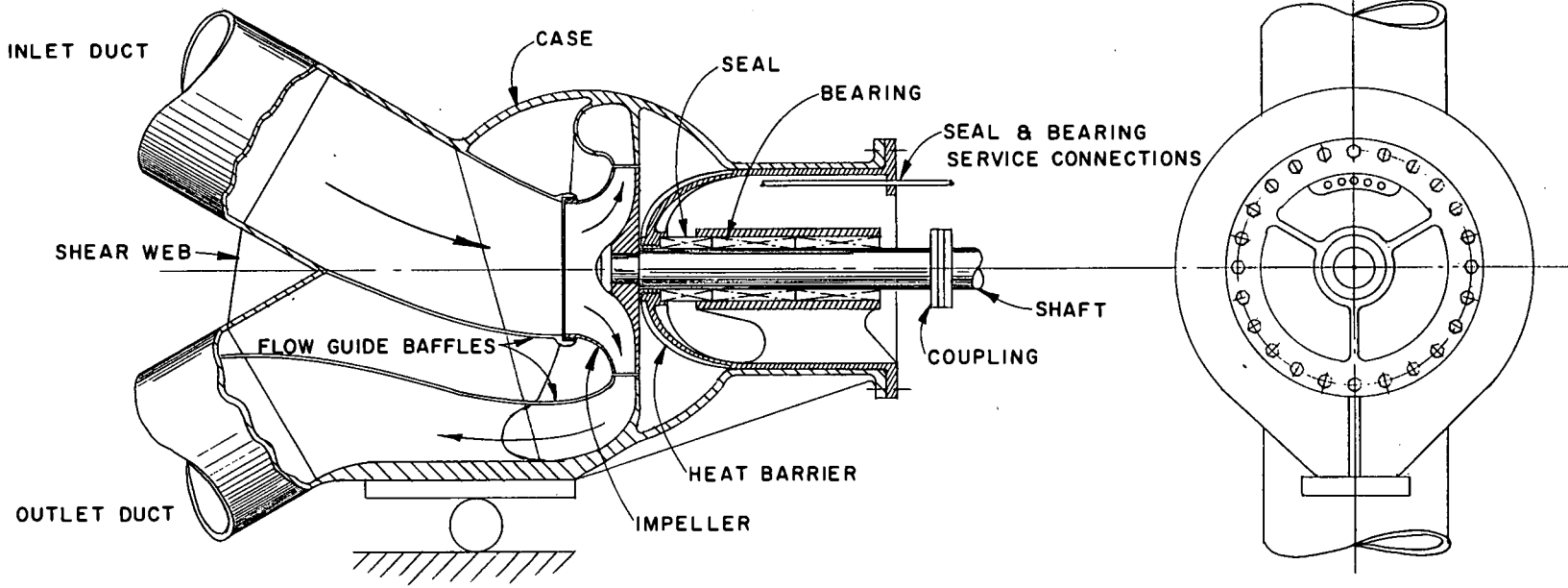


Fig. 9.1. Schematic Diagram of Blower for PBR.

Maintenance of the compressor would be accomplished by first removing the quill shaft between the compressor and the turbine drive. The flanged plug assembly containing the shaft, bearings, seal, and impeller would then be removed and replaced. The shaft seal and flange seal would be similar to those suggested for the PBRE.

Since the blower power required will be about 7200 hp per blower and flow control by blower-speed variation is desirable, steam turbine drives appeared to fit this application. Accordingly, a steam turbine drive together with a pony motor for plant shakedown tests have been sized to drive the compressor. The turbine is located behind concrete shielding, as shown in Fig. 4.6, and thus is available for direct maintenance. In order to use standard mechanical-drive turbine components, inlet steam at 2400 psia and 1050°F will be desuperheated to about 900°F with boiler feedwater at 400°F. The turbine will exhaust to the reheater where the steam will be combined with the reheat steam from the main turbine. This system was chosen to give a small turbine and avoid additional penetrations through the containment shell. A steam flow rate of about 165 000 lb/hr per turbine is required, assuming a turbine efficiency of 70%.

A startup motor is connected to the end of the drive turbine. In order to provide a substantial gas flow rate for shakedown testing, the motor was designed to give a gas flow of 10% of the design value, which requires a motor of approximately 50 hp for each blower.

10. BALL-HANDLING SYSTEM

The core layout of Fig. 3.1 represents a first attempt to indicate one approach to the design of a pebble-bed reactor for a large power plant, with particular attention given to the graphite shrinkage cracking problem. One of its principal values is that the resulting layout brings to light quite a number of ball-handling problems that had not been anticipated. The present design and the development problems anticipated for this and related designs are discussed here.

Ball Loading

The fuel-loading arrangement shown in Fig. 3.1 consists of two sets of ball ducts leading to the top of the reflector from the floor above the reactor. Twelve equally spaced feeders for 1 1/4-in.-diam unfueled balls are located on a circle at the core perimeter. The 2 1/2-in.-diam fueled balls are added at seven locations; one feeder is at the center of the core and six are spaced equally on a circle over the fuel bed. The individual ball-loading devices for these 19 positions could be designed as suggested in the PBRE report.¹

It is not clear how the top of the core should be shaped to give both good filling and good flow distribution for both the fueled and unfueled balls. The problems introduced by the use of two ball sizes and regions appear to be much greater than was anticipated when the layout of Fig. 3.1 was initiated. Not only does it appear to be difficult to maintain a uniform thickness of the unfueled ball layer, both circumferentially and axially, but there may be difficulties with the fueled balls mixing with unfueled reflector balls and vice versa. Both types of intermixing are to be avoided, since large fueled balls in the reflector region would not be sufficiently cooled, and small unfueled balls in the fuel bed would obstruct the coolant flow.

¹"Preliminary Design of a 10-Mw(t) Pebble-Bed Reactor Experiment," ORNL CF-60-10-63, November 1, 1960, chap. 14, esp. Fig. 14.2.

Since balls cannot be used for the inner layers of the top and bottom reflector regions in continuously fueled cores, these will require replacement by some sort of servicing machine during extended shutdowns for such operations. This being the case, it appears that it would be better to design for replacement of the inner layer of the side reflector at the same time with the same machine rather than to attempt to line the reflector with unfueled balls. Such a provision would greatly simplify the design of the ball-handling system and would remove the basic uncertainties introduced by an uncontrolled interface between two ball regions. Several reflector structures could be considered. A variation of the graphite rod cluster suggested in Fig. 3.2 for the top and bottom reflectors might be employed, or a wall of graphite blocks might be designed for easy removal and replacement by a "brick-laying machine." These and other concepts should be carefully considered before a core design is selected.

Ball Removal

For a cylindrical core of relatively small diameter, such as that described by Sanderson & Porter,² preliminary experiments suggest that, by careful experimentation and design, a favorable radial distribution of ball flow rate through the core can be achieved with one central ball feed tube at the top and one central drain tube at the bottom. For the much larger cores and much smaller core length-to-diameter ratios of interest here, a single centrally located drain port for spent fuel balls will probably not be sufficient, and the zoning of the round core support grid to accommodate six ball drain ports creates noncircular "funnel zones." There are few experimental data to demonstrate the extent or type of ball flow control which can be induced by contouring these funnels in various ways, but it does appear that the bottom of the core should slope toward the exit port at an angle of at least

²Sanderson & Porter, "Pebble-Bed Reactor," S & P 1963.

15 deg relative to the horizontal. An investigation of this problem represents a major test and development item, even for a core containing only uniformly sized fuel balls, and an indeterminately greater effort for a core with two ball sizes in separate zones.

The general arrangement contemplated for the design of Fig. 3.1 employs six ball drain ducts similar to that shown in the PBRE report.¹ By arranging the drain ducts into two groups of three to route the balls outward to opposite sides of the reactor vessel, as shown in Fig. 4.7, the central area under the reactor is kept clear for the service machine, and accessibility to each of the six drainage systems should be good.

Development Problems

The problems of ball flow through the core can be approached effectively only by experimentation. The initial work should be directed at the problems of obtaining a favorable ball flow distribution across the core with multiple feed and drain points. The tests should include ball-feeding devices that will introduce balls into the core at a low velocity to avoid the sort of damage encountered in the Sanderson & Porter tests carried out at Babcock & Wilcox.³ The effects of the core-reflector interface geometry, including several different angles of inclination away from the feed points at the top and toward the drain points at the bottom, should be investigated, together with devices such as V-shaped valleys radiating from each drain point, as shown for the bottom of the core of Fig. 3.1.

After the basic work on single-region cores has been completed and a satisfactory design developed, the situation should be reviewed to determine whether it would be advisable to attempt to develop a two-region core with two ball sizes. If so, the first step would be to determine the extent to which the thickness of an outer layer of smaller diameter balls can be kept constant. The effects of the number and location of feed points and relative ball flow through individual feed points for both unfueled and fueled balls should be determined. Irregularities in the thickness of the unfueled region, both circumferentially and axially, would have to be checked by following

³C. A. Leeman, "Pebble Bed Friction Factor and Thermal Expansion Tests," B & W Research Report No. 4316, NYO-9069, Aug. 31, 1960, p. 15.

some particular loading and feeding procedure and then unloading the bed from the top while taking pictures as each successive layer is removed. If the results are to be significant, the scale of the model should be at least one-quarter that of a full-scale core, which would give 5/16-in.-diam balls in the reflector and 5/8-in.-diam balls in the core. At least two or three different geometries for the top and bottom reflector would probably have to be tested to obtain a good idea of the feasibility of the two-region bed concept.

Some sort of servicing machine would have to be developed for maintaining the fuel-handling system and replacing the graphite in the upper, lower, and (probably) side reflector regions. Servicing equipment for the fuel-handling system will entail the use of moving parts in high-temperature zones subject to intense radiation. Much experimental work must be carried out on bearings, gears, feed screws, and other devices to establish a good basis for the design of such equipment.

Developmental work will also be required for components of the ball-handling systems. Devices such as valves for ball feed and drain lines, ball cutoff and counting mechanisms, and the ball-withdrawal assemblies for the bottom of the core will require design, development, and test work. These latter assemblies, in particular, will require special attention because their locations at or near the core boundary will subject them to conditions which will make both materials selection and design difficult. Since the ball-removal assemblies would probably contain moving parts and would stay in place in the core during operation, the design problems will be particularly difficult because of the radiation field.

In comparing the above problems with those of the Dragon and the HTGR to give perspective, it appears that many of the problems are common to all-ceramic reactors and that the pebble bed concept should make possible a simplification of both the fuel handling machinery and the fuel handling operations.

11. HELIUM PURIFICATION SYSTEM

The purification system for the helium coolant includes provisions for removing gaseous and particulate impurities, both radioactive and nonradioactive. The process is essentially the same as that proposed in the PBRE report,¹ in which a discussion of the chemistry involved is presented.

A sidestream of helium is withdrawn from the circulating loop at the discharge of one of the helium compressors, and it re-enters the main stream at the compression suction; thus advantage is taken of the pressure rise through the compressor to drive the gas through the cleanup system. The system has been sized to remove impurities evolved from the graphite, including hydrogenous gases, CO₂, and CO, equivalent to an inleakage of 50 lb/day. The normal steam inleakage by diffusion through the steam generator is estimated to be about 3 lb/day, and the rate of graphite outgassing after the first month of operation is expected to yield gases equivalent to between 5 and 20 lb of water per day, depending on the temperature experience of the graphite during the first month.² The extra capacity is provided for operational flexibility and as a cushion in an emergency. Although the economically optimum impurity level is not known, the system has been designed to hold the impurity concentration down to 30 ppm at the maximum inleakage rate by essentially complete removal of impurities from a bypass stream having a flow rate equal to 1% of the flow rate of the main coolant system.

A flow sheet of the proposed system is shown in Fig. 11.1. The temperature of the helium sidestream, which is withdrawn from the cold end of the circulating system (550°F), must be raised to 750°F before

¹"Preliminary Design of a 10-Mw(t) Pebble-Bed Reactor Experiment," ORNL CF-60-10-63, November 1, 1960, chap. 16.

²"Gas-Cooled Reactor Project Quarterly Progress Report for Period Ending September 30, 1960," ORNL-3015, pp. 125-36.

UNCLASSIFIED
ORNL-LR-DWG 54380

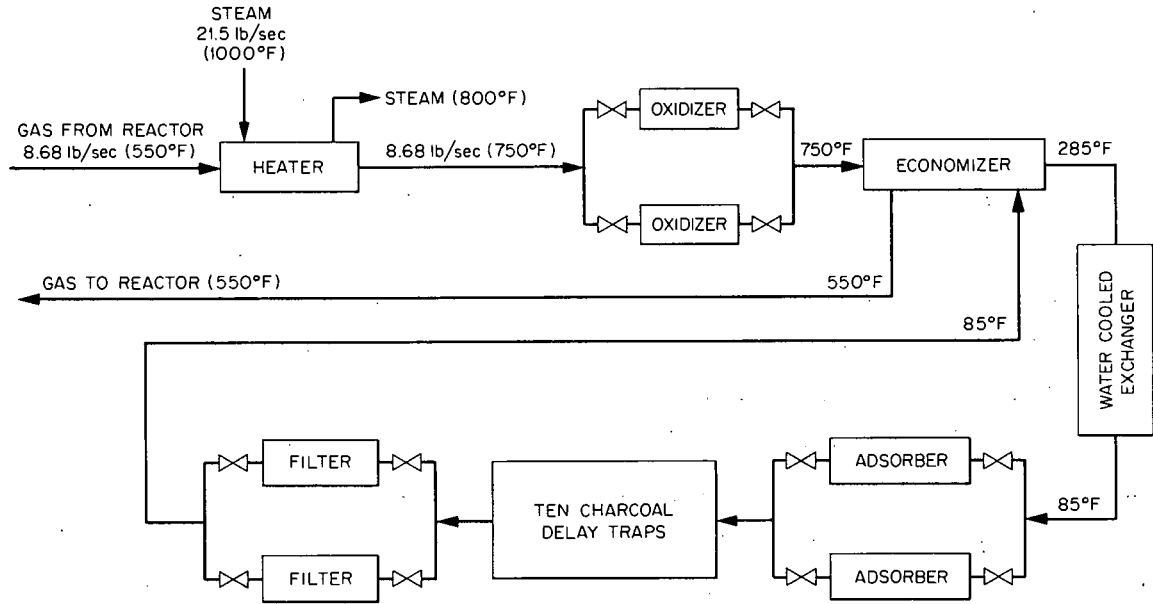


Fig. 11.1. Helium Purification System.

catalytic oxidation of hydrocarbons, hydrogen, and carbon monoxide will occur. The temperature is raised by passing the gas through a countercurrent heat exchanger heated by a small stream of reheat steam, which then passes to the feedwater heaters. The heater is a typical tube-and-shell heat exchanger with about 166 ft² of heat transfer surface. The heat exchanger shell is about 9 ft long and 10 in. in diameter. Since the sidestream will be operated continuously, duplicate units for the oxidizer, adsorber, and filter are provided so that one unit is onstream at all times, while the other one is being regenerated or replaced. The oxidizers consist of fixed beds of copper oxide pellets (1/8 in. in diameter and 1/8 in. long), each containing 441 lb of copper oxide. The copper oxide container is about 12 in. in inside diameter and 48 in. long; it is surrounded by a heating coil and insulation that bring the outside diameter to 20 in.

The temperature of the hot gas leaving the oxidizer must be reduced from 750 to about 85°F before the gas enters the adsorbers. This is accomplished with a regenerative heat exchanger so that about 70% of the heat is transferred to the cold, clean gas that is to be returned to the main circulating stream. The economizer is a shell-and-tube heat exchanger containing 292 tubes, 3/4 in. o.d., on a 1-in. square pitch. It is about 15 ft long and contains 786 ft² of heat transfer area. After leaving the economizer at 285°F, the gas is water cooled to 85°F in another shell-and-tube exchanger containing 292 tubes, 3/4 in. o.d., on a 1-in. square pitch. Its length is about 17 ft, and it contains 892 ft² of heat transfer surface.

The adsorbers are fixed beds of type-5A Linde molecular sieves. Two units, each containing 714 lb of sieve material, are provided. The sieve container is about 24 in. in inside diameter and 75 in. high. It is wrapped with heating coils and insulation for regeneration, and the resulting outside diameter is about 30 in. From the adsorbers the gas goes to the charcoal delay trap, which consists of 10 beds of 6- to 8-mesh charcoal in series. Each bed contains about 3200 lb of charcoal and is about 24 in. in outside diameter and 35 ft long.

Since the purpose of the charcoal delay trap is to reduce the gaseous radioactivity in the circulating helium, an estimate has been made of the total activity both with and without the delay trap in service in order to obtain the decontamination factor. The values on which the estimate is based are given in Table 11.1.

Table 11.1. Estimated Loop Activity and Decontamination Factors for the Fission-Product Delay Trap

Isotope	Half-Life	Loop Activity Without Purification (curies)	Loop Activity with Purification (curies)	Decontamination Factor
Kr ⁸⁵	10.3 y	1.04×10^5	1.04×10^5	1
Kr ⁸⁷	78 m	2.48×10^2	1.33×10^2	1.86
Kr ⁸⁸	2.77 h	1.6×10^3	8.3×10^2	1.92
Xe ^{131m}	12 d	1.01×10^4	7.44×10^2	13.5
Xe ^{133m}	2.3 d	1.92×10^3	1.6×10^2	12
Xe ¹³³	5.27 d	2.23×10^5	1.71×10^4	13
Xe ¹³⁵	9.13 h	6.97×10^3	6.8×10^2	10.3
I ¹³¹	8.05 d	1.76×10^5	3.2×10^2	556
I ¹³²	2.4 h	1.12×10^5	1.4×10^4	8
I ¹³³	20.7 h	1.92×10^4	3.12×10^2	61
I ¹³⁵	6.68 h	4.56×10^3	2.24×10^2	20.1
Total activity		6.36×10^5	1.39×10^5	

From the charcoal trap the gas goes to either one of two filters for the removal of particulate matter that may have been picked up in the trap. These filters consist of Fiberglas sheets enclosed in steel pressure containers (Flanders type 6C21-C), each about 30 in. in outside diameter and 12 in. in depth.

After leaving the particulate filter at 85°F, the gas is heated regeneratively to 550°F by the hot gas from the oxidizers and returned to the suction side of one of the main blowers.

An advantage of the proposed sidestream purification system is the simplicity of operation. Since there are no moving components, it is expected that the system will be essentially maintenance-free.

It will probably be necessary to regenerate the copper oxide beds and the molecular sieves after each seven days of reactor operation. In order to do this the oxidizer should be removed from service and regenerated with air for approximately 8 hr at operating temperature, whereas the adsorber can be regenerated by purging with dry air at atmospheric pressure and a temperature of 600°F for approximately 8 hr. The life of the delay trap will depend on the poisoning effect of the iodine and some of the daughter products of the fission gases, for which no experimental data are available at the present time. It is expected, however, that the life of the charcoal in the delay trap will exceed several years.

12. STEAM AND ELECTRICAL PLANT

A coal-fired plant designed for completion of construction in 1964 was chosen as a point of departure¹ in order to expedite the design study of the steam and electrical portions of the plant. Some modifications were required, including a reduction in the feedwater temperature, to give a well-proportioned steam generator with the 550°F reactor helium inlet temperature used, and allowances were made for the steam required for the blower drive turbines.

Turbine Plant

A 330-Mw, tandem, compound-turbine-generator unit for indoor service was chosen for the plant, partly because of its lower cost and partly because it gave a favorable layout for the steam piping. The steam conditions are 2400 psig, 1050°F, with a single reheat to 1000°F. The turbine exhausts at 1.5 in. Hg absolute. The generator is rated at 345 000 kva for a 0.85 power factor and a short-circuit ratio of 0.64 and is cooled with hydrogen at 30 psig. The unit is complete, with accessories, including a directly connected exciter, a lube oil system, and a gland sealing system.

Electric-motor-pumps are employed in the feedwater system. A regenerative cycle is employed to heat the feedwater to 400°F. Further heating would increase both the steam-generator capital charges and the blower pumping-power requirements. This system includes six feedwater heaters, with the deaerator preceding the highest pressure heater. Electric motors are used for the boiler-feed-pump drives. The exhaust steam from the blower drive turbines is passed through the reheater and fed to the intermediate turbine.

A flow sheet for the steam plant is presented in Fig. 12.1 to show the principal features of the plant. It may be seen that the

¹Study of a Typical 306 Mw Net Coal-Fired Installation, Contract AT(10-1)-1010 between the Division of Reactor Development, USAEC, and Ebasco Services Inc., April 1959.

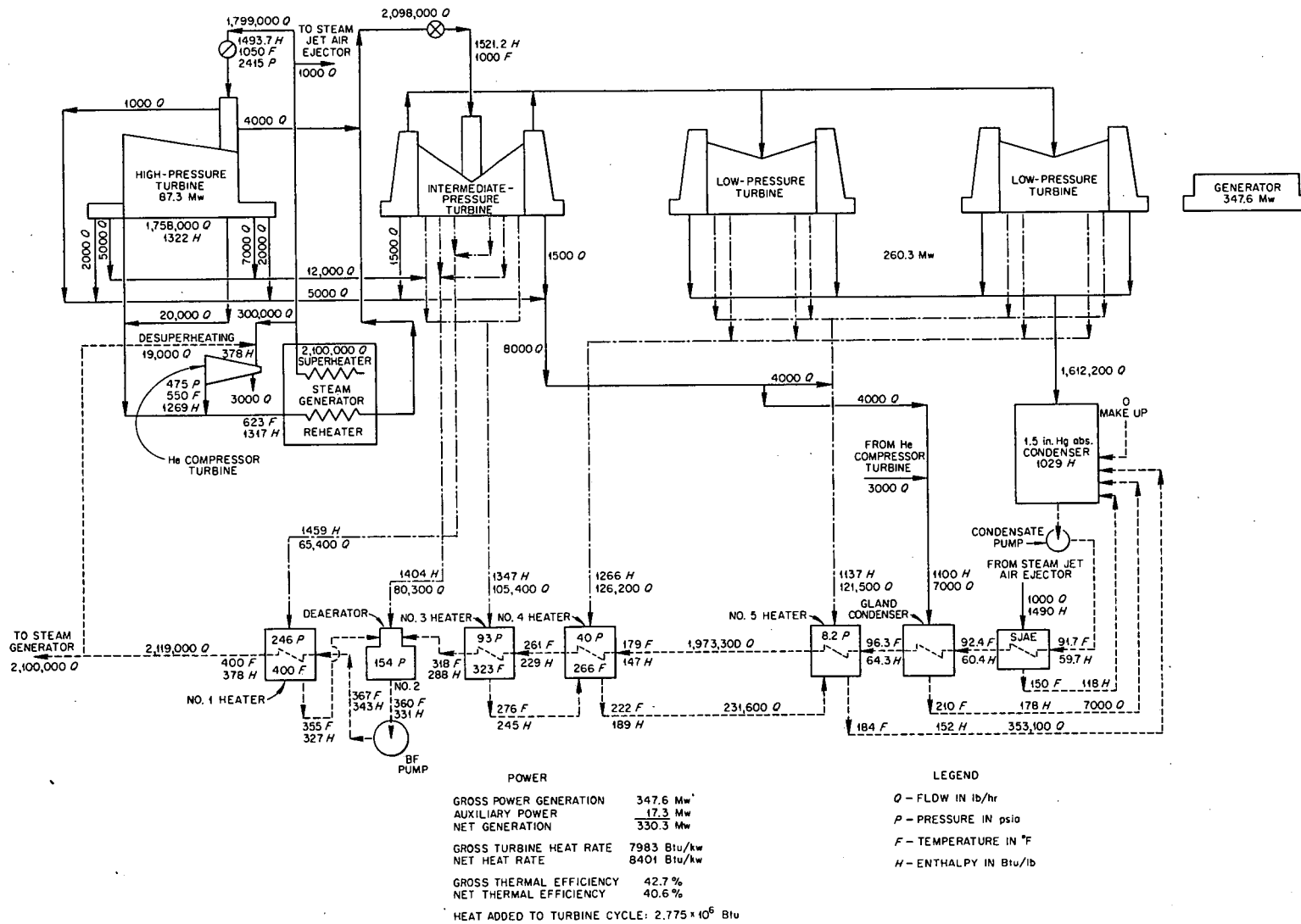


Fig. 12.1. Diagram of Steam and Electrical Plant.

heat balance gives an over-all thermal efficiency close to 40%. No allowances were made for heat losses from the steam generator, since these should be only about 0.1%.

The main condenser is a twin-shell, 150 000-ft² unit employing a two-pass, divided-water-box design. The condenser cooling-water system includes trash racks, traveling screens with wash equipment, and algae control equipment.

The accessory equipment includes isolated phase-generation leads, exciter connections, transformer and cables, control wiring, storage batteries with a charger, an emergency generator set, and station-grounding protection.

Miscellaneous plant equipment includes cranes, cleaning equipment, fire-fighting gear, air-gas-oil facilities, office and laboratory services, tools, and communication provisions.

The outdoor switch yard includes an oil circuit breaker, disconnect switches, and relaying devices. A single transmission-line takeoff is provided.

A cost estimate for the steam and electrical plant is presented in Table 12.1. A summary of these data is presented in Table 12.2, which shows that this portion of the total plant is, as expected, competitive with the best coal-fired plants now under construction.

Table 12.1. Estimated Costs for Steam and Electrical Plant

	Labor	Material and Other	Total
Land	Not estimated here		
Site work			
Improvements	Not estimated here		
Intake and discharge structures ^a	\$100,000	\$ 100,000	\$ 200,000
Buildings			
Turbine	750,000	1,350,000 ^b	2,100,000
Other buildings related to turbine plant	50,000	150,000	200,000
Total			\$ 2,300,000
Power generation			
Turbine generator	500,000	11,350,000 ^c	\$11,850,000
Auxiliaries for turbine	20,000	60,000 ^a	80,000
Condenser with auxiliaries	140,000	1,260,000 ^a	1,400,000
Circulating-water system	150,000	350,000	500,000
Pedestal ^a	60,000	100,000	160,000
Total			\$13,990,000
Feedwater and steam supply systems			
Equipment			\$ 1,750,000
Piping			1,750,000
Total			\$ 3,500,000
Accessory Electrical Equipment			
Panel boards	5,000	255,000	\$ 260,000
Controls	120,000	760,000	880,000
Direct-current gear	10,000	26,000	36,000
Connections and supports	250,000	280,000	530,000
Diesel-generators	5,000	15,000	20,000
Total			\$ 1,726,000

^aTypical 306-Mw net coal fired station, EBASCO Contract AT(10-1)-1010.

^bEstimated on 7 ft³/kw (Elec. World, Oct. 5, 1959) with \$1/CF total cost charge.

^cWestinghouse price list 1252 (September 28, 1959), plus 10%.

Table 12.1 (Continued)

	Labor	Material and Other	Total
Miscellaneous Plant Equipment			
Cranes	\$ 15,000	\$ 125,000	\$ 140,000
Station air	35,000	35,000	70,000
Communication	10,000	10,000	20,000
Fire protection	5,000	10,000	15,000
Other	30,000	150,000	180,000
Total			\$ 425,000
Transmission Plant			
Transformers	25,000	750,000	\$ 775,000
Controls	35,000	165,000	200,000
Connections and supports	30,000	30,000	60,000
Total			\$ 1,035,000

Table 12.2. Summary of Investment Data for 330-Mw-Net Steam and Electrical Plant

	Capital Charges (\$/kw)
Land	Not estimated
Structure and improvements (turbine room only)	7.7
Turbine generator	46.3
Accessory electrical equipment	5.8
Miscellaneous plant equipment	1.4
Transmission plant	3.5
Feedwater and steam system	<u>11.7</u>
Total for steam and electrical plant	76.4

13. HAZARDS ANALYSES

The hazards associated with operation of a reactor include both hazards to the public from the release of radioactivity and hazards to plant personnel during the course of operation. In assessing the hazards to the public, the two conditions of activity release accompanying the maximum credible accident and activity release during normal operation must be considered. A major question relating to the safety of plant employees involves the dose levels to which personnel would be exposed in performing maintenance operations.

Maximum Credible Accident

There has not been a sufficiently extensive hazards analysis made of the PBR to establish the maximum credible accident. The factors of importance can, however, be determined by considering the results of some simplified computations and making comparisons with the PBRE.¹

The maximum credible accident for the PBRE was postulated to be simultaneous rupture of the primary system and the steam system, succeeded by oxidation of all the core and part of the reflector by oxygen present in the containment vessel. Computations indicated that after all steel and graphite had come to temperature equilibrium with the gas, the temperature would be 700°F and the pressure 20 psig. The containment vessel appeared to be capable of withstanding this pressure; hence no attempt was made to justify an assumption of a lesser energy release.

Oxidation of the PBRE core was assumed to release 100% of the noble gases, 50% of the other volatile nuclides (halogens and alkali metals), and 5% of the nonvolatile nuclides to the containment vessel. The amount of fission products present was taken as that associated with a long period of operation at 10 Mw(t). It was further assumed that

¹"Preliminary Design of a 10-Mw(t) Pebble-Bed Reactor Experiment," ORNL CF-60-10-63, November 1, 1960, chap. 19.

fission products would leak from the container in proportion to their concentration (without allowance for deposition) and that all leakage would be at ground level. Even with these conservative postulates, a leakage rate from the container of 0.4% of its volume per day would not result in a dose exceeding 25 rem in an 8-hr period 1000 ft from the reactor.

Making assumptions for the PBR similar to those for the PBRE would lead to more extreme conditions, both with regard to pressure in the containment vessel and the amount of activity which escapes by leakage from the vessel. If all the steel (including the containment vessel), graphite, water, and gases in the PBR came to temperature equilibrium after rupture of the primary system, the temperature would be about 510°F and the pressure about 20 psig. Heat storage in the shield concrete would lower the temperature after a sufficient time, but it was not included because the low thermal diffusivity of heat in concrete makes the heat storage rate low. As shown in Table 13.1, reaction of all free oxygen present with graphite would raise the temperature to 690°F and the pressure to 27 psig. Rupture of one heat exchanger would make the pressure higher by increasing the gas content of the containment

Table 13.1. Effect of Reactor Rupture on Conditions in Containment Vessel After All Steel, Graphite, Water, and Gas Come to Temperature Equilibrium

Event	Temperature (°F)	Pressure (psig)
Rupture of primary system	510	20
Rupture of primary system plus oxidation of graphite	690	27
Rupture of primary system and one heat exchanger	470	30
Rupture of primary system with blowdown of both heat exchangers	400	16

vessel. Rejection of the heat content of the heat exchangers to the condenser by blowdown would relieve conditions, and continued operation of the heat exchangers might help further.

The pressures given in Table 13.1 represent rather high values for which to design a containment vessel of the size specified. If more detailed analyses confirm that such high pressures are credible, pressure suppression schemes may have to be included in the design to protect the containment vessel.

The fission-product activity present in the PBR would be about 80 times that present in the PBRE, but an assumption of oxidation of the core by oxygen from the containment vessel would not result in 80 times the activity release. Whereas there would be more than enough oxygen available to oxidize all the PBRE fuel, all the air in the containment vessel would oxidize less than 5% of the PBR fuel. Combustion of 5% of the core would release fission products associated with 40 Mw of thermal power, if activity is released only from that fuel which actually burns (the energy from the reaction if all stored in graphite in the core and reflector would only raise the graphite temperature about 600°F). Making the same conservative assumptions as those used for the PBRE, a leakage rate from the containment vessel of 0.1%/day would be permissible if the fission products equivalent to 40 Mw(t) were evolved from the fuel.

Much more than 5% of the total activity might be evolved from the core if a large fraction of the fuel melted. A meltdown of the PBR, core, however, is made unlikely, both by provision for emergency cooling and by the low core power density.

Natural circulation of helium will easily remove fission-product decay heat from the core as long as the coolant pressure remains near the design value. The reactor is therefore not likely to be subjected to excessive temperatures when at high pressures, even if both blowers cease to operate. Natural circulation, however, will not remove the decay heat at atmospheric pressure without the occurrence of high gas

and high fuel temperatures. The system is, therefore, designed so that operation of one blower is sufficient for cooling the core in the event of a loss of pressure in the primary system. Overheating of the reactor is thus prevented, even at atmospheric pressure, as long as the heat can be rejected to a heat exchanger.

Simultaneous loss of power to both blowers is extremely unlikely. If the steam supply to the turbine drives were interrupted, the electrically driven pony motors would supply sufficient power to remove the fission-product decay energy. For operation of the pony motors, emergency power generated on the station would be available, as well as power from the distribution system to which the plant would be connected. A station generating 300 Mw of electricity is likely to be connected to other systems by several independent lines, and electricity from any one could be used to drive the helium blowers.

If both blowers failed (which may not be credible) after a rupture of the primary system, the core temperature would rise until the heat loss became equal to the fission-product energy release rate. Heat would be transferred by radiation and natural convection from the outer surface of the reactor vessel and by natural convection inside the reactor. A detailed analysis would be required to determine whether melting of the fuel would occur if no other method of cooling could be supplied. Under any circumstances, however, the large heat capacity of the core will prevent the temperature from rising very rapidly. Allowing for heat storage in the core and reflector graphite, the fission-product energy would raise the core temperature less than 300°F/hr during the first hour after shutdown and more slowly after that. Hence, time would be available for taking emergency action in the event cooling of the core were completely interrupted.

A preliminary examination thus indicates that melting of the core will be extremely unlikely. If, however, a detailed analysis showed melting to be credible, means could be provided for reducing the hazard from the large amount of activity which might be evolved. Limiting the leakage rate from the containment vessel to a very low value is obviously

desirable, but there is a practical limit to what can be achieved. Making provision for escaping activity to be conducted to a high elevation before entering the atmosphere would help. A thin sleeve around the outside of the containment vessel is one possible way of doing this. The dose beyond the plant boundary during an inversion would be reduced perhaps tenfold if the release were at an elevation of 75 ft rather than at ground level.

The concentration of gaseous and suspended activity in the containment vessel would be reduced by the filters in the recirculating building ventilating system. While this might have little effect on the rate of activity escape immediately following an accident, it could considerably reduce the total release during, say, the 8 hr afterward, particularly if adsorbers were added.

Activity Release to the Surroundings Under Normal Conditions

During normal operation of the PBR, air is drawn into the containment vessel for ventilation. Air passing through the shield becomes slightly radioactive from the production of $7.4s\ N^{16}$, $29s\ O^{19}$, and $1.8h\ A^{41}$. In addition, it picks up any gaseous activity accompanying helium leakage from the reactor gas-cooling system. Contamination of the reactor building by these activities is avoided by maintaining the pressure of the air within the shield ventilating and cooling system below that in the rest of the containment vessel. The movement of air toward and into the shield prevents the escape of activity into the areas to which personnel normally have access.

The ventilating air exhausted from the building is passed through a filter and adsorber to minimize the amount of activity released and is then discharged from a high stack to insure dilution of any activity discharged before it returns to ground level. Iodine adsorbers appear to be quite effective in reducing the release of this particularly noxious activity, and filters are more than 99% effective in removing particulate matter.

An indication of the normal activity release from the PBR can be obtained by using the results of analyses performed for the PBRE and for the EGCR.²

Activation of Shield Cooling Air

For the 84-Mw(t) EGCR, it was estimated that 400 curies/day of A⁴¹ would be generated in the shield cooling air. Lesser amounts of N¹⁶ and O¹⁹ would be produced, but, in any case, these activities would decay to insignificant levels before reaching the ground. The A⁴¹ generation rate for the PBR has not been computed, but it would be expected to be of the same magnitude as that in the EGCR. The PBR has a thicker reflector and pressure vessel than the EGCR, which will reduce the neutron leakage, but this will probably be offset by the larger volume of air around the reactor. Assuming a discharge of 400 curies/day of A⁴¹ from a 200-ft stack with the meteorological parameters characteristic of the EGCR site, the maximum ground concentration during a large inversion would be about five times the maximum permissible concentration (MPC) for other than operating personnel. While this concentration would be excessive if sustained for a long period, it actually represents a condition that would exist only periodically at any particular location. The calculated release would be reduced to tolerable levels if allowances were made for wind variability. No definite conclusion is possible in the absence of a specific analysis, but, from the preceding discussion, it appears that the argon activity must be considered early in the design of a reactor. The A⁴¹ generation rate could be reduced by designing the shield so as to restrict the volume of air between it and the pressure vessel. This problem is, however, in no way unique to pebble-bed systems, since it could exist in connection with any large power reactor.

²"Experimental Gas-Cooled Reactor Preliminary Hazards Summary Report," ORO-196 (supplement), May 1959.

Activity Escape from Reactor

In the hazards study¹ for the 10-Mw(t) PBRE, an estimate was made that under normal conditions there would be about 900 curies of gaseous fission-product activity circulating in the helium system. This activity was assumed to leak from the reactor with the helium coolant at a rate of 0.1%/day. Maximum ground concentrations were computed for the more important nuclides, assuming release from a 200-ft stack with the meteorological conditions that prevail at the EGCR site. Without allowance for purification of the stack gas, the largest fraction of the non-occupational MPC for an inversion condition was represented by 1.1% for I¹³². Assuming that iodine is removed by an adsorber in the stack, no nuclides were computed to attain a ground concentration exceeding 0.2% of the nonoccupational MPC.

An assumption that the normal activity release from the 800-Mw(t) PBR would run 80 times that of the 10-Mw(t) PBRE would still not lead to an excessive computed activity level for the meteorological conditions used. Achievement of fuel having better fission-product retention than that assumed for the PBRE or a reduction of the helium leakage rate to below 0.1%/day would reduce the maximum ground concentration to well below permissible levels.

Dose at Helium Blowers

The radiation dose level at the surface of an unshielded helium blower is the major factor in determining whether direct maintenance of the blowers is feasible. Calculations for the PBRE indicated that Ba^{137m} and I¹³² will be the major activity sources affecting maintenance if their cesium and tellurium precursors are deposited in the primary systems more rapidly than they are removed in the side-stream processing system. An estimate of the Ba^{137m} and I¹³² dose rates at the surface of a helium blower has been obtained for the PBR by assuming that cesium and tellurium are deposited uniformly on all metal surfaces in the primary system. The values in Table 13.2 were based on the fractional

Table 13.2. Estimated Dose at Blower Surface Based on Fractional Release Values from PBRE Study

Nuclide	Fractional Release (PBRE Basis)	Activity in Blower (curies)	Dose at Blower Surface (r/hr)
2.4h I ¹³²	0.0026	280	98
2.6m Ba ^{137m}	0.050	580	67

release values for Te¹³² and Cs¹³⁷ from the PBRE study and the assumption of a uniform volumetric radiation source 7 ft in diameter surrounded by 1 1/2 in. of steel.

The dose rates indicated by Table 13.2 are obviously too high for direct maintenance, and they would not decrease significantly in a reasonable time period because of the long half-life of 26.6y Cs¹³⁷. The fractional release values used for the PBRE study were, however, based on present experience with alumina-coated UO₂ particles. Fuel having better fission-product retention properties will probably be available by the time a PBR is ready for operation. Dose values are therefore presented in Table 13.3 that were obtained by arbitrarily assuming the more favorable fission-product escape rates shown. With moderate success in decontamination of the blowers, the activities given in Table 13.3 would be reduced to tolerable levels for direct maintenance. If the fission-product deposition were not uniform in the gas system, but, rather, occurred preferentially on the first cold surface that the gas contacted, there might be a factor of 10 difference in deposition rate between the steam generator and the blower. This coupled with a decontamination factor of 100 would permit limited contact maintenance of the blowers, even with the dose levels indicated by Table 13.2 for the fuel currently being tested.

The uncertainties in these values should be emphasized. Because of the lack of applicable data, both the fractional release of fission products from the fuel and the distribution of fission products in

Table 13.3. Estimated Dose at Blower Surface Assuming Improved Fission-Product Retention in Fuel

Nuclide	Fractional Release	Activity in Blower (curies)	Dose at Blower Surface (r/hr)
2.4h I ¹³²	10 ⁻⁵	1.1	0.38
2.6m Ba ^{137m}	10 ⁻⁴	1.2	0.14

the primary system were based on arbitrary assumptions. The possible range of these values is large enough to introduce an error of several orders of magnitude in the dose rate. The activity in the blower would be less than quoted if cesium and tellurium were removed by a side-stream processing system at a rate competitive with deposition in the primary system or if they deposited in the heat exchanger or elsewhere before reaching the blower. However, the dose might be higher if the low temperatures and high turbulence in the blower housing led to greater deposition than assumed. The dose rates would also be increased by including other nuclides than the two considered, particularly if nonvolatile elements were separated from the gas by centrifugal forces in the blower.

Conclusions

The hazards analysis of the PBR has not been sufficiently detailed to establish the maximum credible accident. A preliminary examination suggests, however, that a meltdown of the core would not be found to be credible. Combustion of the core following rupture of the primary system is probably preventable by coating the fuel spheres, but, even if it is not, the oxygen content of the containment vessel is sufficient to burn only 5% of the fuel. The fission products evolved by combustion would thus be only those associated with 40 Mw of thermal power.

Estimates of the pressure which could exist following a primary system rupture yield values which may be excessive for the containment vessel. If detailed analyses confirm that high pressures are credible, means for suppressing the pressure will be required.

If the ability of the fuel to retain fission products is at least an order of magnitude better than the values used for the PBRE, the normal activity leakage from the reactor will not be at a rate which is excessive for discharge from the stack. However, care may have to be taken in designing the reactor shield to limit the rate of $1.8h A^{41}$ generation in the shield cooling air.

An estimate of the unshielded radiation dose levels at the blowers was made by assuming that tellurium and cesium deposit uniformly on all surfaces in the primary system. The values obtained using the fission-product retention properties estimated for the PBRE fuel are too high for direct maintenance, even after reasonable decontamination. The blowers may be approached for direct maintenance after decontamination, however, if improved fuel leads to fission-product escape fractions in the range below 10^{-4} .

14. CONSTRUCTION COSTS

While reasonably good cost estimates can be made for the conventional portion of the steam plant, the design is not sufficiently detailed for a good cost estimate of the reactor portion of the plant. As was the case with the PBRE design, the best way to estimate construction costs for the reactor appeared to be to use the EGCR costs as a point of departure. Estimates were made of the quantities of materials required for the design outlined, and the costs were extrapolated from the EGCR costs by considering the costs to be proportional to the quantities of materials for the two plants. This approach seems reasonable, since the size of the reactor building is not much greater than that required for the EGCR, and the service area, control room, and related facilities are comparable. Probably less uncertainty lies in the cost of the facilities of the size proposed than in the adequacy of the proposed facilities. It may be that substantially more building space will be needed or that a considerable amount of equipment not included may be required. There are also major uncertainties in the cost of the fuel-handling and servicing equipment, since no designs are available to serve as a basis for cost estimation.

The cost estimates are summarized in Tables 14.1 and 14.2. In reviewing the data of Tables 14.1 and 14.2, a number of points are evident. About two-thirds of the basic costs are either for conventional plant or for items such as the containment shell, for which firm cost-estimating data are available. The top charges imposed on these items may be excessive. Of the remaining one-third of the construction costs, the uncertainties arise from the lack of detailed designs. Items such as the closures for the access tubes in the reactor pressure vessel, the fuel-handling equipment, the servicing machine and the special tools required for it, and the steam generator are all unconventional and will require much detailed design work before firm cost estimates can be made. Some indication of the fine

Table 14.1. Summary of Cost Data and Estimates for the EGCR, PBRE, and PBR

Cost Code	Description	EGCR		PBRE		PBR	
		Quantity	Cost	Quantity	Cost	Quantity	Cost
21.210	Access road and water main	0.876 mile	\$ 180,000	0.1 mile	\$ 45,000	0.89 mile	\$ 183,000
21.211	General yard improvements	120 000 ft ²	660,000	40 000 ft ²	160,000	120 000 ft ²	660,000
21.212	Reactor service building	512 000 ft ³	432,000	250 000 ft ³	250,000	476 000 ft ³	476,000
	Turbine building	17 500 ft ²					
	Control building	665 000 ft ³	611,000	90 000 ft ³	90,000	1 350 000	1,350,000
		358 000 ft ³	373,000	150 000 ft ³	150,000	247 000 ft ³	247,000
		25 200 ft ²					
	Guard, stack, chlorine, etc., buildings	800 ft ²	300,000		95,000		300,000
	River pumping station	30 000 gpm	527,000	5000 gpm	100,000		700,000
21.213	Reactor building		3,902,000		1,960,000		4,002,000
21.214	Experimental cells	7000 ft ²	930,000				
22.220	Reactor equipment		3,527,000		777,000		4,978,000
22.221	Heat transfer system		2,249,000		624,000		6,976,000
22.222	Fuel handling and storage		2,358,000		600,000		2,200,000
22.224	Radioactive waste treatment		93,000		100,000		400,000
22.225	Instrumentation and controls		1,812,000		800,000		1,500,000
22.226.7	Steam system		533,000		200,000		3,500,000
23	Turbine generator unit	25 Mw	1,267,000			330 Mw	13,490,000
24	Accessory electrical equipment		1,235,000		310,000		1,726,000
25	Miscellaneous power plant equipment		128,000		60,000		425,000
	Transmission plant		198,000		30,000		1,035,000
	Miscellaneous		146,000		70,000		150,000
Total direct costs			\$21,461,000		\$6,421,000		\$44,298,000
Indirect costs (general and administrative, at 12% of direct) ^a					770,000		5,315,760
Total direct and indirect costs					\$7,191,000		\$49,613,760
Engineering, design, and inspection (at 15%) ^{a, b}					1,078,000		7,442,064
Total direct + indirect + engineering					\$8,269,000		\$57,055,824
Contingency (at 10% of direct + indirect + engineering) ^a					827,000		5,705,582
Total					\$9,096,000		\$62,761,406

^aCharges assigned are based on those used in the USAEC "Civilian Power Reactor Program, Part 3, Status Report on Gas-Cooled Reactors," 1959.

^bActual indirect, engineering, design, inspection, and contingency figures are not yet available for the EGCR.

Table 14.2. Approximate Quantity and Cost Estimates for the Reactor Building and Reactor for the EGCR, the PBRE, and the PBR

Cost Code	Description	EGCR		PBRE		PBR	
		Quantity	Cost	Quantity	Cost	Quantity	Cost
21.213.1	Excavation and gunniting	53 250 yd ³	\$ 120,000	26 000 yd ³	\$ 50,000	100 000 yd ³	\$ 226,000
.3	Concrete	23 200 yd ³	1,565,000	12 500 yd ³	800,000	19 500 yd ³	1,310,000
.4	Containment shell and related items	2 600 000 lb	1,761,000	1 300 000 lb	880,000	2 965 000 lb	2,010,000
.6	Building services and miscellaneous		456,000		230,000		456,000
21.213	Total reactor building		<u>\$3,902,000</u>		<u>\$1,960,000</u>		<u>\$4,002,000</u>
22.220.1	Reactor vessel and internals	700 000 lb	\$1,600,000	150 000 lb	\$ 320,000	750 000 lb	\$1,720,000
.2	Control rods and drives	21	480,000	6	137,000		458,000
.4	Cooling facilities		400,000		40,000		1,000,000
.6	Graphite	313 000 lb	887,000	64 000 lb	200,000	410 000 lb	1,160,000
	Miscellaneous		160,000		80,000		640,000
	Total		<u>\$3,527,000</u>		<u>\$ 777,000</u>		<u>\$4,978,000</u>
22.221.11	Main blowers and drives	6200 hp	\$ 465,000	500 hp	\$ 200,000		\$1,206,000
.12	Main coolant piping and valves		237,000	3500 lb	3,500	80 000 lb	194,000
.31	Steam generators	88.1 Mw	700,000	10 Mw	100,000	800 Mw	3,801,000
.32	Attemperators		132,000				100,000
.4	Coolant charging and discharging	244 000 ft ³	184,000	20 000 ft ³	50,000		475,000
.5	Coolant purification equipment		193,000		200,000		500,000
.6	Burst slug detection system		162,000				
	Miscellaneous		176,000		70,000		700,000
22.221	Total heat transfer system		<u>\$2,249,000</u>		<u>\$ 624,000</u>		<u>\$6,976,000</u>

structure is given by Table 14.3, which shows a breakdown for cost code item 22.222, fuel handling, storage, and reactor servicing equipment. The costs given are simply rough estimates based on an appraisal of the operations required, which seem to be substantially simpler than the corresponding operations for the EGCR.

Table 14.3. Fuel Handling and Servicing

Service machines, basic structure	\$ 800,000
Service machine servicing tools, etc.	500,000
Fuel feed at 19 points	190,000
Fuel withdrawal at 6 points	180,000
Mobot	80,000
Steel wall lining	40,000
Remote hoist	60,000
Special tools, television equipment, etc.	150,000
Casks	150,000
Decontamination	50,000
Total	\$2,200,000

The fuel-cycle costs for the PBR have been estimated for a first loading of U^{235} and thorium. The initial conversion ratio has been calculated to be 0.75, but it is expected to rise, eventually, to some value greater than 0.8 as the proportion of U^{233} in the core increases. A complete calculation of fuel-cycle costs would take into account the change in reactivity lifetime, and the change in value of the U^{235} as it is recycled. Since a complete calculation could not be made within the time limit imposed on this study, the value of U^{235} burned was considered to be constant at the price for fresh fuel, and the conversion ratio was assumed to be constant at 0.8 to permit a preliminary estimate of the fuel cycle costs.

The fuel cycle cost has been broken down into the following five items: (1) net U^{235} burned, (2) fuel-handling costs at the power station, (3) fuel fabrication costs, (4) reprocessing, conversion, and shipping costs, and (5) interest charges on the average total U^{235} inventory.

1. Net U²³⁵ Burned. The price of U²³⁵ has been taken as \$17.10/g, with 1.3 g equivalent to 1 Mw-day of thermal energy. The net uranium consumption is considered as the power equivalent of fissionable material times one minus the conversion ratio, and the cost is

$$\begin{aligned} \text{Cost} &= (17.10 \times 10^3) \frac{\text{U burned}}{\text{kwhr}(t)} (1 - \text{CR}) \frac{1}{\text{efficiency}} \\ &= 17,100 \frac{1.3}{1000 \times 24} (1 - 0.8) \frac{1}{0.406} \\ &= 0.457 \text{ mill/kwhr.} \end{aligned}$$

2. Fuel-Handling Costs at Power Station. The cost of the facility for handling and packaging spent fuel for shipment has been estimated to be approximately \$2,000,000 for a 500-Mw(e) plant and to be proportional to the square root of the power.¹ The labor costs were estimated to be about \$20,000/year and to vary with power in the same way. The charge rate was taken as 14%/year. For an assumed plant factor of 0.80 (7000 hr/year), the costs are

$$\begin{aligned} \text{Capital charges} &= \frac{(\text{capitalization, mills}) (\text{charge rate})}{(\text{power, kw}) (\text{hr/year})} \\ &= \frac{0.812 (2 \times 10^6) 0.14}{(3.3 \times 10^5) 7000} = 0.098 \text{ mill/kwhr} \\ \text{Labor cost} &= \frac{0.812 (20,000 \times 10^3)}{(3.3 \times 10^5) 7000} = 0.007 \text{ mill/kwhr} \end{aligned}$$

Therefore, approximate total handling costs = 0.11 mill/kwhr.

¹A. P. Fraas and M. N. Ozisik, Relative Capital Charges and Fuel Cycle Costs for All-Ceramic Gas-Cooled Reactors, ORNL CF-60-7-41, July 20, 1960.

3. Fabrication Costs. The power cost assignable to fuel fabrication was calculated from the estimates presented in Chapter 6. The residence time for the fuel in the core depends, from a nuclear standpoint, on the number of fissions per initial fissionable atom (fifa) obtained. If fifa is as low as 1, the residence time is 580 days, and it is twice this for a fifa of 2. It is believed that fifa will exceed 1, and a representative residence time of 700 days was assumed.

The core fuel weight is 134 tons, or 122 metric tons, containing 0.44 wt % U^{235} and 8.45 wt % thorium. The core thus contains 537 kg of uranium and 10 300 kg of thorium. Since each ball contains 21 g of heavy metal, the core contains 5.16×10^5 balls. The fuel reprocessing rate, therefore, is 737 balls/day for a residence time of 700 days. For the minimum and maximum fabrication cost estimates of \$14.28 and \$35.66 per ball, the power cost turns out to be 1.33 and 4.52 mills/kwhr, respectively.

4. Fuel Reprocessing, Conversion, and Shipping. On the assumption that the contained thorium is to be discarded, the characteristic Thorex processing plant² capacity was assumed to be 600 kg/day of heavy metal, as the nitrate, based on criticality limitations. The most economical batch size is obtained when the sum of the reprocessing cost and the interest charges during the period of accumulation, per kilogram of metal, is a minimum. This occurs for a batch size of 1200 kg, accumulated every 77.6 days, and the unit reprocessing cost (exclusive of interest) is \$55/kg. To this must be added the cost of converting the fuel to heavy-metal nitrates, reconversion to the oxide, and shipping. There has been very little experience in converting graphitic fuels, but a conversion cost of perhaps 20% of the Thorex reprocessing cost does not seem unreasonable provided disposal of the graphite and removal of the protective particle coatings does not turn out to be unusually

²WASH-743.

difficult. On this basis the reprocessing cost is \$66/kg of metal, or \$1020/day of full-power operation, or a power cost of 0.129 mill/kwhr.

5. Interest on Fuel. A 4% interest charge on the value of the average total uranium inventory was assumed.

The total average inventory includes the uranium in the core, 30% fresh fuel in storage at the plant, 90 days' accumulation cooling off at all times before shipment, 30 days' accumulation in shipment at all times, and half of 77.6 days' batch accumulation. Therefore,

$$\text{Average inventory} = 537 \text{ kg of U } \left(1.3 + \frac{90 + 38.8 + 30}{700} \right)$$

$$= 537 (1.53) = 820 \text{ kg of U}$$

$$\text{Interest on fuel} = 820 \frac{(17.1 \times 10^6) 0.04}{(3.3 \times 10^5) 7000} = 0.0232 \text{ mill/kwhr}$$

The above costs are summarized in Table 14.4:

Table 14.4. Summary of Fuel Cycle Costs

	Cost (mills/kwhr)
Fuel burned	0.46
Fuel handling	0.11
Fuel fabrication	1.33-4.52
Reprocessing	0.13
Interest on fuel	0.23
Total	2.26-5.45

In the event that the thorium is recovered, rather than discarded, the fuel cycle costs will be increased by about 0.06 mill/kwhr, exclusive

of the value of the thorium. The greatest contribution to the fuel cycle cost is, obviously, the estimated cost of fabrication, and the spread between minimum and maximum is an indication of the great uncertainty of the estimate. If the fuel had to be purchased today, it is unlikely that the price would be much below the maximum, but purchase a few years from now for a "first generation" power station should be at a price approaching the minimum value, provided vigorous development is carried out in the meantime. Second generation reactors might well have fuel fabrication costs below the minimum shown.



ORNL
Central Files Number
60-12-5
Revised

Distribution

- | | |
|------------------------|--|
| 1. S. A. Beall | 41. C. S. Walker |
| 2. M. Bender | 42. A. M. Weinberg |
| 3. A. L. Boch | 43. M. E. Whatley |
| 4. R. B. Briggs | 44. C. E. Winters |
| 5. R. S. Carlsmith | 45. M. M. Yarosh |
| 6. C. E. Center (K-25) | 46-49. ORNL - Y-12 Technical Library
Document Reference Section |
| 7. W. R. Chambers | 50-186. Laboratory Records Department |
| 8. R. A. Charpie | 187. Laboratory Records Department,
ORNL R.C. |
| 9. J. H. Coobs | 188-190. Central Research Library |
| 10. W. B. Cottrell | 191-205. TISE |
| 11. F. L. Culler | 206-225. L. A. Curry |
| 12. E. P. Epler | |
| 13. D. E. Ferguson | |
| 14. J. Foster | |
| 15. A. P. Fraas | |
| 16. B. L. Greenstreet | |
| 17. T. Hikido | |
| 18. W. O. Harms | |
| 19. R. B. Korsmeyer | |
| 20. P. G. Lafyatis | |
| 21. R. N. Lyon | |
| 22. H. G. MacPherson | |
| 23. W. D. Manly | |
| 24. E. R. Mann | |
| 25. H. C. McCurdy | |
| 26. A. B. Meservey | |
| 27. M. N. Ozisik | |
| 28. P. Patriarca | |
| 29. A. M. Perry | |
| 30. R. C. Robertson | |
| 31. M. W. Rosenthal | |
| 32. G. Samuels | |
| 33. H. W. Savage | |
| 34. A. W. Savolainen | |
| 35. O. Sisman | |
| 36. M. J. Skinner | |
| 37. I. Spiewak | |
| 38. J. C. Suddath | |
| 39. J. A. Swartout | |
| 40. D. B. Trauger | |